

BEHAVIOR OF STRENGTHENED AND/OR REPAIRED REINFORCED CONCRETE
COLUMNS UNDER REVERSED CYCLIC DEFORMATIONS

APPROVED:

To my parents

BEHAVIOR OF STRENGTHENED AND/OR REPAIRED REINFORCED CONCRETE
COLUMNS UNDER REVERSED CYCLIC DEFORMATIONS

BY

BART J. BETT, B.S.C.E.

THESIS

Presented to the Faculty of the Graduate School of
The University of Texas at Austin
in Partial Fulfillment
of the Requirements
for the Degree of
MASTER OF SCIENCE IN ENGINEERING

THE UNIVERSITY OF TEXAS AT AUSTIN

May 1984

ACKNOWLEDGMENTS

The author wishes to express his sincere gratitude to Dr. R. E. Klingner for his invaluable direction and assistance throughout the test program and the writing of this report, and also for his concerned guidance of the author's program of graduate study at The University of Texas. Dr. J. O. Jirsa and Dr. R. L. Carrasquillo also were very helpful throughout the test program and their valuable advice is sincerely appreciated. This research was conducted jointly with the firm of H. J. Degenkolb Associates, Inc., San Francisco, California. The author appreciates the help provided by Loring Wyllie, Jr., Chris Poland, Roy Morena, and others of that firm.

This report was funded by Grant No. CEE-8201205 from the National Science Foundation's Directorate for Applied Science and Research Applications, Division of Problem-Focused Research.

The author would like to extend his gratitude to Mr. Tim Overman and Mr. Scott Garner for their many valuable suggestions, endless encouragement and wonderful friendship throughout the test program. The author is indebted to his fellow graduate students Bob Bass, Mark Pavlucik, Kurt Swensson, Chris White, and John Worley, who provided the author with friendship and enthusiastic encouragement. Appreciation is expressed for the willing cooperation and helpful advice of the Ferguson Structural Engineering Laboratory Staff. Assistance from Darrell Miller during the majority of the test program is greatly appreciated.

B.J.B.
May 1984

TABLE OF CONTENTS

Chapter		Page
I	INTRODUCTION	1
	1.1 Background	1
	1.2 Objectives and Scope	2
	1.3 Short Columns in Structures	2
	1.4 Short Column Repair/Strengthening Techniques	3
II	EXPERIMENTAL PROGRAM	9
	2.1 Introduction	9
	2.2 Overall Research Program	9
	2.3 Original Test Specimen 1-1	12
	2.3.1 Design Requirements	12
	2.3.2 Details of Specimen	13
	2.3.3 Calculated Strengths	13
	2.3.4 Specimen Fabrication	17
	2.4 Material Characteristics of Original Test Specimen ...	17
	2.4.1 Concrete	17
	2.4.2 Reinforcement	20
	2.5 Strengthened and Repaired Specimens	21
	2.5.1 Strengthening Technique (Specimens 1-2, 1-3) ..	21
	2.5.2 Repair Technique (Specimen 1-1R)	21
	2.6 Strengthened Specimen 1-2	21
	2.6.1 Details	21
	2.6.2 Calculated Strengths	21
	2.7 Strengthened Specimen 1-3	26
	2.7.1 Details	26
	2.7.2 Calculated Strengths	26
	2.8 Repair of Specimen 1-1	26
	2.9 Fabrication of Strengthened Specimens	31
	2.10 Material Characteristics of Strengthened Specimens ...	36
	2.10.1 Shotcrete	36
	2.10.2 Reinforcement	37
	2.10.3 Epoxy	40
	2.11 Loading History	40
	2.11.1 Axial and Lateral Loading	40
III	LOADING SYSTEM AND INSTRUMENTATION	44
	3.1 Loading System	44
	3.2 Instrumentation	53
	3.2.1 Loads	53
	3.2.2 Deflections	53

TABLE OF CONTENTS (continued)

Chapter	Page
III	LOADING SYSTEM AND INSTRUMENTATION (continued)
	3.2.3 Strains 53
	3.2.4 Slip 58
	3.3 Data Acquisition and Reduction 58
IV	BEHAVIOR OF SPECIMENS 61
	4.1 Introduction 61
	4.2 Description of Test Results 62
	4.2.1 Load-Deflection Curves 62
	4.2.2 Crack Patterns 68
	4.2.3 Strain Distributions 71
	4.2.4 Slip 80
V	DISCUSSION OF TEST RESULTS 84
	5.1 Introduction 84
	5.2 Test Results 84
	5.2.1 Specimen Stiffness and Capacity 84
	5.2.2 Crack Patterns 93
	5.2.3 Strains in Reinforcement 96
	5.2.4 Jacket Slip 106
	5.3 Comparison of Observed and Predicted Behavior 107
VI	SUMMARY AND CONCLUSIONS 112
	6.1 Summary of Investigation 112
	6.2 Summary of Test Results 113
	6.2.1 Original Column Specimen 113
	6.2.2 Strengthened and Repaired Specimens 114
	6.3 Conclusions 116
	6.4 Additional Research 118

LIST OF TABLES

Table		Page
2.1	Test Program Summary	10
2.2	Original Specimen Concrete Strength	22
2.3	Steel Properties (Original Specimen)	22
2.4	Shotcrete Properties	37
2.5	Shotcrete Strengths	39
2.6	Steel Properties (Jacket #3 Long.)	40
2.7	Concresive 1411 Mechanical Properties	42
5.1	Secant Stiffness in First Cycle to Various Drift Levels ..	86
5.2	Reduction in Secant Stiffness Between 1st and 3rd Cycles .	91
5.3	Lateral Capacity	109

LIST OF FIGURES

Figure		Page
1.1	Captive column concept	4
1.2	Relation between end shears and moments in a column subjected to sidesway	5
1.3	Failed columns at Misawa Commercial High School— Tokachi-Oki earthquake, Japan, 1968	6
1.4	Techniques to increase shear capacity	7
2.1	Details of original specimen	14
2.2	Shear capacity-interaction diagram (original specimen)	16
2.3	Details of end block reinforcement	18
2.4	Construction of formwork	19
2.5	Stress-strain curve for original specimen steel reinforcement	23
2.6	Details of Specimen 1-2	24
2.7	Shear capacity-interaction diagram (Specimen 1-2, 1-3)	25
2.8	Details of Specimen 1-3	27
2.9	Post-test, Specimen 1-1	28
2.10	Loose cover removed, Specimen 1-1	28
2.11	Jacket reinforcement, Specimen 1-1.....	29
2.12	Crossties secured by epoxy, Specimen 1-1	30
2.13	Screed guides	32
2.14	Shotcrete test panels	33
2.15	Shotcreting	34
2.16	Shotcreting	35

LIST OF FIGURES (continued)

Figure		Page
2.17	Panel (top) core samples	38
2.18	Panel (bottom) core samples	38
2.19	Stress-strain curve for jacket steel (#3)	41
2.20	Lateral displacement history	43
3.1	Specimen/loading schematic	45
3.2	Floor-wall reaction system	46
3.3	Specimen hold-down bolt details	47
3.4	Loading rams	49
3.5	Test setup	50
3.6	Restraining rams	51
3.7	Vertical and horizontal positioning system	52
3.8	Linear potentiometer locations	54
3.9	Linear potentiometer mounting frame	55
3.10	Strain gage locations (original specimen)	56
3.11	Strain gage locations (jacket)	57
3.12	Slip wire instrumentation	59
3.13	Slip wire locations	60
4.1	Load-deflection curve, Specimen 1-1	63
4.2	Load-deflection curve, Specimen 1-2	64
4.3	Load-deflection curve, Specimen 1-3	65
4.4	Load-deflection curve, Specimen 1-1R	66

LIST OF FIGURES (continued)

Figure		Page
4.5	Load-deflection envelopes, Specimens 1-1, 1-2, 1-3, and 1-1R	67
4.6	Crack patterns, NW column faces, Specimen 1-1	69
4.7	Crack patterns, Specimen 1-3	70
4.8	Envelopes of strain distribution, NW longitudinal #6, Specimen 1-1	72
4.9	Envelopes of strain distribution, NW longitudinal #6, Specimen 1-3	73
4.10	Envelopes of top gage strain, #6/#3, NW longitudinal bars, Specimen 1-3	74
4.11	Strain envelopes, N-S direction, original column ties, Specimen 1-1	76
4.12	Strain envelopes, E-W direction, original column ties, Specimen 1-1	77
4.13	Strain envelopes, mid-height ties, Specimen 1-3	78
4.14	Strain envelopes, N-S crossties, Specimen 1-3	79
4.15	Strain envelopes, E-W crossties, Specimen 1-3	81
4.16	Envelope of mid-height jacket slip, Specimen 1-3	82
4.17	Envelope of bottom jacket slip, Specimen 1-3	83
5.1	Load-displacement envelopes, 1st and 3rd cycles, Specimen 1-1	87
5.2	Load-displacement envelopes, 1st and 3rd cycles, Specimen 1-2	88
5.3	Load-displacement envelopes, 1st and 3rd cycles, Specimen 1-3	89
5.4	Load-displacement envelopes, 1st and 3rd cycles, Specimen 1-1R	90

LIST OF FIGURES (continued)

Figure		Page
5.5	Crack patterns, Specimen 1-1R	94
5.6	Crack patterns, Specimen 1-2	95
5.7	Predicted envelopes of longitudinal bar strains	98
5.8	Strain envelopes, mid-height ties, Specimen 1-1R	103
5.9	Strain envelopes, N-S crossties, Specimen 1-1R	104
5.10	Strain envelopes, E-W crossties, Specimen 1-1R	105

N O T A T I O N

a	Shear span, in.
A_c	Area of concrete core, out-to-out of ties, in. ²
A_g	Gross area of cross section, in. ²
d	Distance from extreme compression fiber to the centroid of the tension reinforcement, in.
d*	Distance from extreme compression fiber to the centroid of the extreme tension reinforcement, in.
E	Modulus of elasticity of reinforcement
E_{STH}	Modulus of elasticity of reinforcement at the onset of strain hardening
f'_c	Concrete compressive strength (6 x 12 in. cylinder), psi (28 day strength for design. Strength at age of test specimen for analysis of data)
f_u	Ultimate tensile strength of reinforcement
f_y	Yield strength of reinforcement
N	Applied axial compression, lbs.
V_{nr}	Nominal shear strength of short columns, lbs
ϵ_{STH}	Tensile reinforcement strain at onset of strain hardening
ϵ_u	Ultimate tensile reinforcement strain

C H A P T E R I

INTRODUCTION

1.1 Background

Reinforced concrete buildings in seismic zones are repaired or strengthened for three reasons: 1) to repair earthquake damage and obtain improved performance during future events; 2) to comply with local building codes and regulations when the building's use is changed; and 3) to satisfy the building owner's concern for the safety of the occupants and protection of his financial investment.

Such strengthening is difficult. The existing building must be thoroughly analyzed to determine the strengths and weaknesses of the original lateral force-resisting system, considering the building's functions and aesthetics. Strengthening schemes may involve the use of materials different from those of the original structure, and the interaction of those materials must be understood. The scheme selected must not create new areas of weakness, and must be economically feasible.

The need for information on the repair and strengthening of reinforced concrete structures is becoming increasingly apparent. Several National Science Foundation-sponsored workshops on this topic have been held in the United States, and a number of U.S. research institutions (Portland Cement Association, University of Michigan, University of California-Berkeley) have studied repair techniques [1,2]. Repair

and strengthening problems have received more attention in Japan [3,4]. Because experimental work in the area of repair and strengthening is very complex and expensive, most studies have involved small scale specimens. In addition, there has been little dialogue between researchers and the designers who must incorporate research results into practice. These two concerns are addressed in the overall research program discussed in Chapter II.

1.2 Objectives and Scope

The objective of this study is to evaluate various repair and strengthening techniques for reinforced concrete short columns. Short columns under constant axial compression were subjected to reversed cyclic deformations. Two columns were strengthened before testing, and one column was repaired after testing. Individual column test results were compared. Repair and strengthening techniques were evaluated in terms of strength, stiffness, and damage repair.

1.3 Short Columns in Structures

Field reports following various damaging earthquakes indicate that columns are vulnerable structural elements, particularly if they fail in shear. Shear-dominated behavior is most common in columns having shear-span/depth (a/d) ratios less than 2.5 [5,6,7,8]. Short columns exist in structural systems either as part of the original design, or as the result of structural or architectural changes made during the life of the structure. Members originally designed as short columns can behave satisfactorily under lateral loads if designed for

sufficient shear resistance. However, short (or "captive") columns are sometimes produced unintentionally [8,9] when clear column height is reduced by stiff elements that restrict the lateral deformation of the column over a portion of its length (Fig. 1.1). This change in length is important because a column's applied shear and moment are related by its length, as shown in Fig. 1.2. The original column may have been properly designed to develop its flexural capacity before failing in shear. Due to the reduction in length, the captive column will often fail in shear before developing its flexural capacity. Post-earthquake structural investigations report many failures of captive columns restrained by structural or non-structural elements (Fig. 1.3).

1.4 Short-Column Repair/Strengthening Techniques

Severe seismic loading of columns with small shear-span/depth (a/d) ratios and widely-spaced transverse reinforcement generally results in shear-dominated failure, leading to structural collapse by the formation of a single-story sidesway mechanism. While this can be prevented by increasing column shear capacity, it must be done economically, and without large increases in flexural capacity, which would increase applied shears. Figure 1.4 illustrates four methods now available for increasing the shear capacity of a vulnerable column: 1) encase it with rectangular or circular steel sections; 2) encase it with steel straps; 3) confine it by using welded wire fabric; and 4) confine it by adding spliced ties. A jacket of shotcrete or cement grout is then applied to protect the added steel and make it act integrally with the original column.

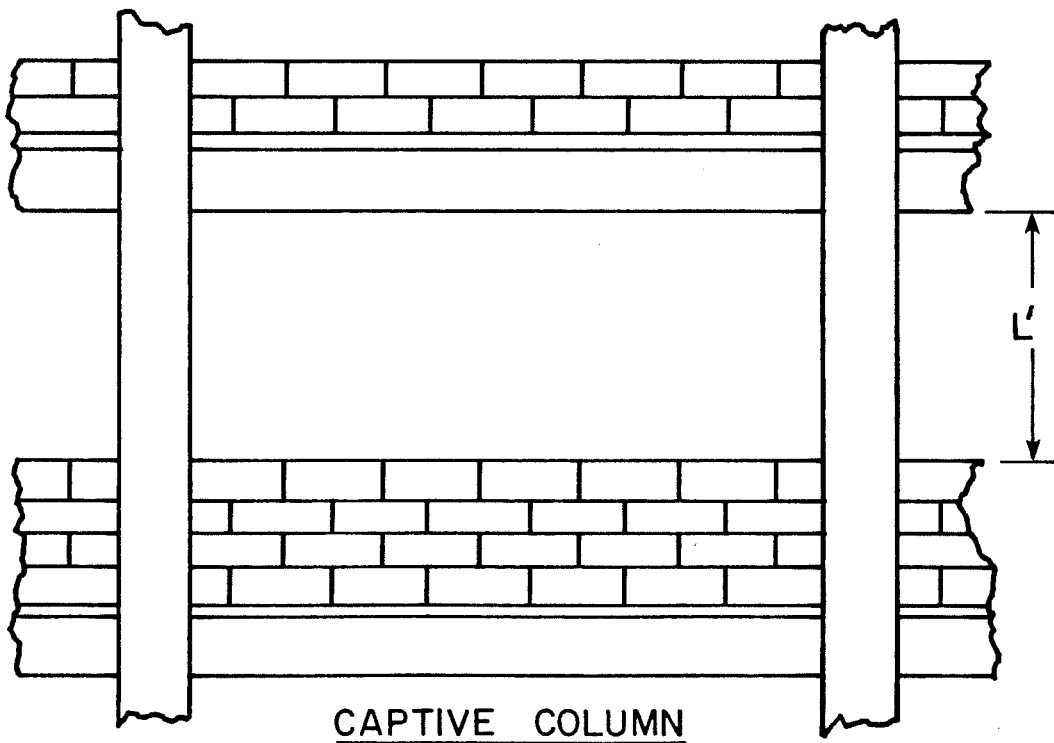
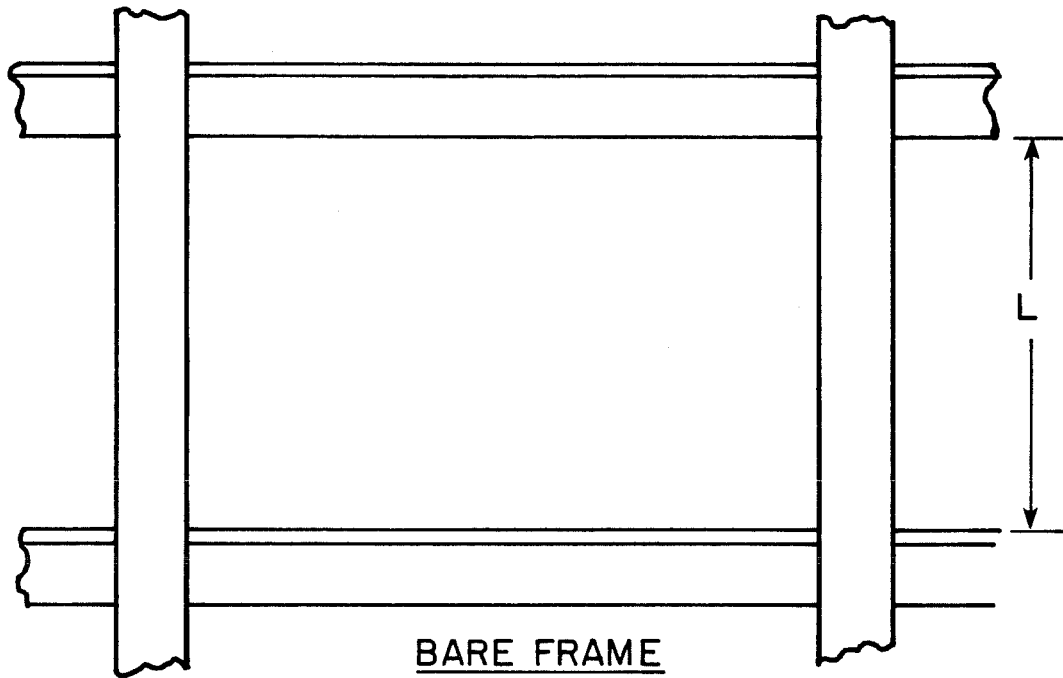


Fig. 1.1 Captive column concept.

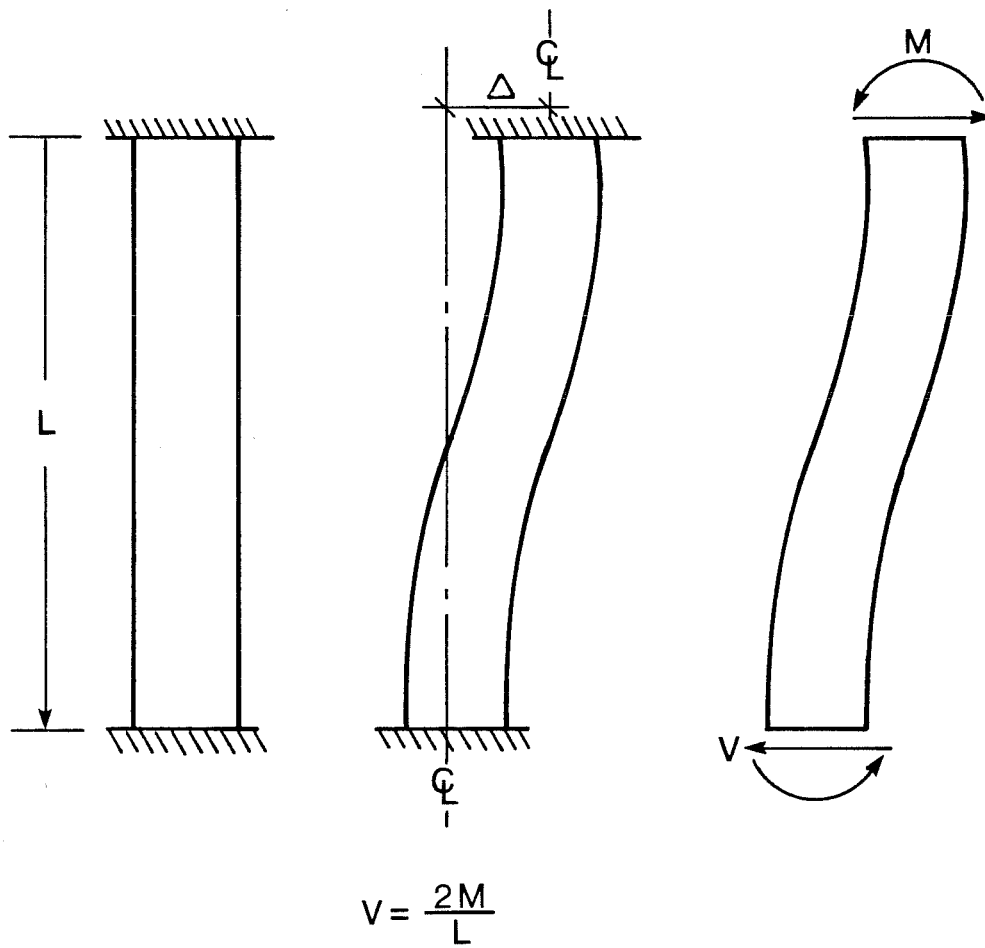


Fig. 1.2 Relation between end shears and moments in a column subjected to sideways.

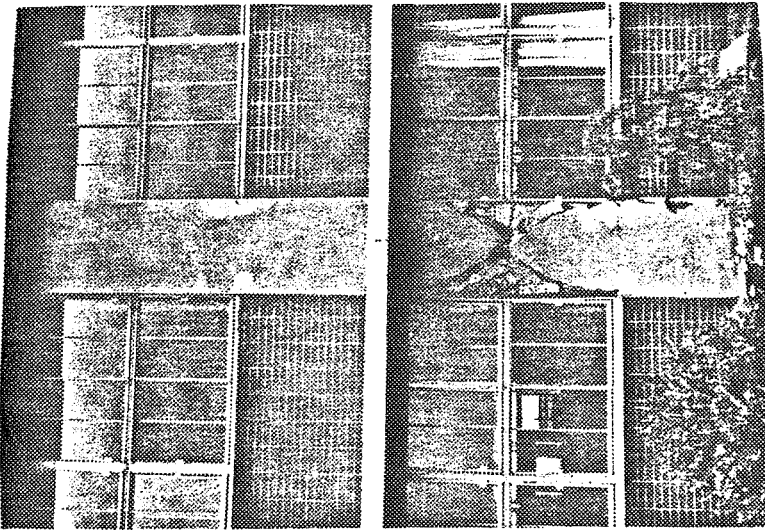
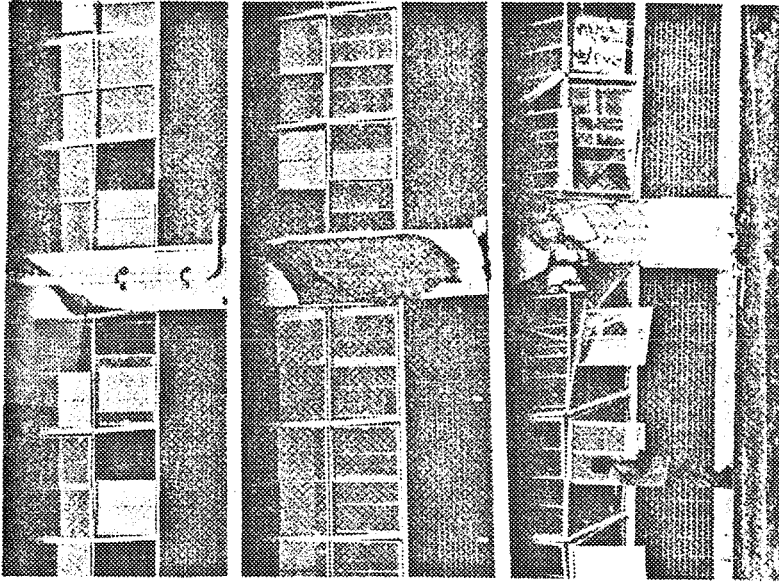


Fig. 1.3 Failed columns at Misawa Commercial High School, Tokachi-Oki earthquake, Japan, 1968.

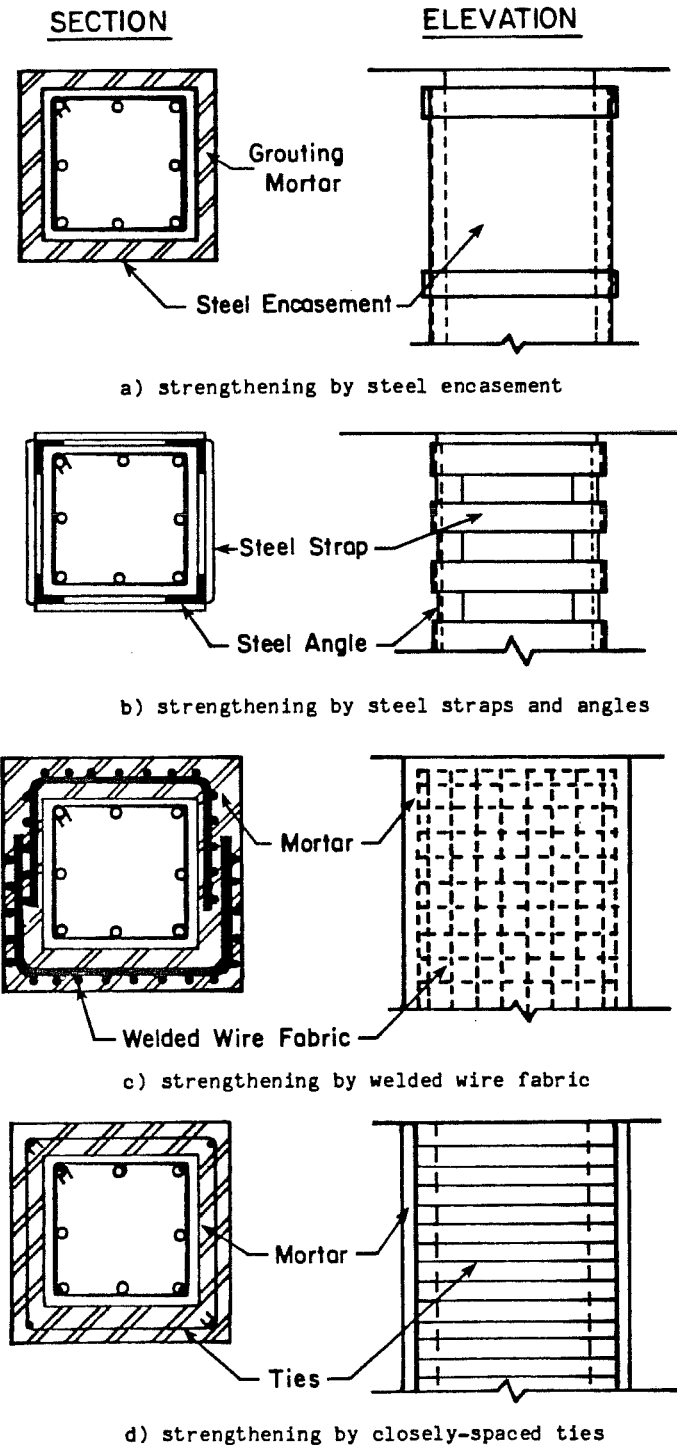


Fig. 1.4 Techniques to increase shear capacity [13].

Jacketing can increase the shear resistance of the column, but may adversely affect the building's seismic resistance: decreased (a/d) ratio and increased moment capacity make shear-dominated column failure more likely; increased column stiffness decreases the building's fundamental period and increases seismic-induced lateral forces. However, jacketing of the original column is still beneficial; 1) due to increased confinement, column shear performance is adequate even at lower (a/d) ratios; 2) judicious selection and placement of jacket longitudinal steel minimizes increases in column flexural capacity; and 3) increased column shear capacity offsets increases in seismic-induced lateral forces.

Retrofitting techniques can be evaluated experimentally in terms of strength and stiffness. The behavior of a column, initially tested, repaired and strengthened, and then retested, can be compared to the behavior of initially strengthened columns, and a correlation developed between retrofitting technique and performance.

C H A P T E R I I

EXPERIMENTAL PROGRAM

2.1 Introduction

The purpose of this study was to evaluate various repair and strengthening techniques for reinforced concrete short columns. Three test specimens were constructed using normal weight concrete and Gr. 60 reinforcement. One specimen was tested in its original form, repaired, strengthened, and retested. The remaining two specimens were strengthened prior to testing. The specimens were numbered sequentially (1-1, 1-2, 1-3) and the repaired specimen was designated by 1-1R. In each test, constant axial compression and numerous cycles of reversed lateral deformations were applied to the specimen. The primary objective of this test program was to study the effect of different strengthening or repair techniques on the strength and response characteristics of reinforced concrete short columns. In this chapter, the experimental program will be discussed. Much of the information is summarized in Table 2.1.

2.2 Overall Research Program

This investigation was part of a larger study of the behavior of reinforced concrete frame systems subjected to cyclic lateral deformations. The overall research program was devoted to evaluation of various repair and strengthening techniques for R/C frame elements. The study reported herein deals only with short columns.

TABLE 2.1 Test Program Summary

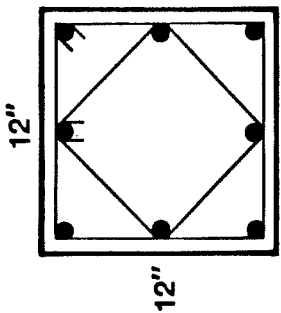
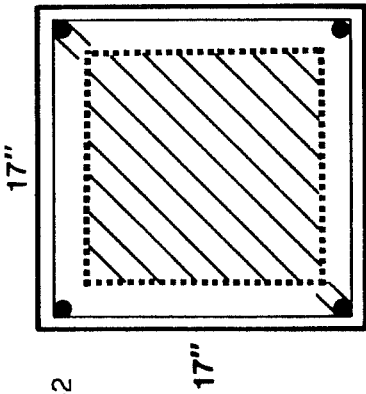
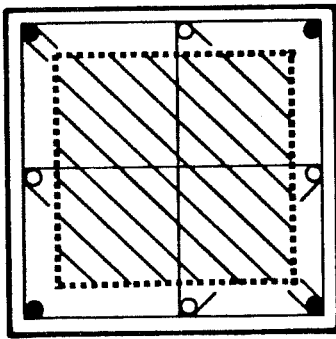
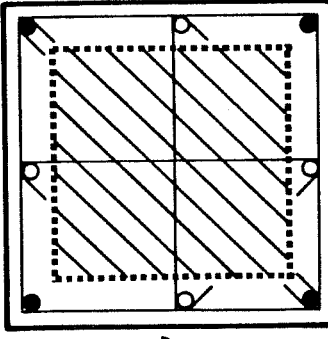
Test Specimen No.	Column Cross Section	Test Description
1 1-1	 <p>Long. steel: #6's Ties: 6mm @ 8" Identical 12" x 12" cores used for all specimens.</p>	<p><u>Description:</u> original specimen</p> <p><u>Test:</u> reversed unidirectional loading</p> <p><u>Deflection limit:</u> 2% drift</p>
2 1-2	 <p>Long. steel: #3's Ties: 6mm @ 2-1/2" 2-1/2" shotcrete shell</p>	<p><u>Description:</u> sandblast, add 4-#3 longitudinal bars and 6mm ties at 2-1/2". Shotcrete to 17" x 17".</p> <p><u>Test:</u> reversed unidirectional loading.</p> <p><u>Deflection limit:</u> 2.5% drift</p>

TABLE 2.1 Test Program Summary (continued)

Test Specimen No.	Column Cross Section	Test Description
3 1-3	 <p data-bbox="423 1481 446 1543">17"</p> <p data-bbox="619 1686 642 1737">17"</p> <p data-bbox="470 1052 501 1297">Long: #3's, #6's</p> <p data-bbox="540 991 564 1297">Ties: 6mm @ 2-1/2"</p> <p data-bbox="603 960 635 1297">Crossties: #3's @ 9"</p> <p data-bbox="666 950 697 1297">2-1/2" shotcrete shell</p>	<p data-bbox="470 265 627 827"><u>Description:</u> sandblast, add 4-#3 corner bars and 4-#6 midface bars. Anchor midface bars w/#3 crossties, secured with epoxy. 6mm ties @ 2-1/2". Shotcrete to 17" x 17".</p> <p data-bbox="666 337 729 827"><u>Test:</u> reversed unidirectional loading.</p> <p data-bbox="760 337 791 827"><u>Deflection limit:</u> 2.5% drift.</p>
4 1-1R	 <p data-bbox="862 1481 885 1543">17"</p> <p data-bbox="1058 1686 1081 1737">17"</p> <p data-bbox="893 1032 925 1297">Long: #3's, #6's</p> <p data-bbox="956 991 987 1297">Ties: 6mm @ 2-1/2"</p> <p data-bbox="1019 960 1050 1297">Crossties: #3's @ 9"</p> <p data-bbox="1089 950 1121 1297">2-1/2" shotcrete shell</p>	<p data-bbox="893 245 1081 827"><u>Description:</u> Remove all loose cover Add 4-#3 corner bars and 4-#6 midface bars. Anchor midface bars w/#3 crossties, secured with epoxy. 6mm ties @ 2-1/2". Shotcrete to 17" x 17".</p> <p data-bbox="1121 337 1183 827"><u>Test:</u> reversed unidirectional loading.</p> <p data-bbox="1215 337 1246 827"><u>Deflection limit:</u> 2.5% drift.</p>

The overall research program is distinguished from other repair and retrofitting investigations in two respects: first, it combines the capabilities of a university research laboratory and a structural engineering design firm. Repair and strengthening is a specialized area in which professional experience is extremely important. Design requirements for strengthening techniques and details are not as codified as requirements for original construction. Second, experiments were conducted using nearly full-scale specimens fabricated especially for studying repair and strengthening procedures, and not as an adjunct to a study with other primary objectives. The success of most repair techniques lies in the details utilized, and scale effects may be important.

2.3 Original Test Specimen 1-1

2.3.1 Design Requirements. The objective of the project was to study the behavior of a reinforced concrete column that would fail in shear if it were not strengthened. To avoid the cost of designing and constructing a new test frame, it was decided to use short column specimens of the same size as those studied in previous test programs [5,6,7,8,9]. The test specimen selected was a short column framing into enlarged end blocks, which provided both for attachment of the specimen to the test frame and for anchorage of the longitudinal column reinforcement.

The prototype short column was designed as an 18-in. (45.7 cm) square section meeting the column design provisions of ACI 318-63 [16], particularly Section 806 and Chapter 19. It was 4.5 ft (1.37 m) high,

and reinforced with eight #9 longitudinal bars ($P_g = 0.025$) and two sets of #3 ties at 12 in. Cover was 1-1/2 in. Transverse reinforcement spacing and details were selected as typical for structures designed for seismic regions of the U.S. during the late 1950's and early 1960's. Columns of such structures usually had transverse reinforcement which would be insufficient by current standards, resulting in shear-dominated behavior under severe lateral loads.

Column loads in the structures mentioned above vary widely. Based on actual load data [14], typical compressive stresses ranged from about 350 psi to 550 psi, with an average of about 450 psi. The axial load required to develop an average compressive stress of 450 psi on the prototype 18-in. square column is about 146 kips.

To reduce fabrication and testing costs, yet permit the use of commercially available deformed reinforcement, the test specimens were constructed to two-thirds scale. Analyses indicated that the previously used connection details between the frame and a strengthened specimen would be inadequate. Those details were subsequently modified as described in Chapter III.

2.3.2 Details of Specimen. Details of the original test specimen are shown in Fig. 2.1. The two-thirds scale model was a 12-in. (30.5 cm) square section, 3.0 ft (0.92 m) in height, containing eight #6 longitudinal bars, sets of special 6 mm deformed ties at 8 in., and 1 in. cover.

2.3.3 Calculated Strengths. The test specimen's theoretical moment and shear capacities were calculated using the computer program

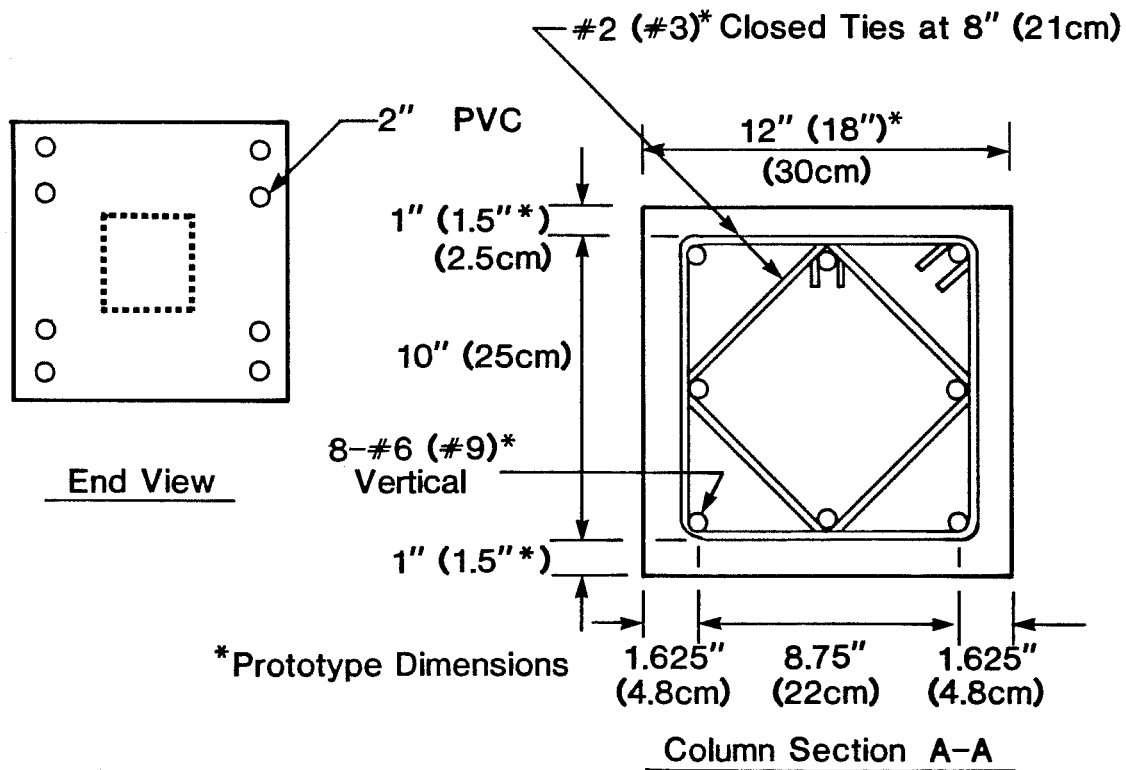
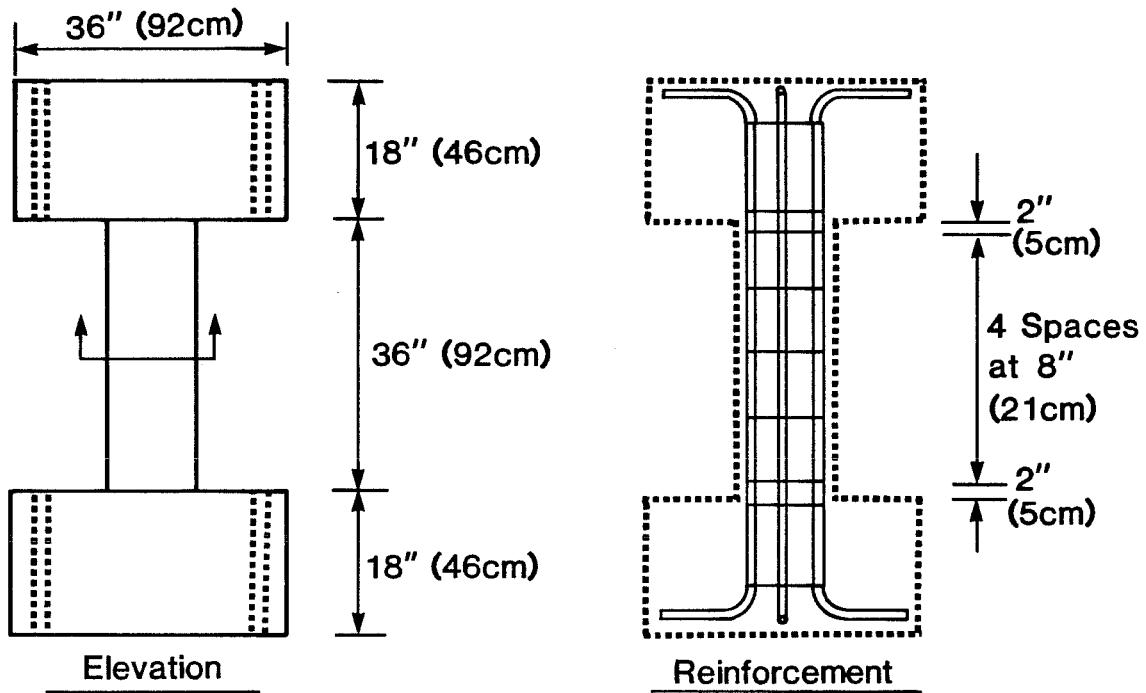


Fig. 2.1 Details of original specimen.

RCCOLA, developed for inelastic flexural analysis of reinforced concrete sections [15]. Although moment capacity can be estimated fairly accurately, shear capacity is more difficult to predict. The program used an empirical relationship (2.1) based on University of Texas short column test results [23].

$$V_{nr} = \left(11 - 3 \frac{a}{d^*} \right) A_c \sqrt{f'_c} + \frac{0.2 N}{\frac{a}{d^*}} \quad (2.1)$$

$$\frac{0.2 N}{\frac{a}{d^*}} \leq \frac{160 A_g}{\frac{a}{d^*}}$$

$$1 \leq \frac{a}{d^*} \leq 2.5$$

Using the above shear resistance, and the statical relations between shear and moments in a column subjected to sidesway (Fig. 1.2), a diagram of moment capacity as governed by shear was produced (Fig. 2.2). Capacities are shown for both the initial (entire) and confined cross sections. The shear capacity plot indicates the level of end moment required to generate the column's shear capacity at any axial load. Inspection of Fig. 2.2 reveals that the shear capacity curve becomes vertical for large axial loads. This conservative limit was due to the absence of test results for large axial loads. Neglecting the beneficial effects of axial compressive load on a column's shear capacity may be appropriate in the analysis of columns subjected to earthquakes. It is entirely possible that during a severe seismic event, the effect

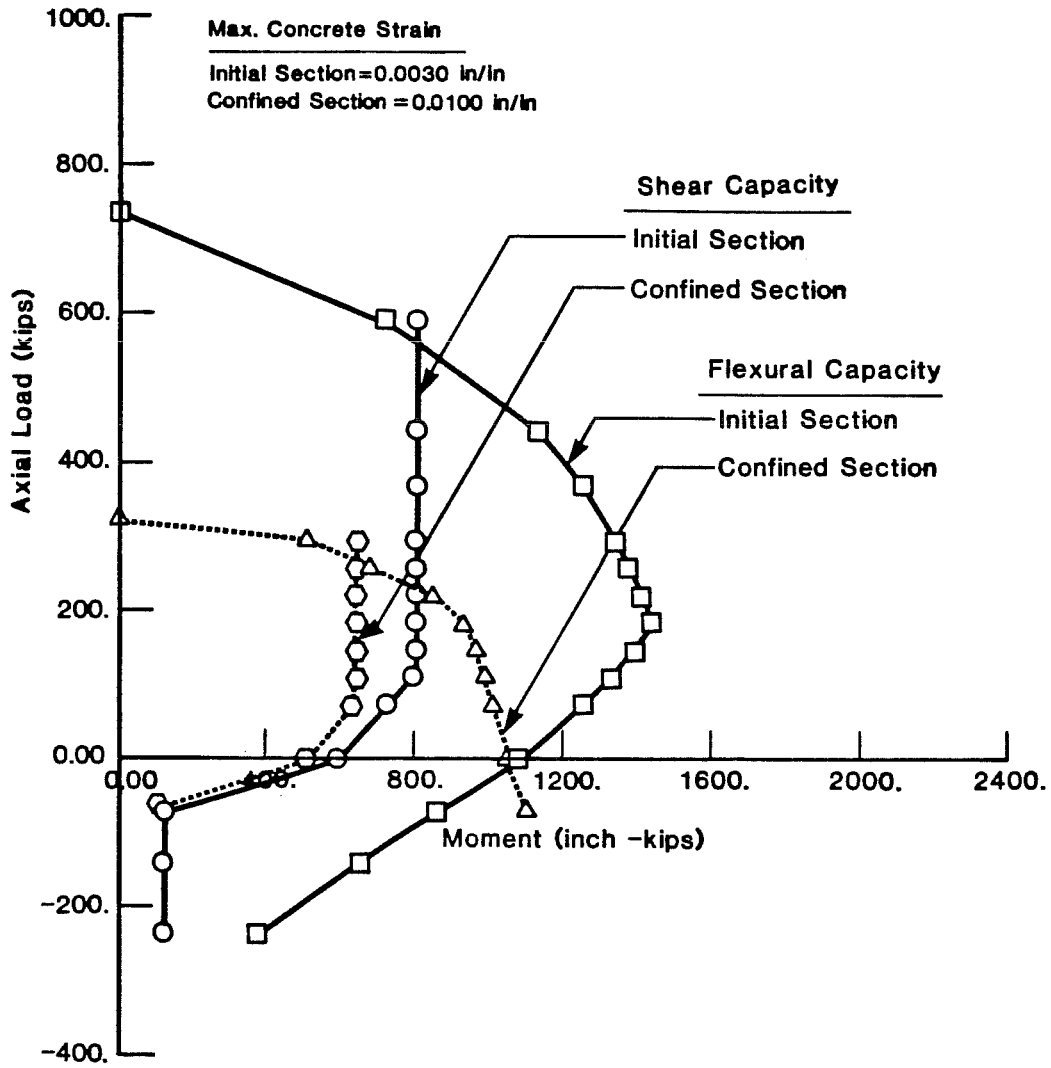


Fig. 2.2 Shear capacity-interaction diagram (original specimen).

of overturning or vertical accelerations may reduce the level of axial compression significantly. Considering a 12-in. square column subjected to 450 psi compression (64.8 kips), the predicted end moment corresponding to flexural failure of the initial section is about 1150 in.-kips, and that corresponding to shear failure about 720 in.-kips. Based on the analytical model of Fig. 1.2, the corresponding lateral capacities are 64 kips (flexure) and 40 kips (shear). The original column could therefore be expected to fail in shear.

2.3.4 Specimen Fabrication. Dimensions of the end block were based on the requirements for attaching the test specimen to the test frame and for anchoring the longitudinal column reinforcement. Details of the end block reinforcement are shown in Fig. 2.3.

To simplify formwork, specimens were cast in two stages. First, the bottom end block was cast with the column and top block formwork already in place. Four days later the column and top end block were cast. This casting sequence produced a cold joint at the bottom of the column, and is similar to that used in reinforced concrete buildings. Figure 2.4 illustrates the specimen formwork.

2.4 Material Characteristics of Original Test Specimen

2.4.1 Concrete. Ready-mixed concrete was obtained from a local supplier, with the following mix proportions:

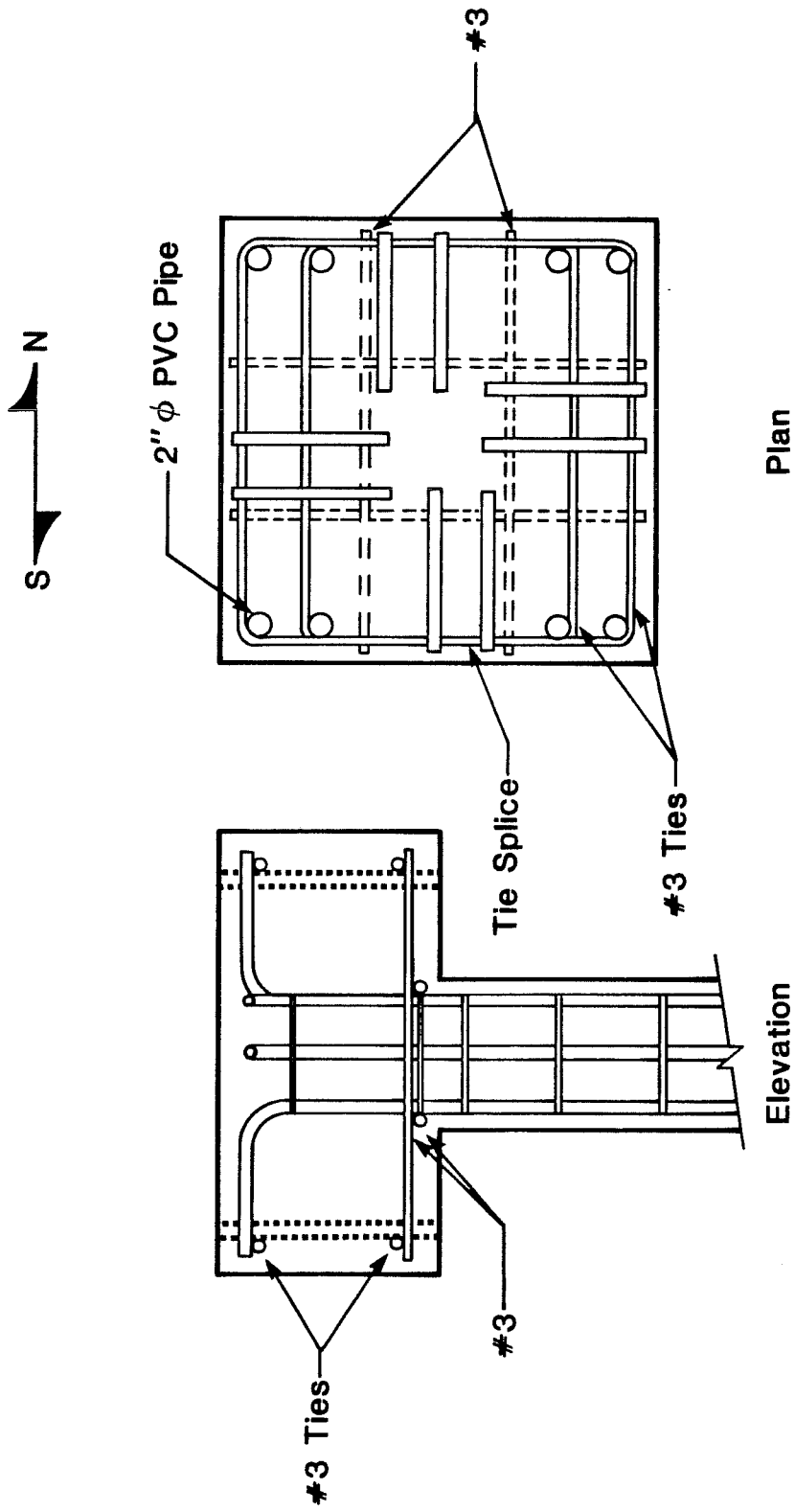


Fig. 2.3 Details of end block reinforcement.

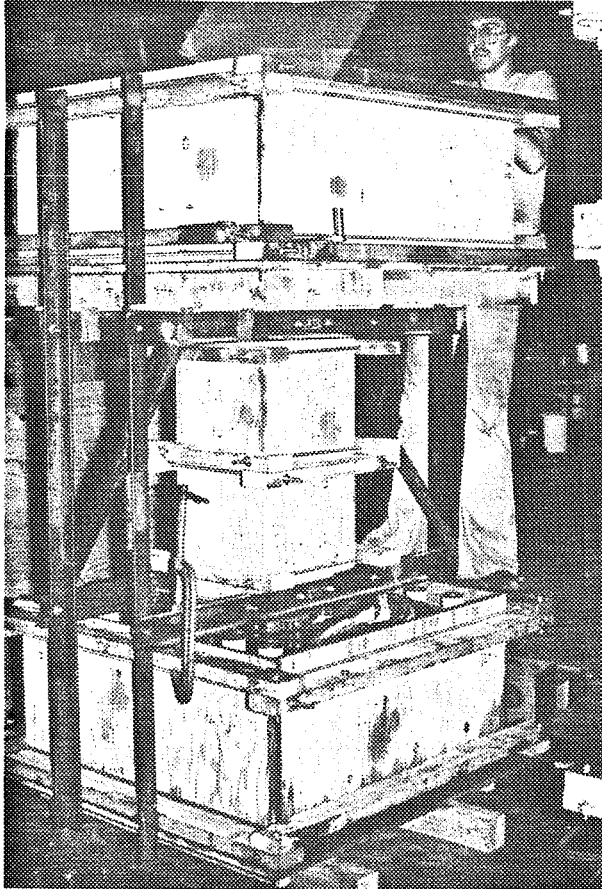


Fig. 2.4 Construction of formwork.

Concrete Mix Design (4000 psi)Proportions of 1 yd³

Water	210 lb
Cement (5 sacks)	470 lb
Fine aggregate	1530 lb
Coarse aggregate (5/8 in.)	1830 lb
Trisene L (retarding admixture)	15 oz

(w/c = 0.45 by weight)

The aggregate was Colorado River sand and gravel. Because of congestion of reinforcement, a relatively high slump was necessary to ensure proper placement of concrete. The concrete was ordered with a slump less than the desired 7 in., and water was added on site to achieve the required slump. Twelve control cylinders were cast and cured with the specimens. All three specimens were cast in the same operation, and moist-cured under polyethylene sheets for seven days prior to stripping the forms.

Three control cylinders were capped and tested at 28 days, and at the conclusion of the first, second, and fourth tests. Table 2.2 summarizes the results of the cylinder tests.

2.4.2 Reinforcement. Number 6 deformed reinforcement (ASTM A-615 Gr. 60) was used for the longitudinal steel, and 6 mm deformed reinforcement for the transverse steel. The 6 mm deformed bars were

fabricated in Sweden and obtained through the Portland Cement Association Laboratories. Mechanical characteristics of reinforcement are shown in Table 2.3, and typical stress-strain curves in Fig. 2.5.

2.5 Strengthened and Repaired Specimens

2.5.1 Strengthening Technique (Specimens 1-2, 1-3).

Strengthening involved encasing the original column with a shotcrete jacket reinforced with closely-spaced transverse steel. Additional longitudinal steel was placed at each corner of the jacket to support the transverse steel. Details of the strengthening technique for each specimen will be described in subsequent sections.

2.5.2 Repair Technique (Specimen 1-1R). The repair technique consisted of two operations. First, all loose cover was removed with a chipping hammer, exposing the longitudinal steel. Holes were then drilled through the columns, and crossties used to anchor additional longitudinal steel were inserted and cemented with epoxy. Second, closely-spaced ties were placed around the column core, and it was encased with shotcrete. Details of the repair technique will be shown later.

2.6 Strengthened Specimen 1-2

2.6.1 Details. The strengthening technique used for Specimen 1-2 consisted of a shotcrete jacket reinforced as shown in Fig. 2.6.

2.6.2 Calculated Strengths. Theoretical moment and shear capacities, calculated as described previously [15], are shown in Fig. 2.7. Inspection of Fig. 2.7 reveals that for a 64.8 kip (224 psi) axial

TABLE 2.2 Original Specimen Concrete Strength

	Age (days)	Cylinder Compressive Strength (psi)	Average (psi)
	28	3961 3784 3749	3831
Test 1-1	57	4333 4386 4280	4333
Test 1-2	147	4350 4403 4445	4399
Test 1-1R	204	4792 4421 4669	4627

TABLE 2.3 Steel Properties (Original Specimen)

Bar Size	f_y (ksi)	E (ksi)	ϵ_{STH}	E_{sth} (ksi)	f_u (ksi)	ϵ_u
#6	67	25463	0.0079	1344	112	0.1445
6mm	60*	26625	0.00265	870	88	0.0975

* 0.2% offset

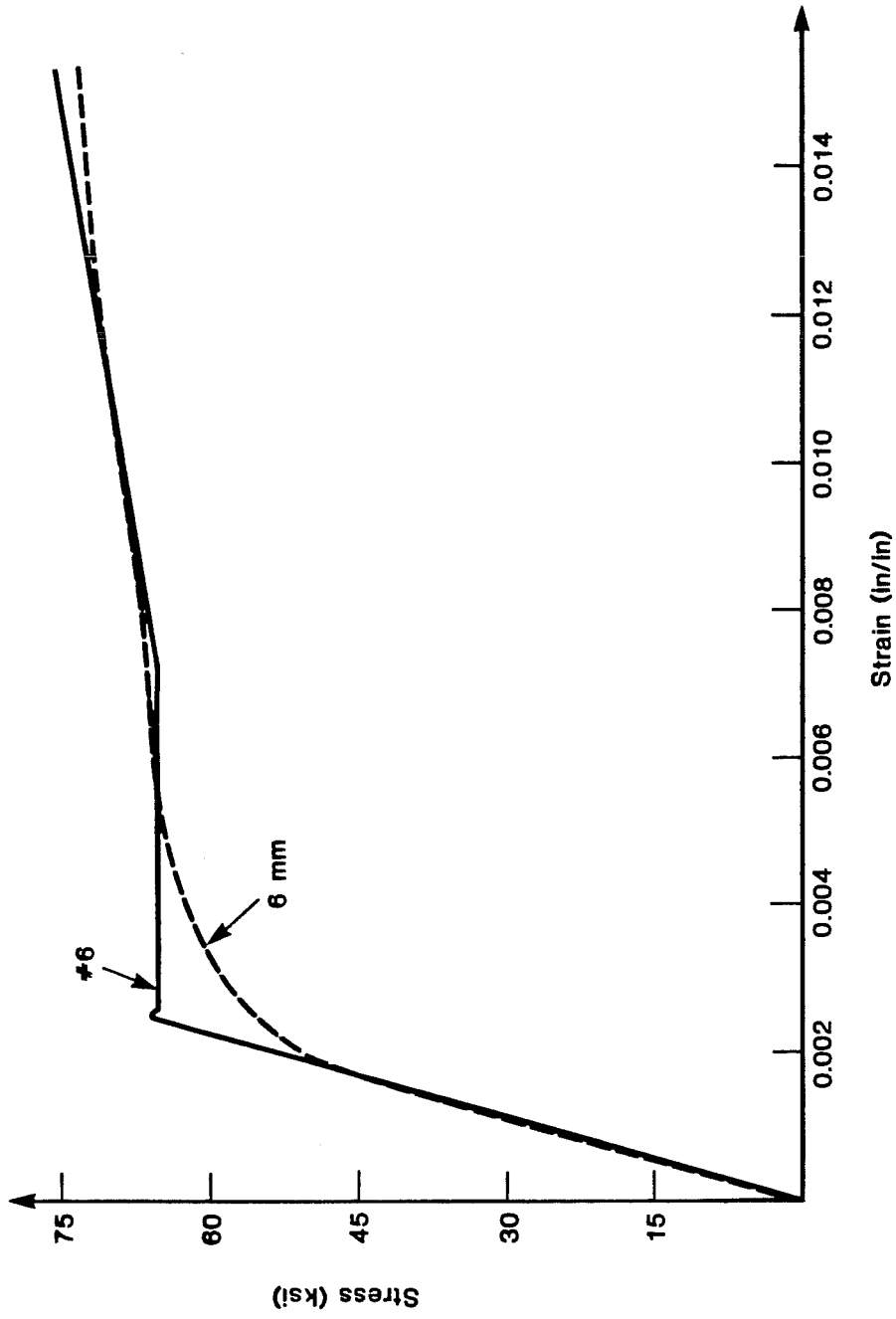


Fig. 2.5 Stress-strain curve for original specimen steel reinforcement.

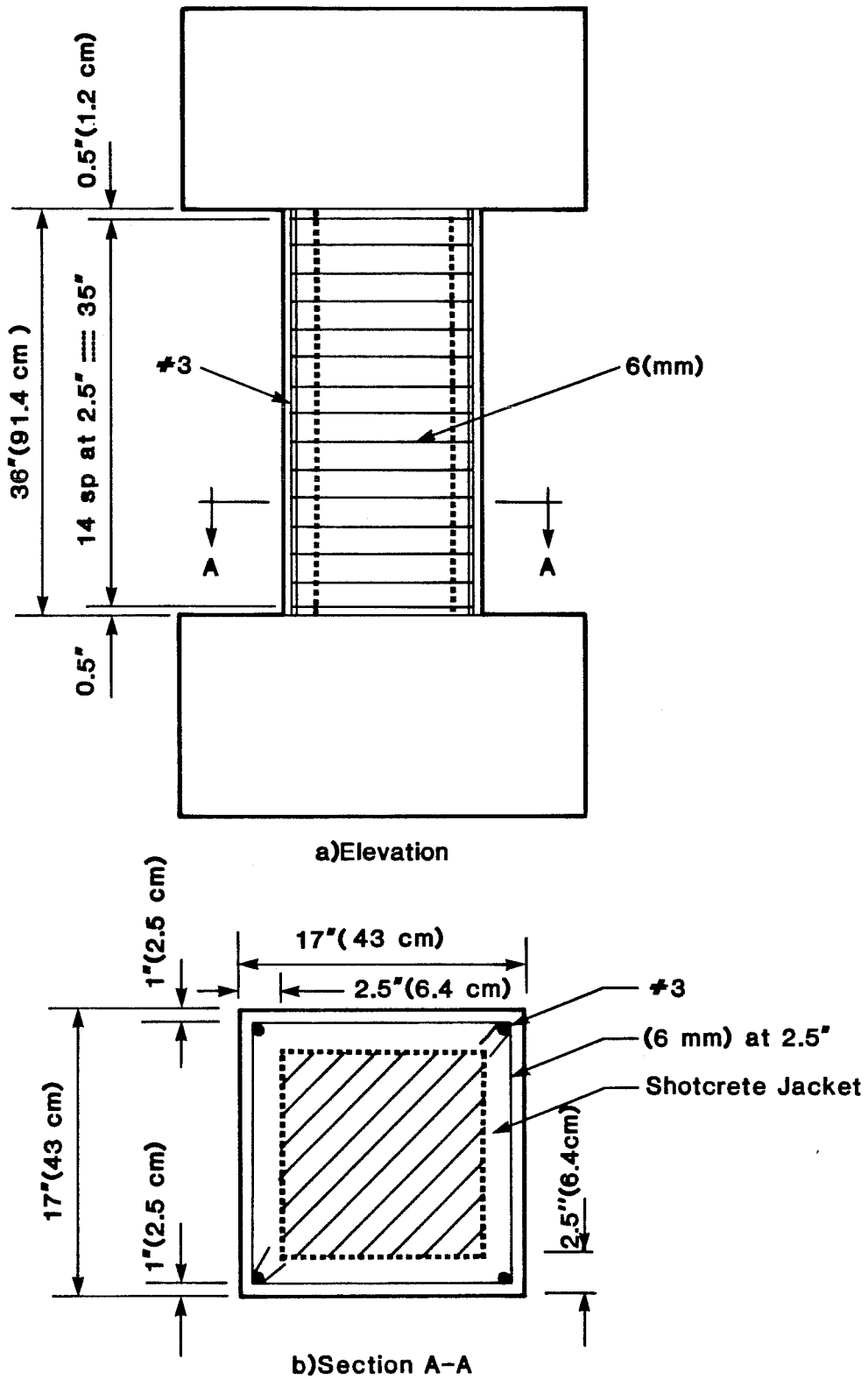


Fig. 2.6 Details of Specimen 1-2.

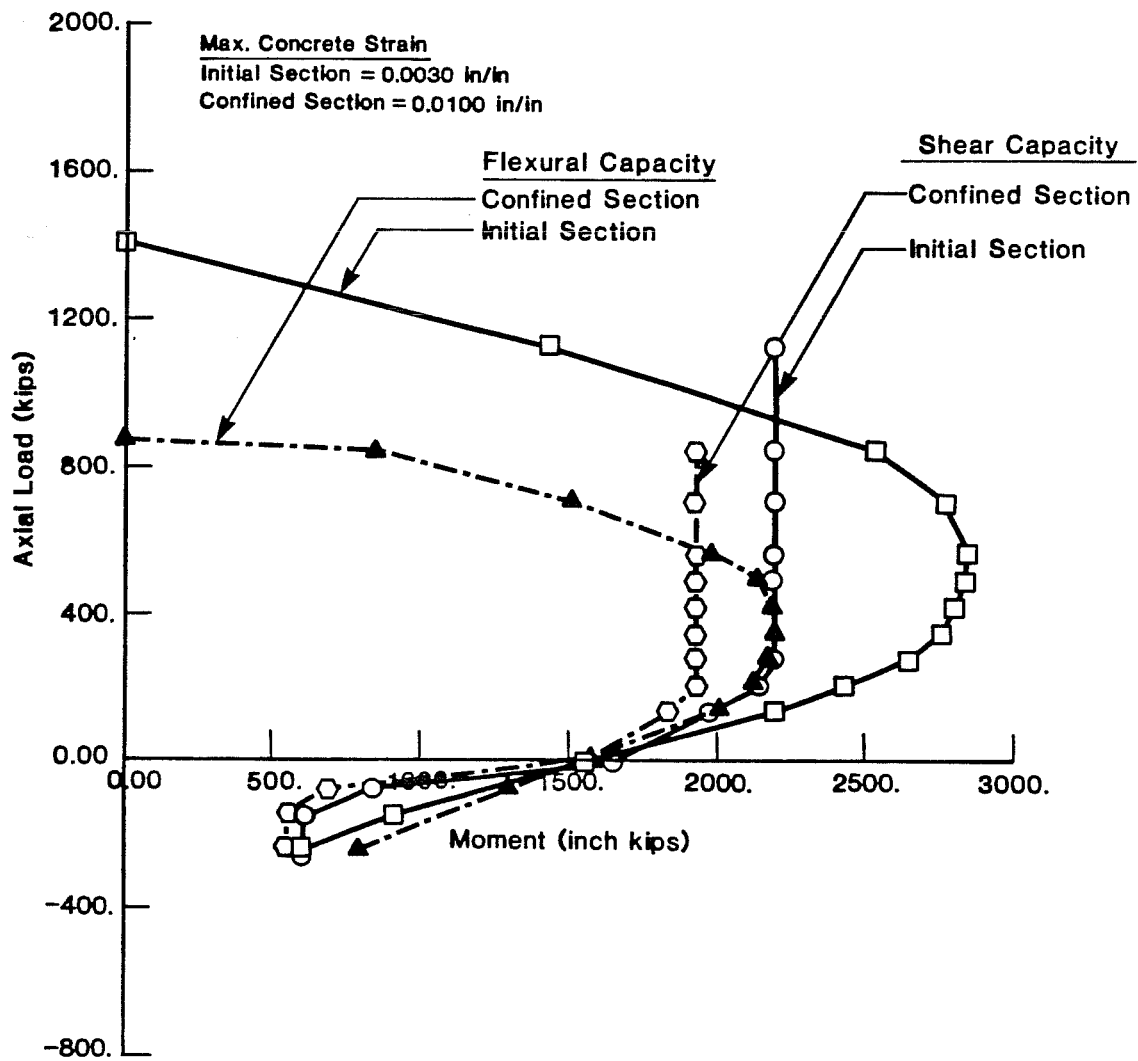


Fig. 2.7 Shear capacity-interaction diagram (Specimens 1-2, 1-3).

load, the end moment corresponding to flexural capacity is about 1800 in.-kips, and that corresponding to shear capacity is about 1650 in.-kips. The corresponding lateral capacities are 104 kips (flexure) and 100 kips (shear). The strengthened specimens could therefore be expected to fail by combined shear and flexure.

2.7 Strengthened Specimen 1-3

2.7.1 Details. The strengthening technique used for Specimen 1-3, shown in Fig. 2.8, consisted of the same basic reinforced shotcrete jacket, plus #6 longitudinal bars at each midface. Holes were drilled through the column, and #3 crossties, secured with epoxy, anchored opposite face longitudinal bars. Holes were 1/4 in. oversize and were cleaned using a tight-fitting bottle brush. One end of each crosstie was field-bent around the midface bar before the epoxy had set.

2.7.2 Calculated Strengths. Neglecting the contribution of the crossties, theoretical moment and shear capacities are identical to those of Specimen 1-2 (Fig. 2.7) [15].

2.8 Repair of Specimen 1-1

Following the first test, Specimen 1-1 was removed from the test frame for repair and strengthening. After removing all loose cover (Figs. 2.9, 2.10), jacket reinforcement (Fig. 2.8) was constructed identical to that used for Specimen 1-3, as shown in Fig. 2.11. Cross-ties through the cracked column core were secured by epoxy (Fig. 2.12), and a shotcrete jacket was added to increase the column size to 17 by 17 in.

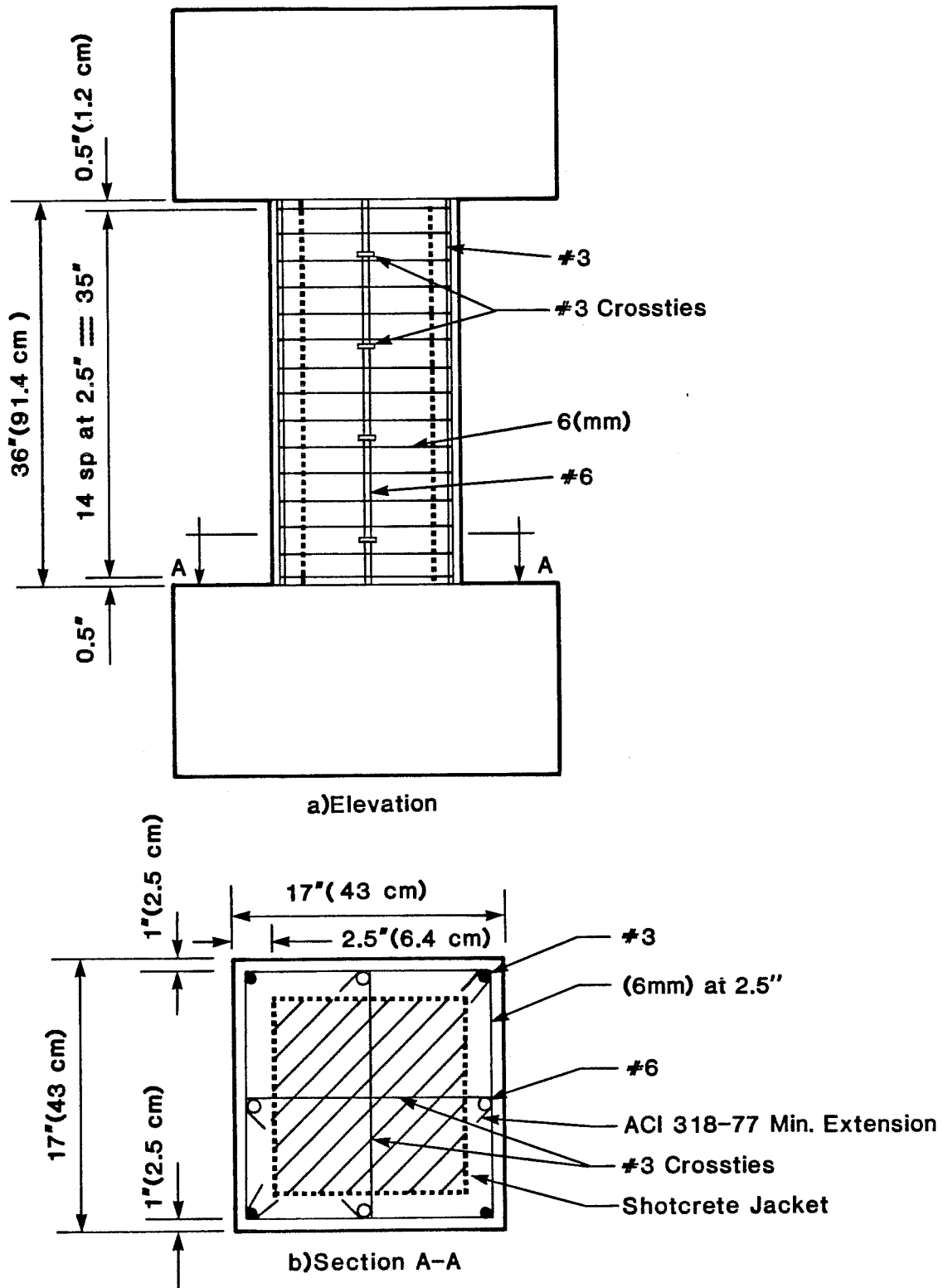


Fig. 2.8 Details of Specimen 1-3.

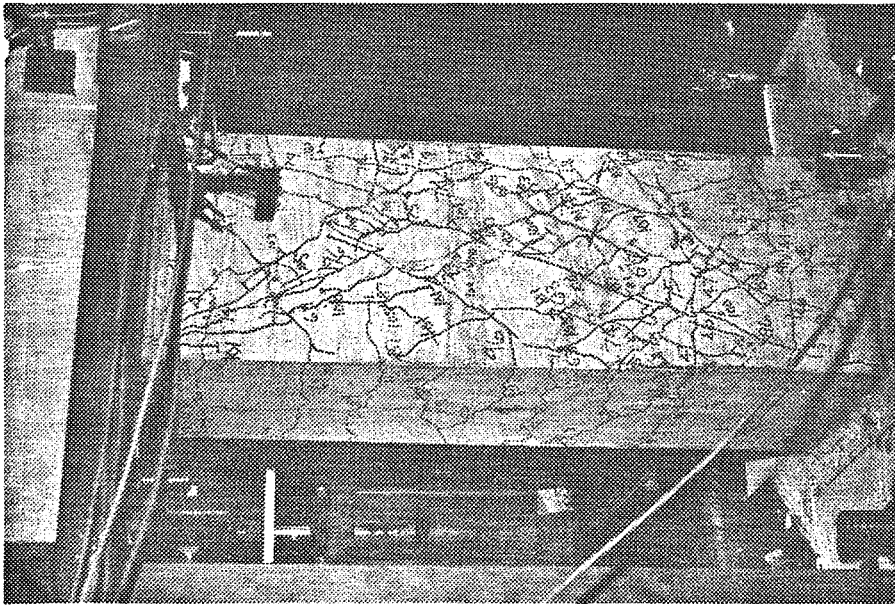


Fig. 2.9 Post-test, Specimen 1-1.

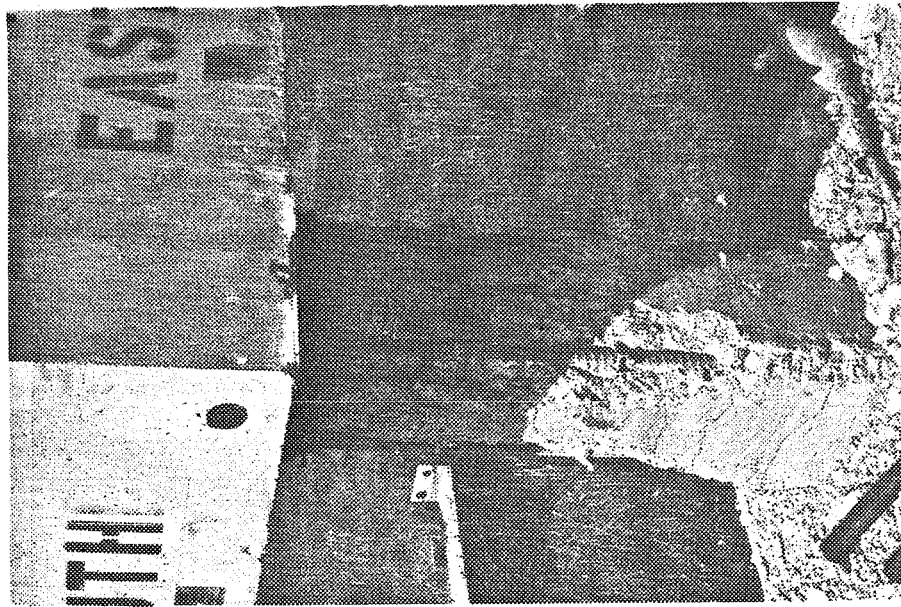


Fig. 2.10 Loose cover removed, Specimen 1-1.

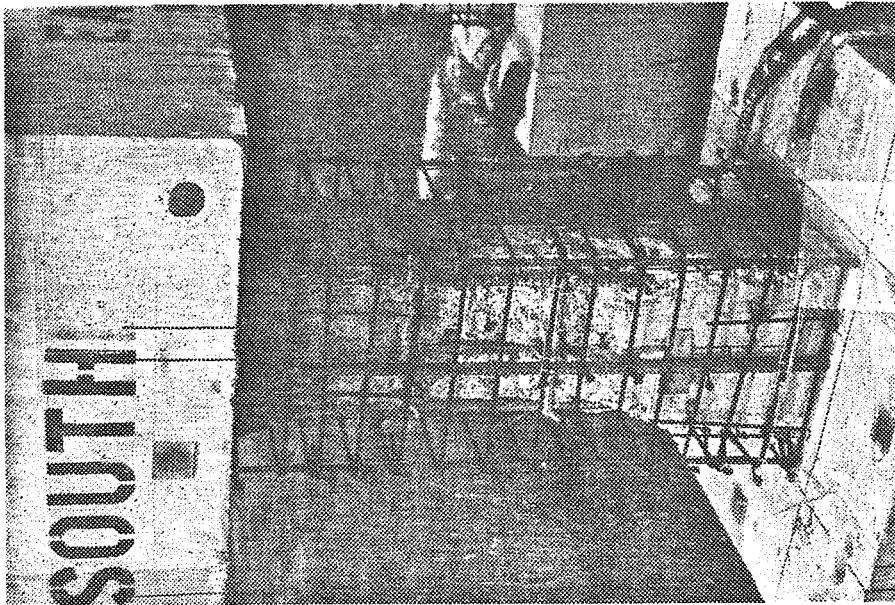
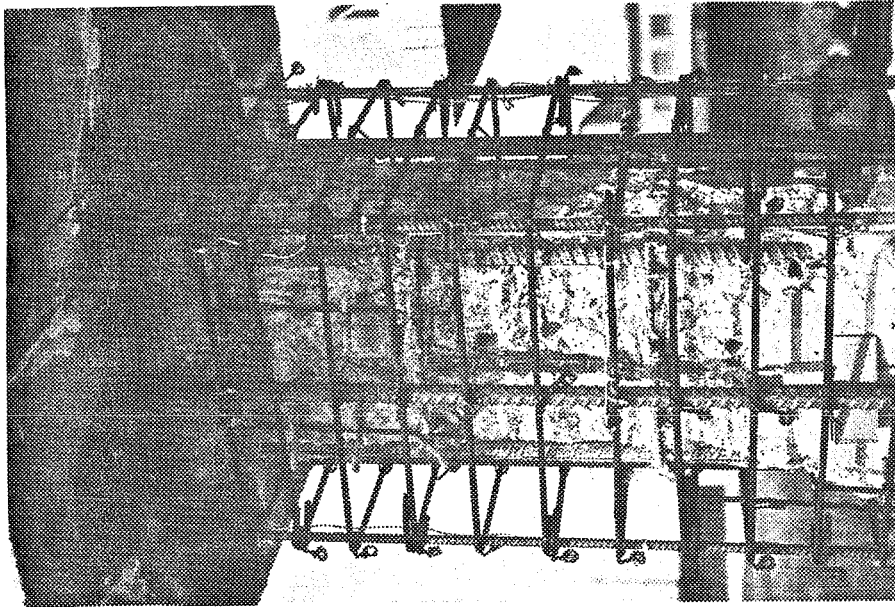


Fig. 2.11 Jacket reinforcement, Specimen 1-1.

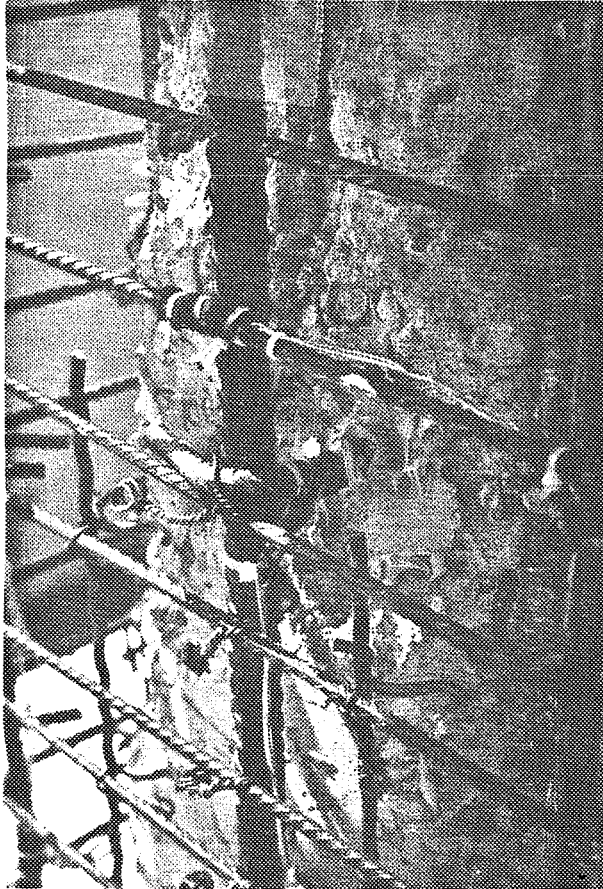


Fig. 2.12 Crossties secured by epoxy, Specimen 1-1.

2.9 Fabrication of Strengthened Specimens

Fabrication of strengthened specimens consisted of tying the jacket reinforcement cages and then shotcreting. Specimens were roughened by light sandblasting using a No. 6 venturi nozzle and a fine sand (No. 6). As shown in Fig. 2.13, wooden screed guides were attached to each specimen's end blocks using ramset nails. Shotcrete quality was monitored using two vertical test panels (36 x 18 x 3 in.), shown in Fig. 2.14. One of the panels had a wood back while the other had a concrete back. The two types of materials were used to determine if shotcrete test panel rebound characteristics different from the actual column applications might alter quality control information. Half of each panel was reinforced identically to the jacket of Specimen 1-3, without crossties. Two sizes of core samples were to be taken from each panel. Large cores (4 x 3 in.) from the reinforced side of each panel were used to monitor void formation behind individual bars. Small cores (1-3/4 x 3 in.) from the unreinforced side were used for compressive strength tests. An experienced contractor shotcreted and float-finished (Figs. 2.15, 2.16) the specimens and panels, both of which were cured under polyethylene sheets for seven days. When the specimens were shotcreted, concrete temperature, slump, unit weight, and air content were measured. Two sets of control cylinders were cast; one set was taken using concrete directly from the ready-mix truck, the other set was taken using shotcrete placed in a wheelbarrow by the nozzle.

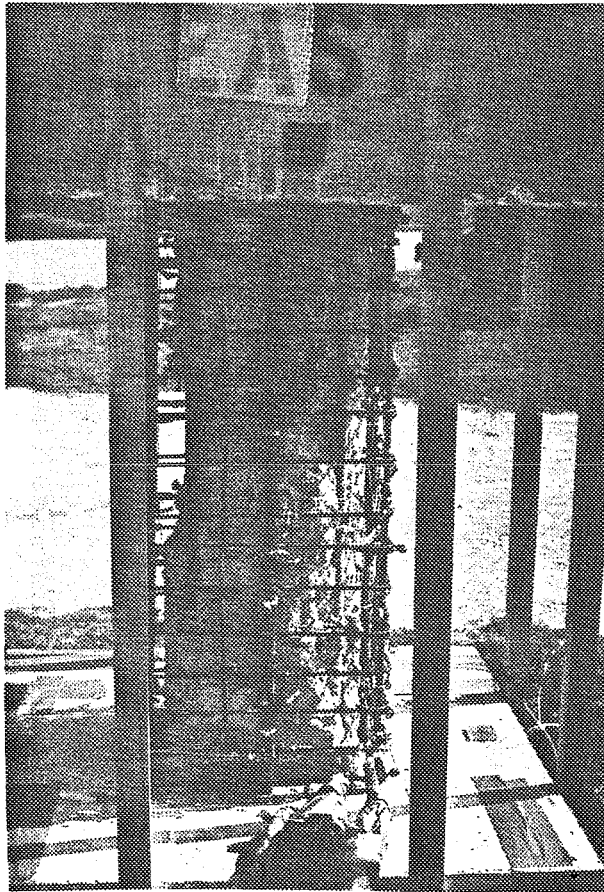


Fig. 2.13 Screed guides.

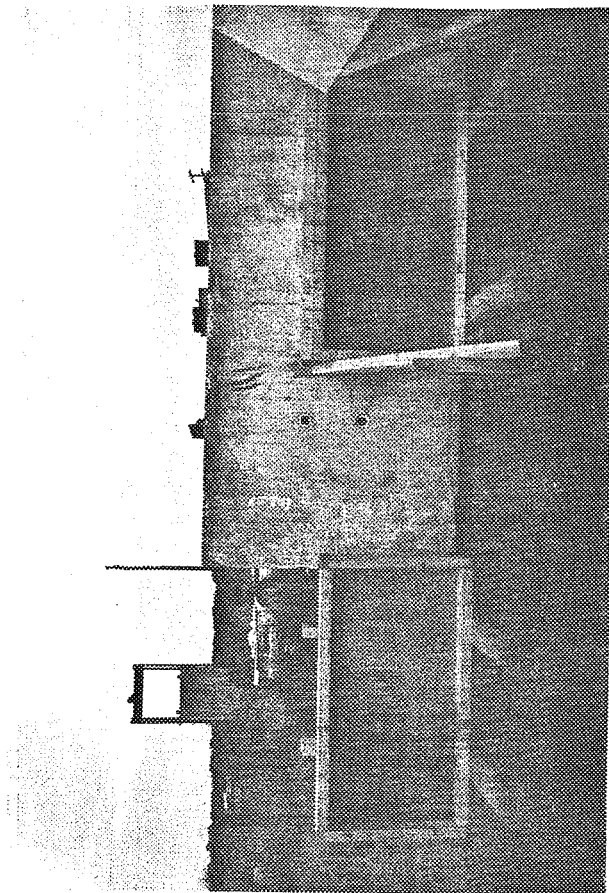


Fig. 2.14 Shotcrete test panels.

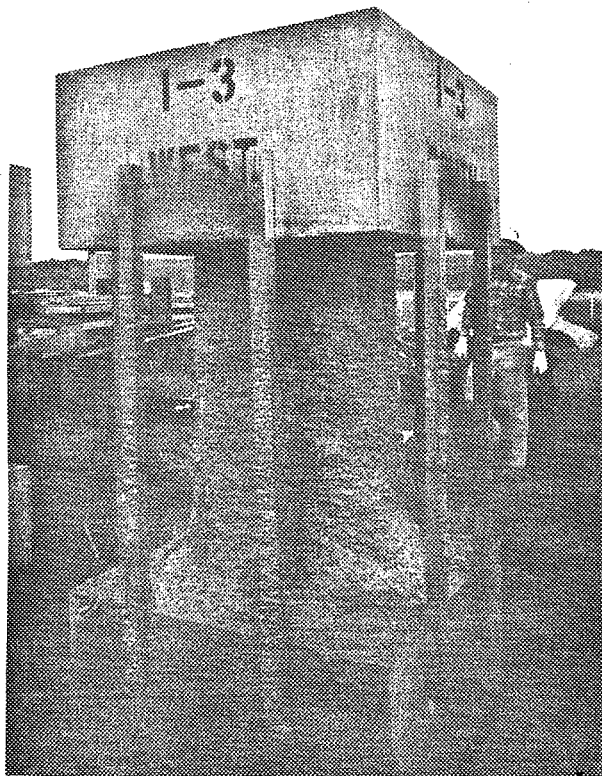


Fig. 2.15 Shotcreting.

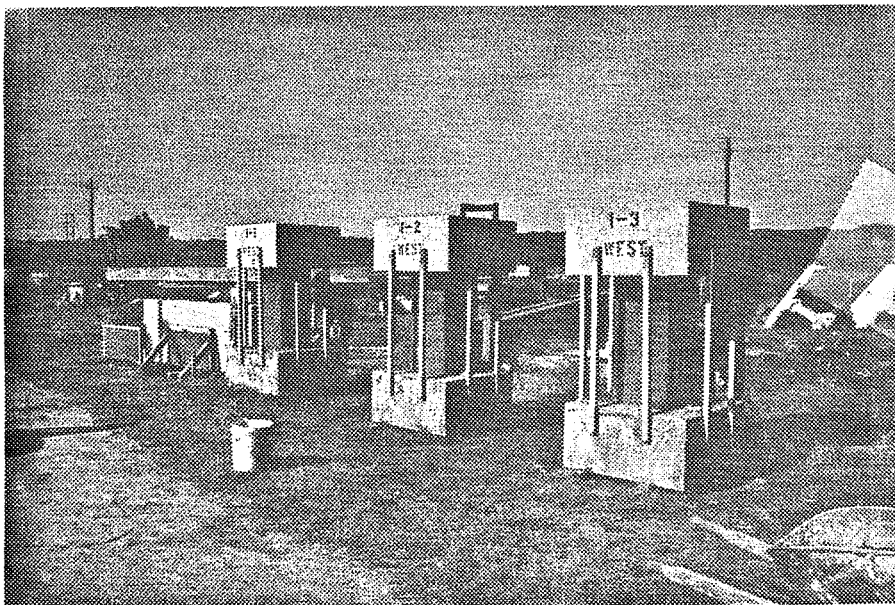
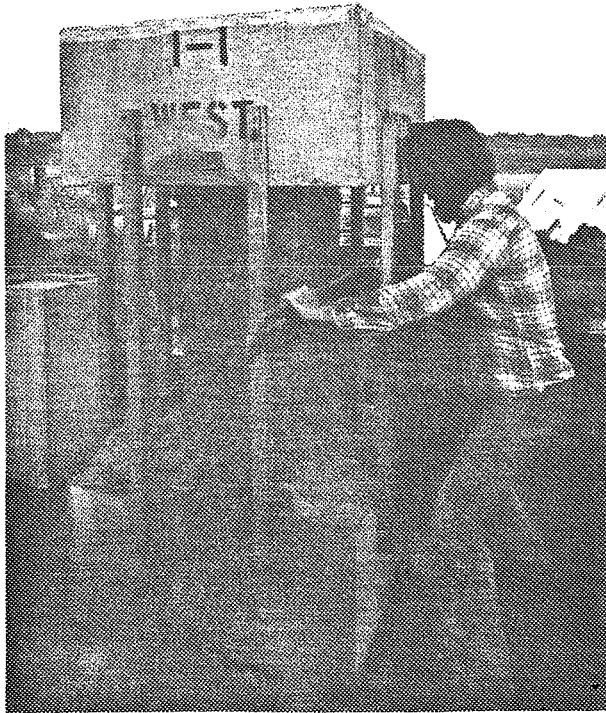


Fig. 2.16 Shotcreting.

2.10 Material Characteristics of Strengthened Specimens

2.10.1 Shotcrete. Ready-mixed concrete was obtained from a local supplier for the shotcrete. Mix proportions for the shotcrete [18] were as follows:

Shotcrete Mix Design (4000 psi)

Proportions for 1 yd³

Water	250 lb
Cement	658 lb
Fine Aggregate	2100 lb
Coarse Aggregate (3/8 in.)	750 lb
Sol Air (3% air entrainment)	10 oz
CCC 494 (water reducing agent)	21 oz

(w/c = 0.38 by weight)

The aggregate was Colorado River sand and gravel. To facilitate pumping, a small quantity of pumping agent [20] was added on site. Table 2.4 summarizes the shotcrete properties.

TABLE 2.4 Shotcrete Properties

Slump (in.) (from truck)	5-1/2
Unit Weight (lbs/ft ³) (from truck)	130
Air Content (%) (from truck)	4-1/2
Air Content (%) (from nozzle)	4

Four-inch cores (Figs. 2.17, 2.18) were taken from both the concrete-backed panel (CB) and the wood-backed panel (WB) to determine if voids were present behind the reinforcing. A single small void (1/4 x 1/4 in.) was found in one (CB) of the six samples. There was virtually no difference between the wood or concrete-backed panel samples. Smaller cores (1-3/4 x 3 in.) were taken from both panels, capped and tested in compression, with the results shown in Table 2.5.

2.10.2 Reinforcement. Jacket reinforcement consisted of #6 longitudinal bars at column midfaces, #3 crossties and longitudinal bars at corners, and 6 mm deformed ties. All U.S. sizes conformed to ASTM A-615, Gr. 60. Data on the #6 and 6 mm bars were provided in Section 2.4.2. Samples of the #3 bars were tested to obtain the averaged steel properties shown in Table 2.6, and the typical stress-strain curve of Fig. 2.19.



Fig. 2.17 Panel (top) core samples.

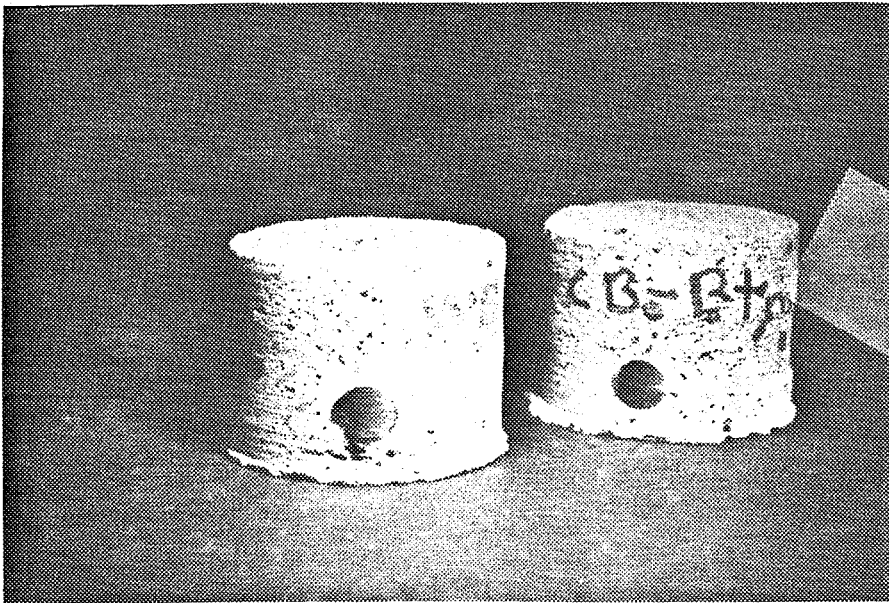


Fig. 2.18 Panel (bottom) core samples.

TABLE 2.5 Shotcrete Strengths

	Age (days)	f'_c (psi)	Average f'_c (psi)
From ready-mix truck	28	4562	4692
	28	4704	
	28	4810	
From nozzle	28	5093	5152
	28	5270	
	28	5093	
Concrete-backed panel	107	3651	3037
	107	3143	
	107	2295	
	107	3343	
	107	2753	
Wood-backed panel	107	4058	2905
	107	2528	
	107	3193	
	107	2844	
	107	1904	

TABLE 2.6 Steel Properties (Jacket #3 Long.)

Bar Size	f_y (ksi)	E (ksi)	ϵ_{STH}	E_{sth} (ksi)	f_u (ksi)	ϵ_u
#3	75	26923	0.010	1182	114	0.117

2.10.3 Epoxy. Crossties (#3's) were anchored to the original column using Concrete 1411, a two-component paste epoxy bonding agent produced by Adhesive Engineering [19]. Minimum mechanical properties are summarized in Table 2.7.

2.11 Loading History

2.11.1 Axial and Lateral Loading. Axial compression was maintained at 64.8 kips for all tests, and was based on typical column load data [14]. The corresponding compressive stress was 450 psi for the 12- x 12-in. column (Test 1), and 224 psi for the 17- x 17 in. columns (Tests 2, 3, and 4).

The lateral loading history (Fig. 2.20) was displacement controlled. Specimen 1-1 was limited to 2 percent drift, while Specimens 1-2, 1-3, and 1-1R had maximum drifts of 2.5 percent. Each test consisted of two cycles at low load levels for system checkout, followed by sets of three cycles at increasing displacement levels. Drift was increased in increments of 0.5 percent.

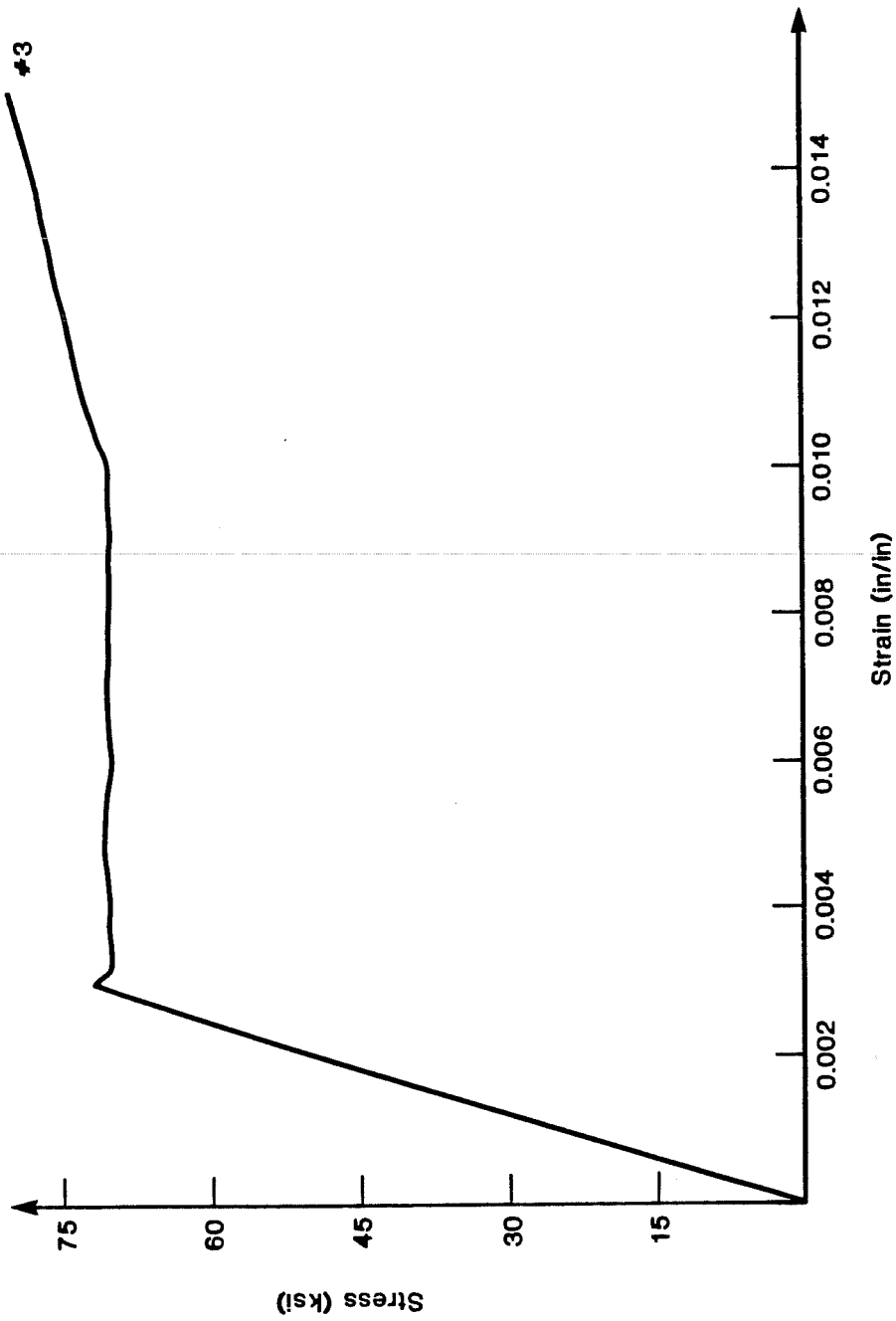


Fig. 2.19 Stress-strain curve for jacket steel (#3).

TABLE 2.7 Concrete 1411 Mechanical Properties

Tensile Strength (psi)	1500
Elongation at Break (%) (ASTM D638)	4
Compressive Yield Strength (psi)	8000
Compressive Modulus (psi) (ASTM D695)	4.0×10^5
Heat Deflection Temperature (°F) (ASTM D648)	105
Slant Shear Strength (psi)	75000
Damp to Damp Concrete (AASHTO T-237)	100% concrete failure

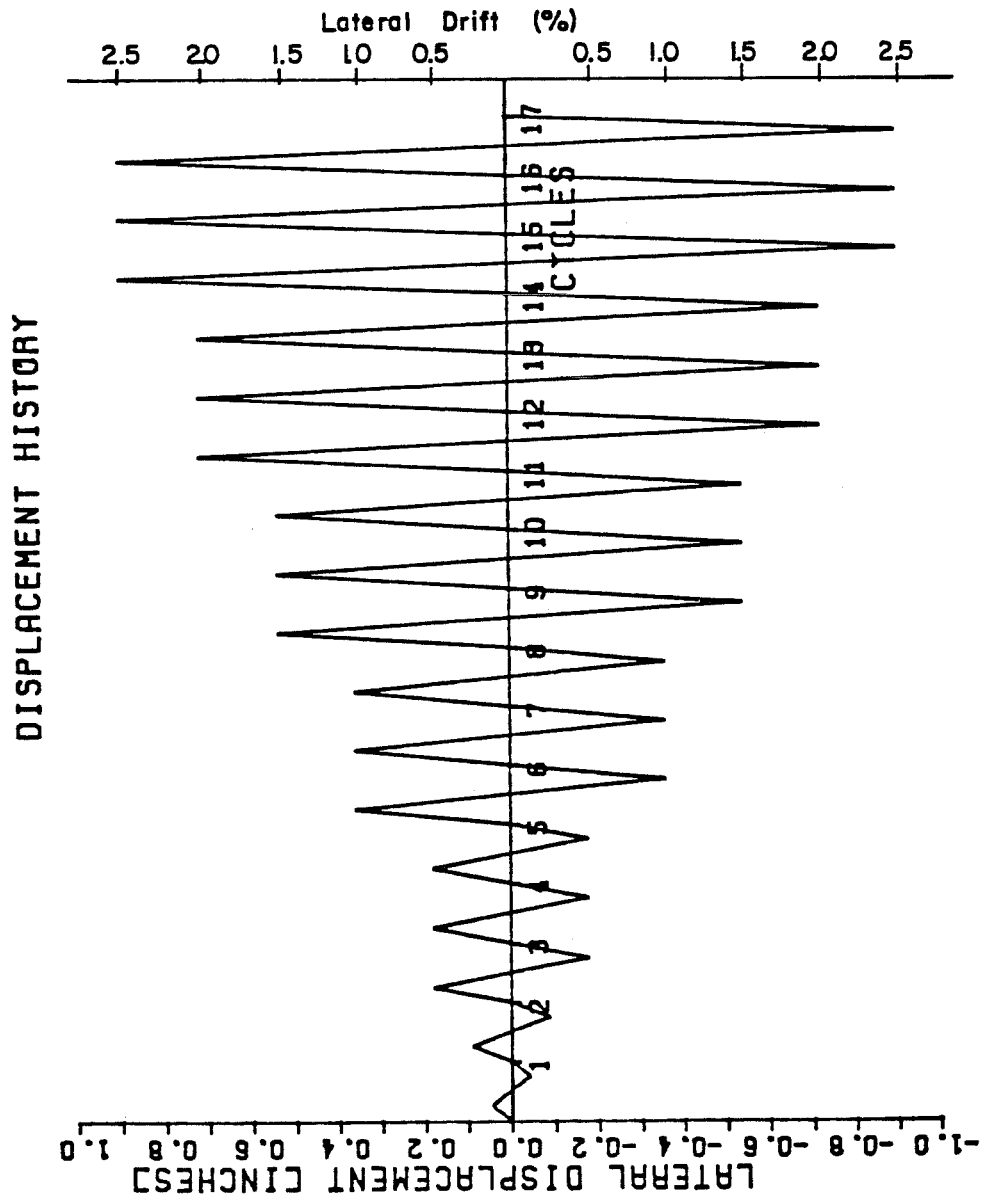


Fig. 2.20 Lateral displacement history.

C H A P T E R I I I

LOADING SYSTEM AND INSTRUMENTATION

3.1 Loading System

The objectives of this research program required a loading system capable of loading the specimen laterally while applying an axial load as shown in Fig. 3.1. The loading system utilized the reinforced concrete floor-wall reaction system of Fig. 3.2 [5].

The loading system consists of three independent components: 1) a mechanically-controlled hydraulic system for controlling the axial load; 2) a closed-loop, servo-controlled hydraulic system for controlling the lateral load; and 3) cross-coupled hydraulic rams for restraining the end blocks from rotating during loading.

The axial loading system was made up of a 300-kip static capacity ram connecting the specimen's upper loading head with the vertical reaction frame. Axial loads were adjusted manually using an Edison load maintainer [21] while monitoring load cell readings. The lateral loading system was composed of two rams, an accumulator, servo-controller, and a central pump. Each ram has a tensile static capacity of 113 kips with a piston stroke of 12 in. Because preliminary analyses [15] indicated that a strengthened specimen would have a lateral capacity in excess of 100 kips, the existing test frame was modified to accommodate two rams mounted one above the other, a brace to limit east-west lateral displacement, and a stronger specimen hold-down bolt pattern (Fig. 3.3).

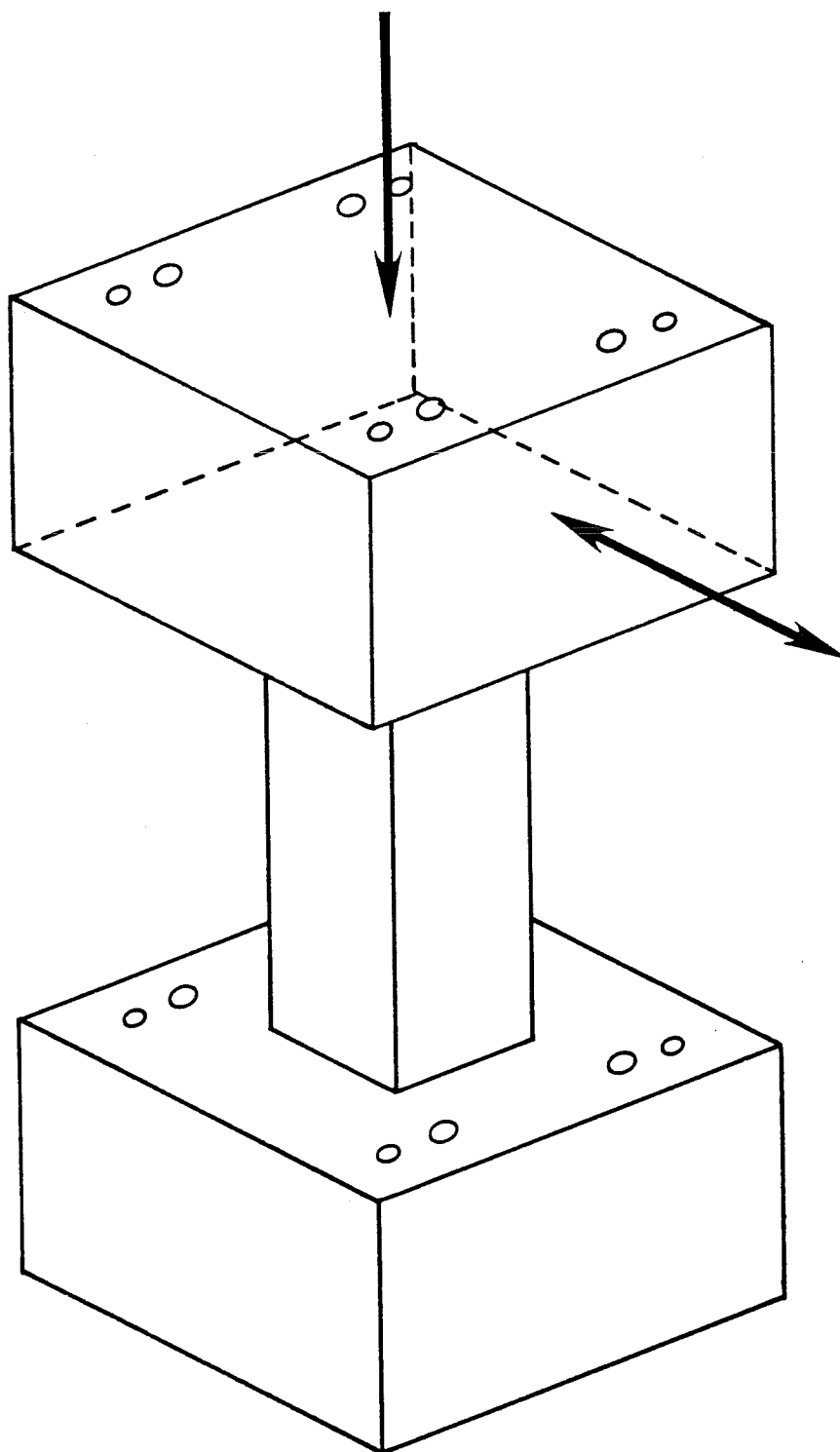


Fig. 3.1 Specimen/loading schematic.

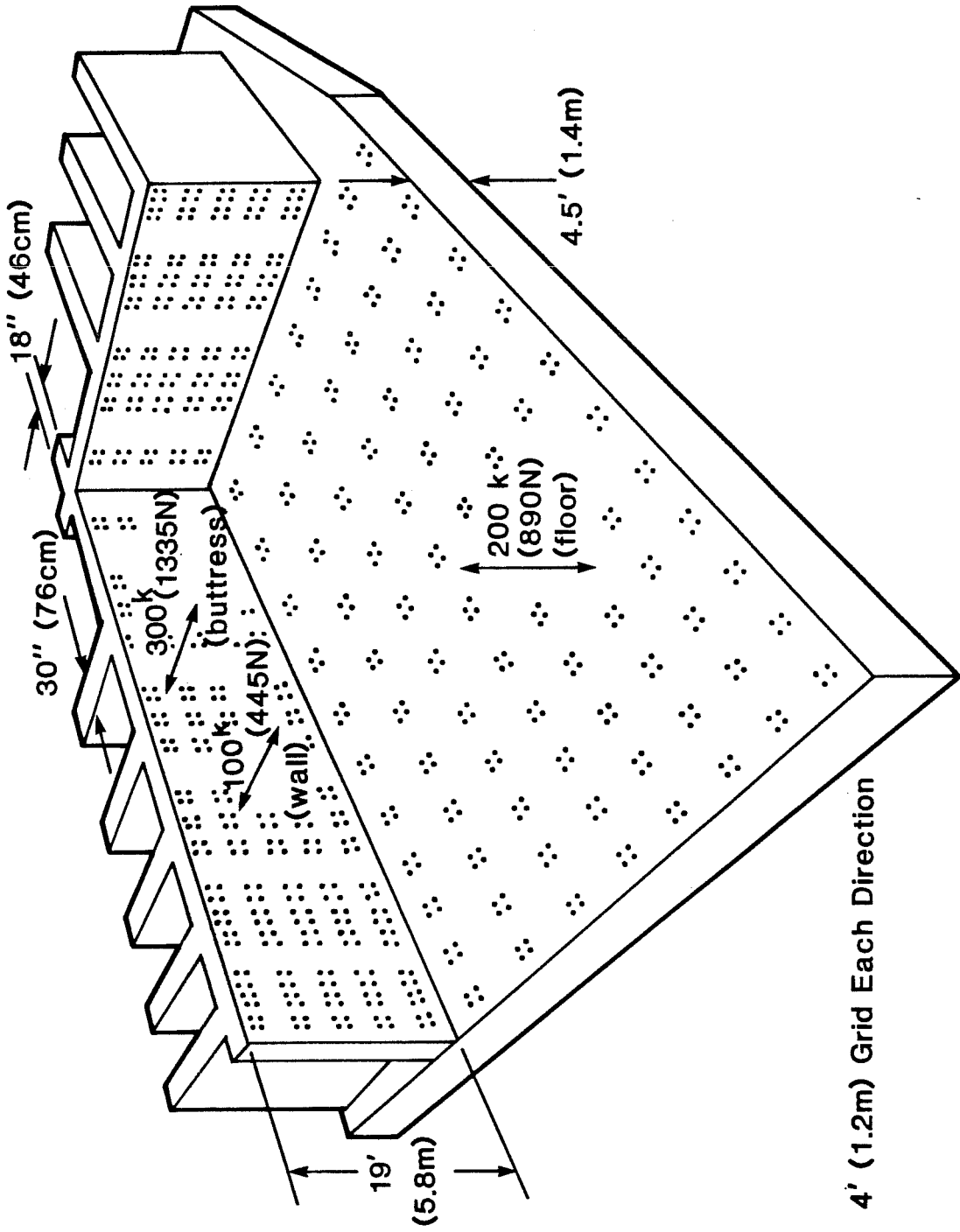


Fig. 3.2 Floor-wall reaction system.

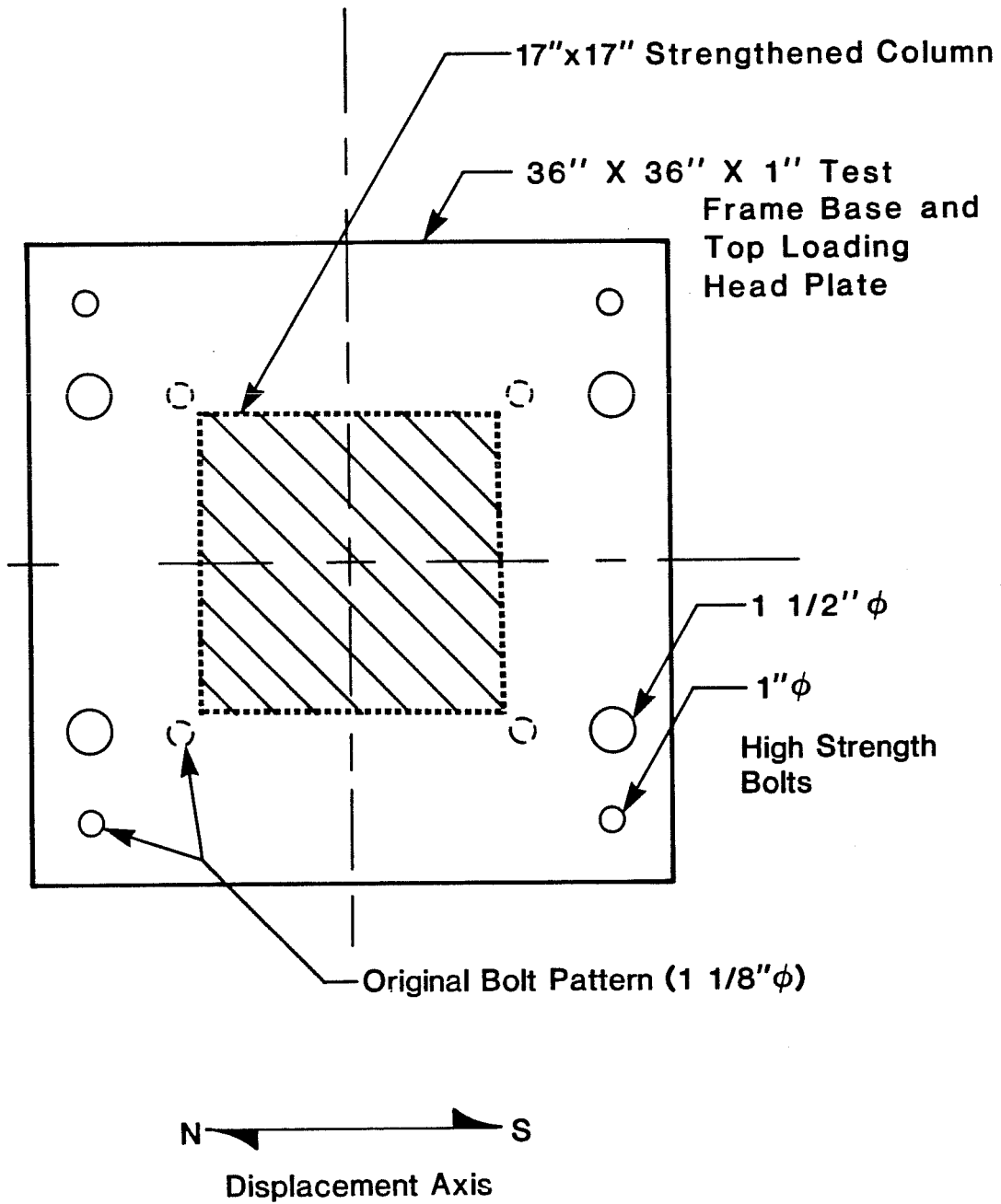


Fig. 3.3 Specimen hold-down bolt details.

The lateral rams were under displacement control. Figure 3.4 illustrates the arrangement of the loading rams with respect to the specimen, and Fig. 3.5 illustrates the actual test setup.

The test specimen is bounded at each end by a loading head which is a welded assembly of wide flange members. The end blocks of the specimen were attached to the loading heads by eight high-strength threaded rods, after placing a coat of gypsum plaster between the loading head and the end block to ensure a smooth bearing surface. The lower loading head is bolted to the testing floor, while the upper crosshead is free to translate in the north-south direction.

The test specimen represents a column bounded by very stiff framing elements. To better model the condition of end fixity, rotations of the upper loading head are restrained by a system of cross-coupled hydraulic rams (Figs. 3.6, 3.7). Two pairs of rams act vertically to restrain rotations of the upper head in two orthogonal vertical planes. The remaining pair of rams is used to resist rotation of the upper head about a vertical axis.

Each pair of cross-coupled rams may extend or retract equally, as in the case of vertical translation of the upper loading head. However, because of cross-coupling, one ram in a pair cannot retract while the other ram extends. This resistance to differential displacements restrains rotation of the upper loading head.

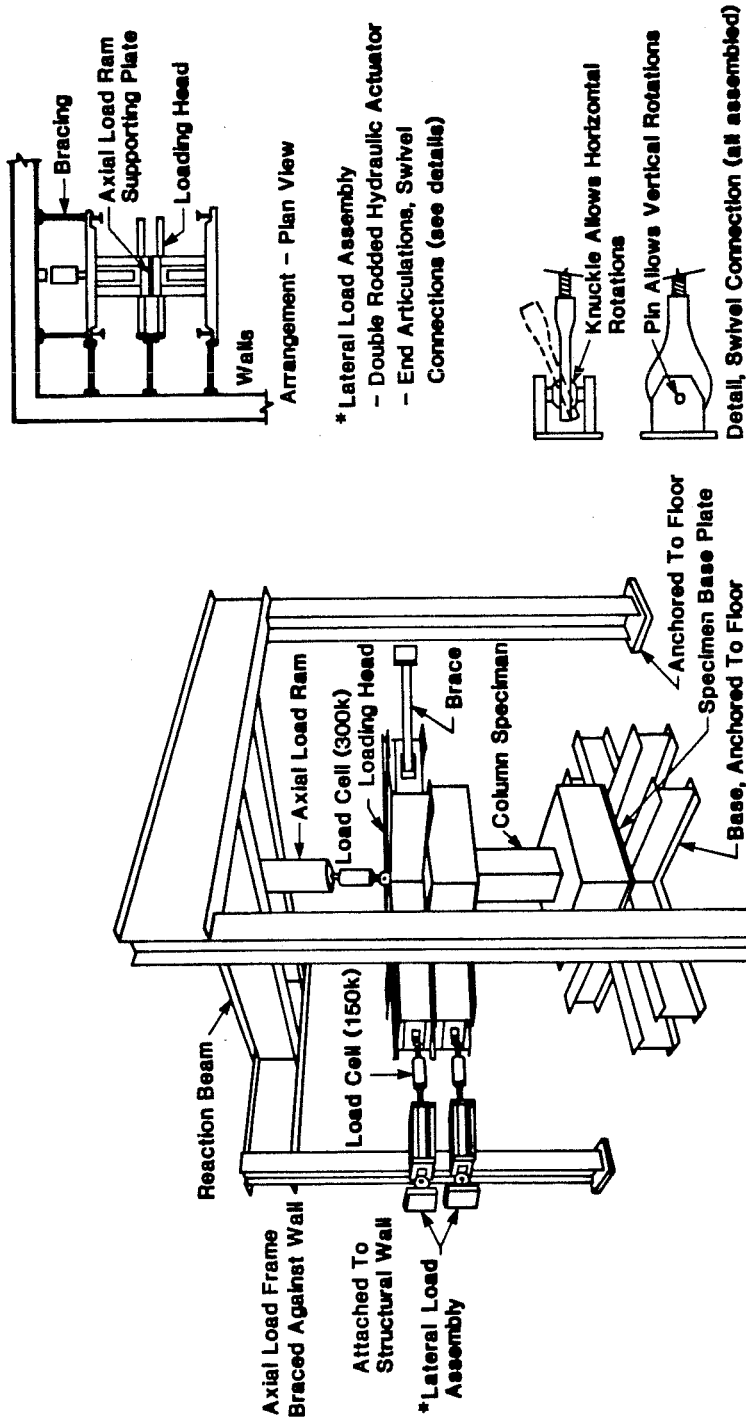


Fig. 3.4 Loading rams.

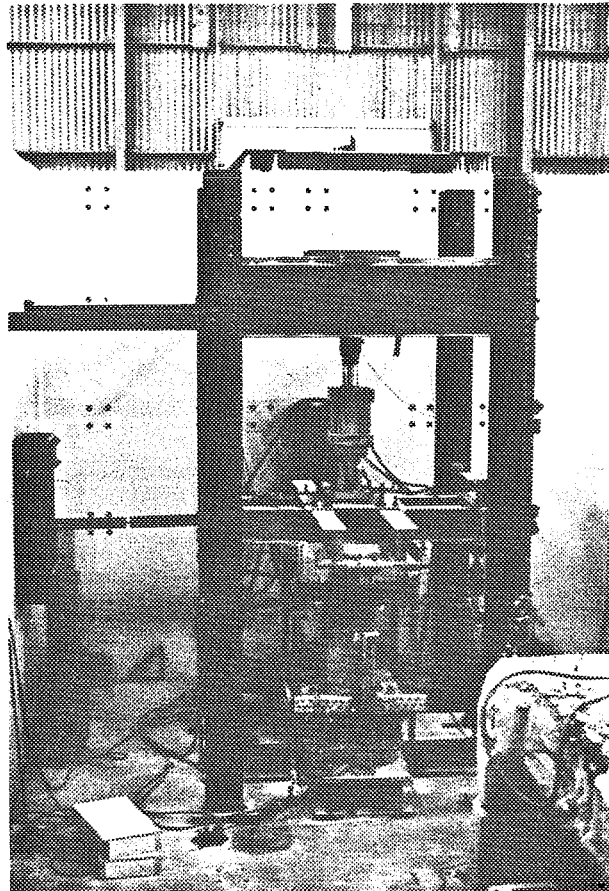


Fig. 3.5 Test setup.

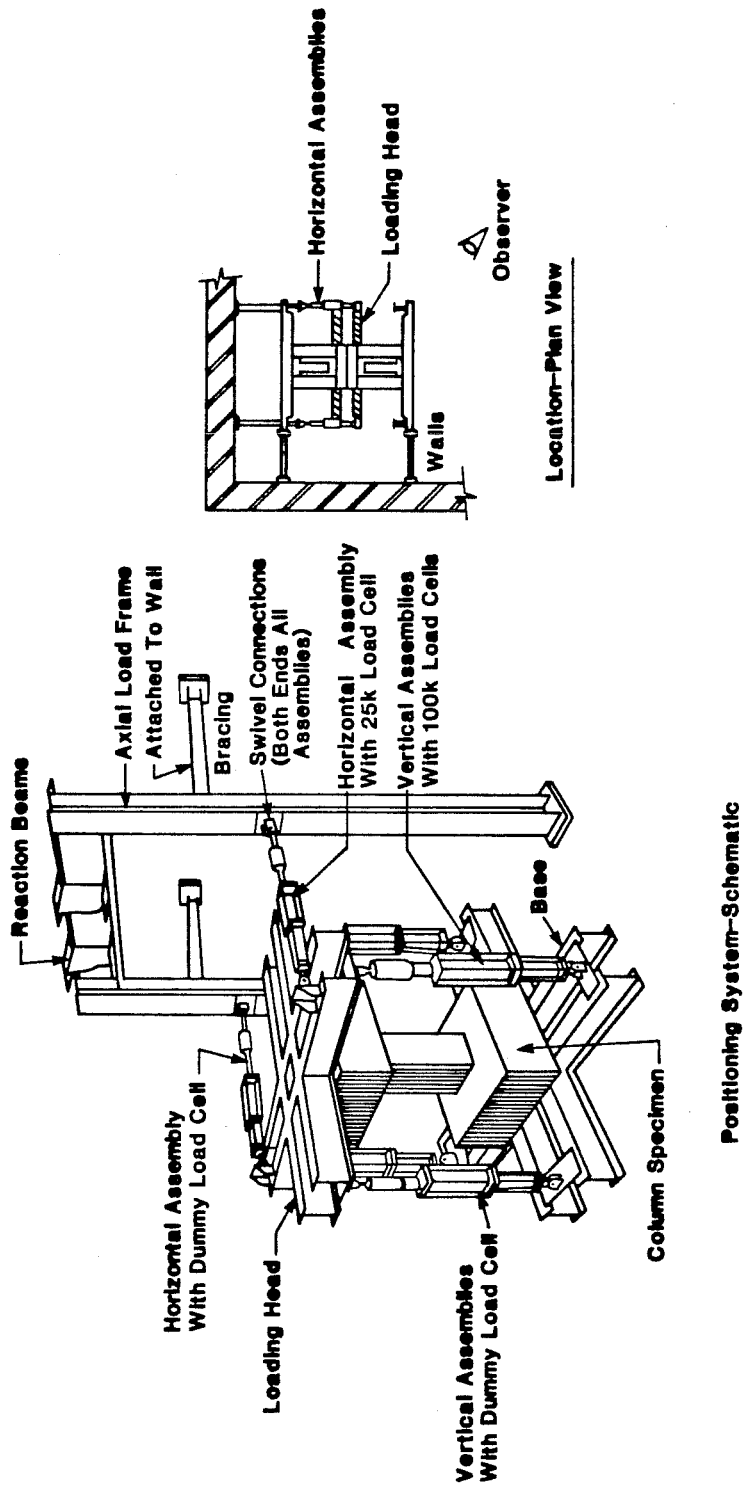
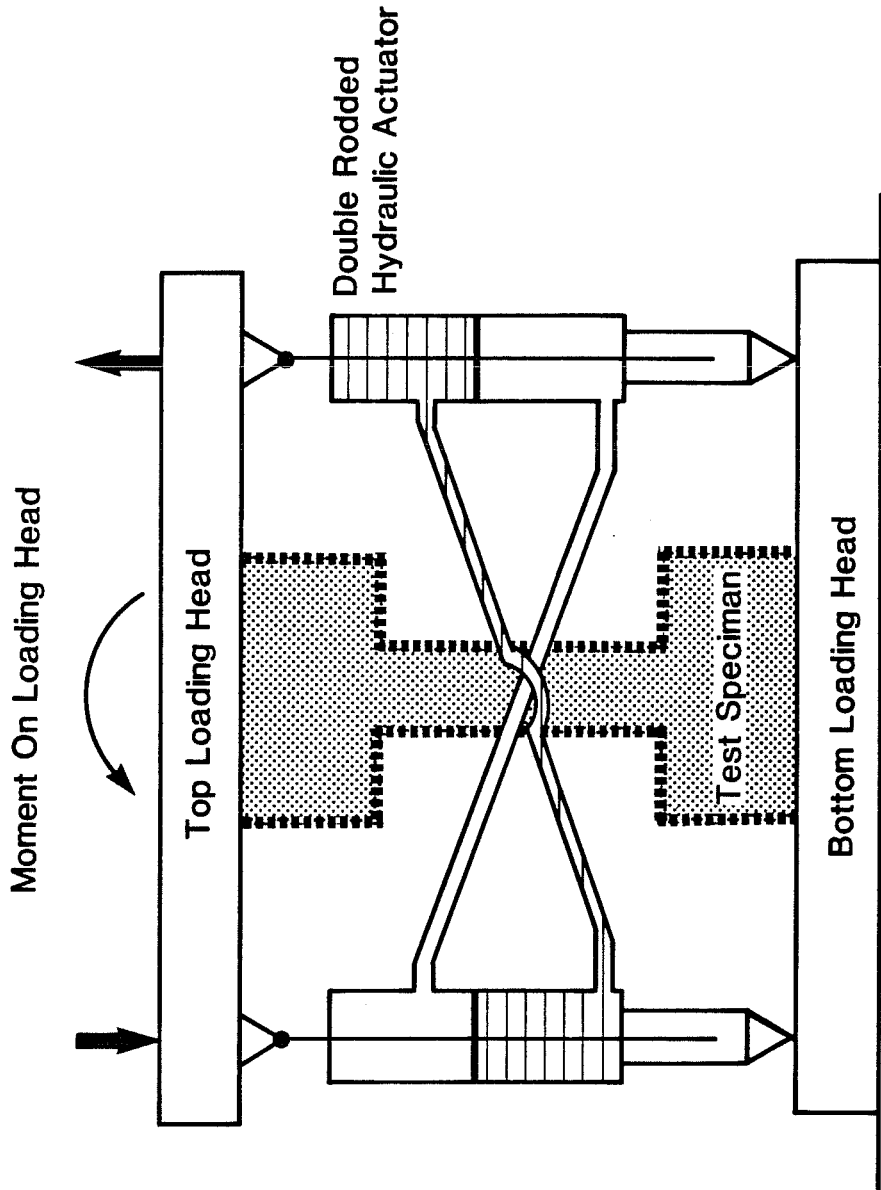


Fig. 3.6 Restraining rams.



Vertical and Horizontal Positioning System

Fig. 3.7 Vertical and horizontal positioning system.

3.2 Instrumentation

Three types of measuring devices were used to monitor the performance of the specimen during testing: 1) load cells; 2) linear potentiometers; and 3) strain gages.

3.2.1 Loads. Load cells were mounted on each loading ram and on one ram in each pair of restraining rams. All load cells were monitored by the data acquisition system, and the force applied by one of the lateral loading rams was plotted on an X-Y recorder as the test progressed.

3.2.2 Deflections. As shown in Fig. 3.8, twelve linear potentiometers were used to monitor the deflections and rotations of the specimen end blocks. As shown in Fig. 3.9, the potentiometers were supported independently of the loading frame. Deflections measured by the potentiometers were recorded by the data acquisition system. The signal from one of the lateral potentiometers, when used in conjunction with the output from a lateral ram load cell, provided a load-deflection plot along the north-south displacement axis used to monitor the response during testing.

3.2.3 Strains. As shown in Figs. 3.10 and 3.11, paper backed strain gages were attached to the tie and longitudinal reinforcement in both the column core and shotcrete jacket. Gages were located on each leg of a jacket reinforcement tie at three levels (top, mid-height, and bottom) of the column. One end of every crosstie was gaged.

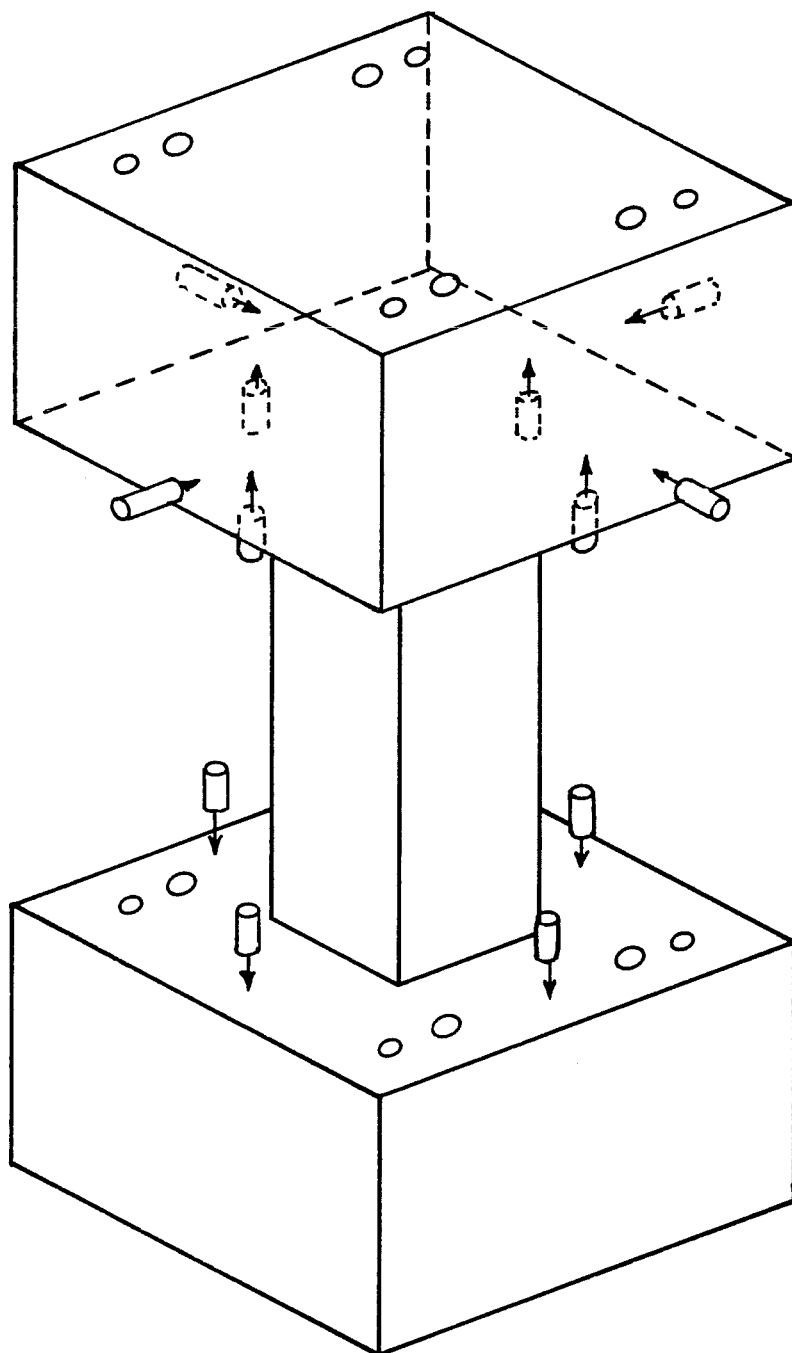


Fig. 3.8 Linear potentiometer locations.

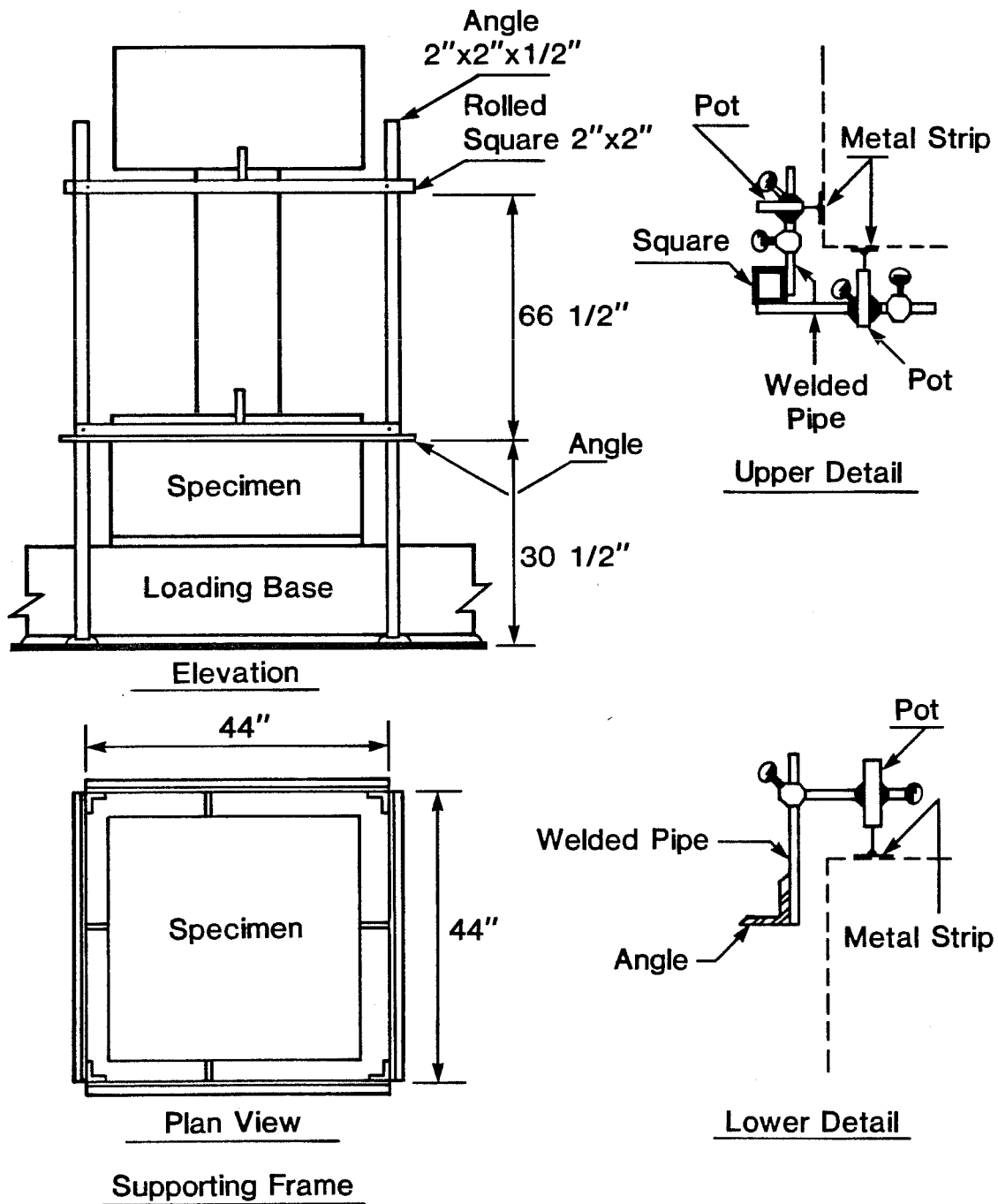


Fig. 3.9 Linear potentiometer mounting frame.

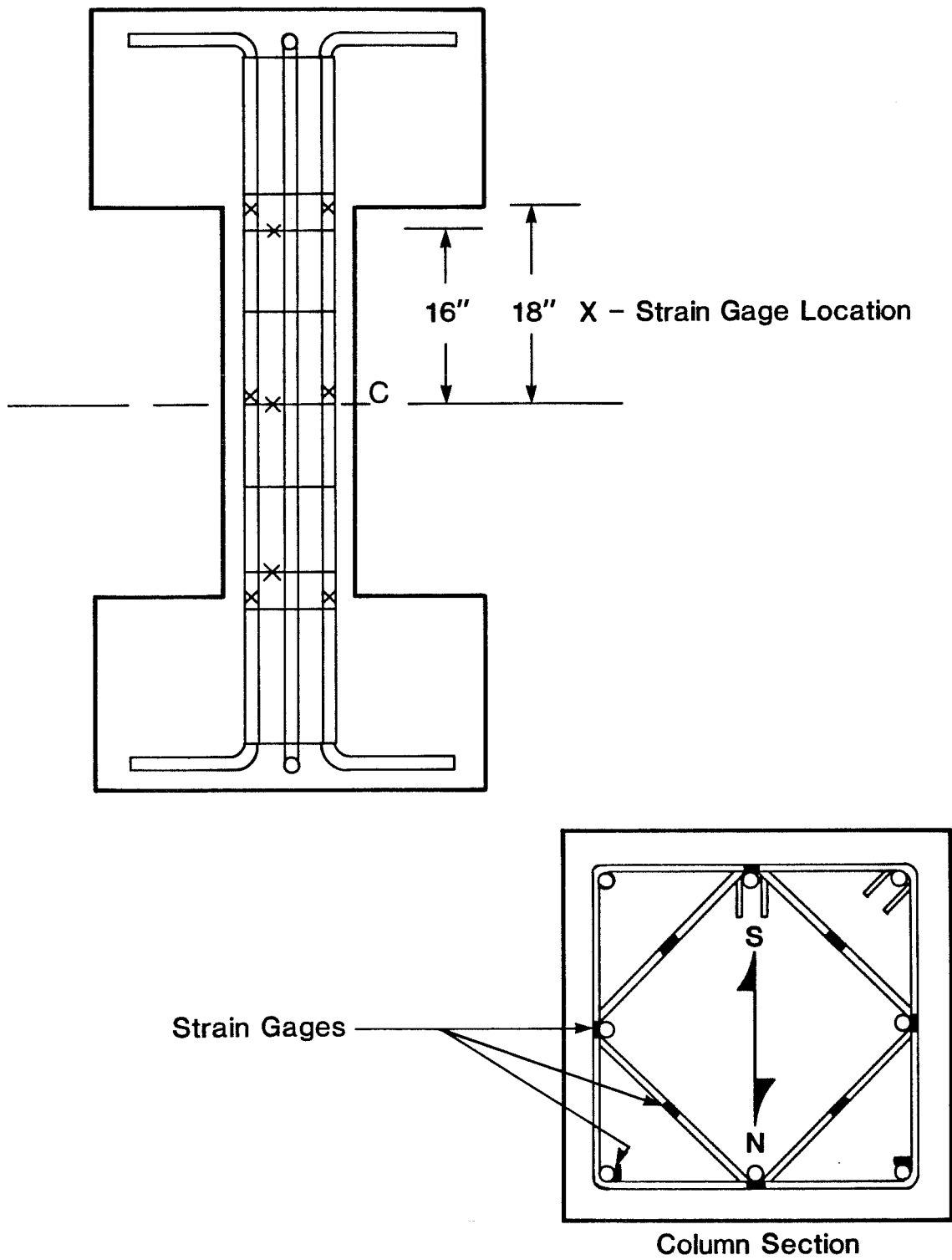


Fig. 3.10 Strain gage locations (original specimen).

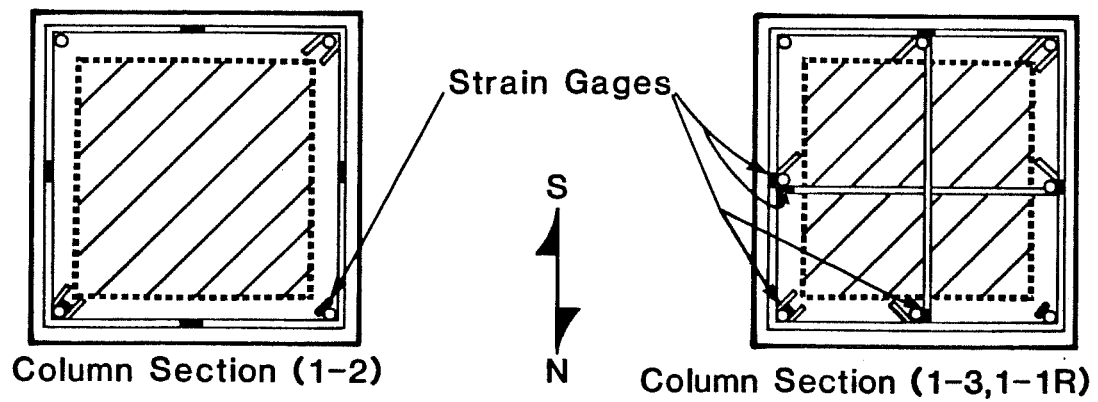
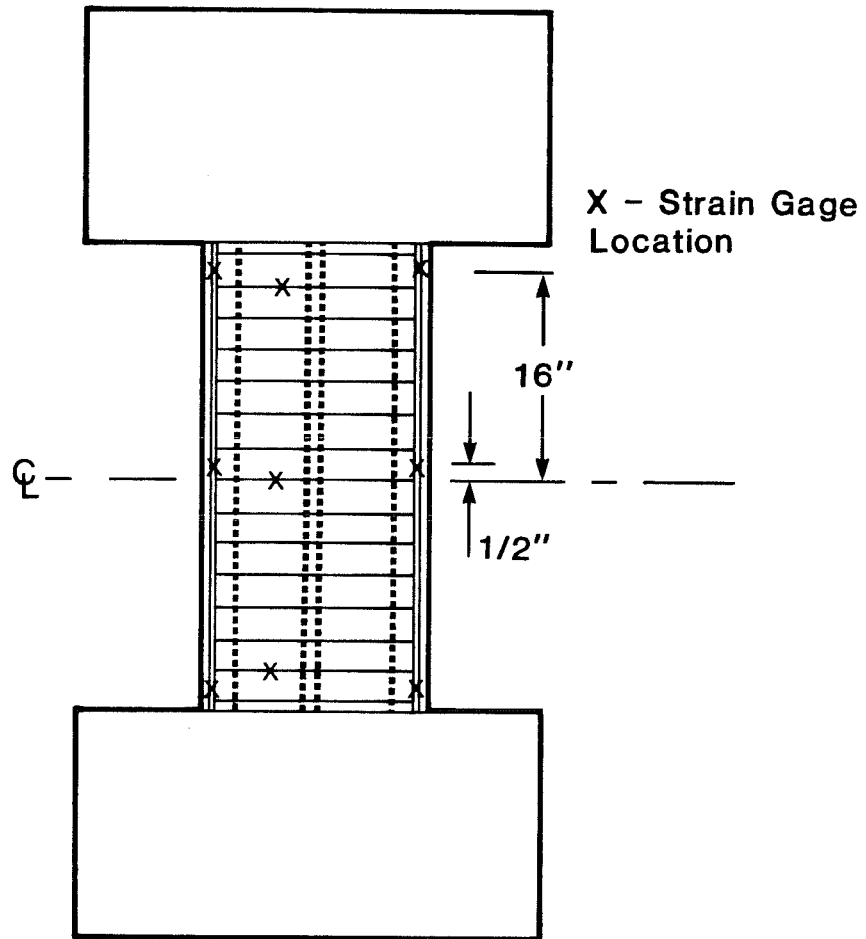


Fig. 3.11 Strain gage locations (jacket).

3.2.4 Slip. Relative slip between the original column and the jacket was measured using slip wires as shown in Fig. 3.12 located at the column mid-height and near the base, as shown in Fig. 3.13.

3.3 Data Acquisition

The main component of the data acquisition system was an Acurex Autodata Datalogger (scanner). The Acurex data scanner read the analog output signal of each instrument, converted it to a digital voltage, and transferred the information to a Data General Nova computer. The Nova then reduced the data to common engineering units as the test progressed.

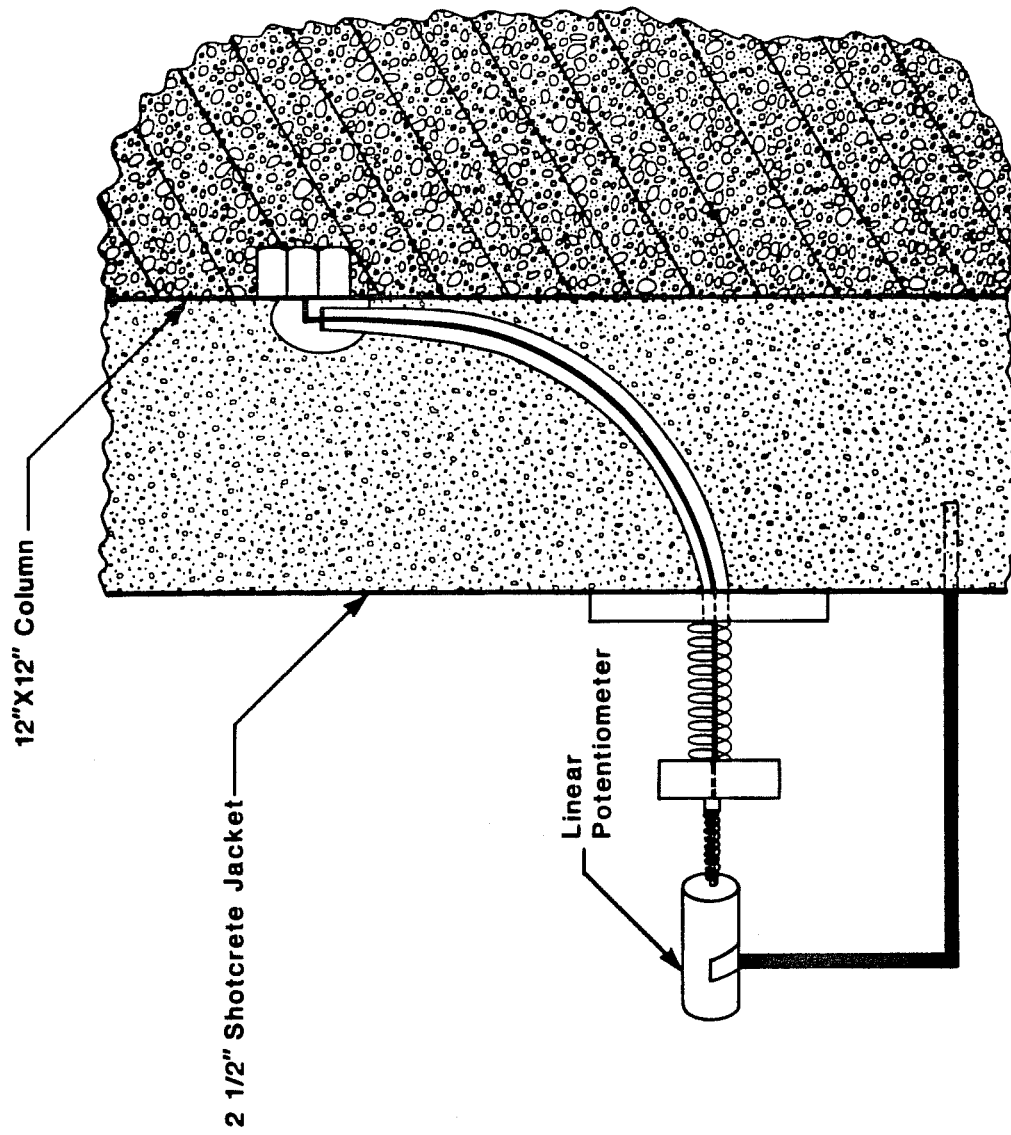


Fig. 3.12 Slip wire instrumentation.

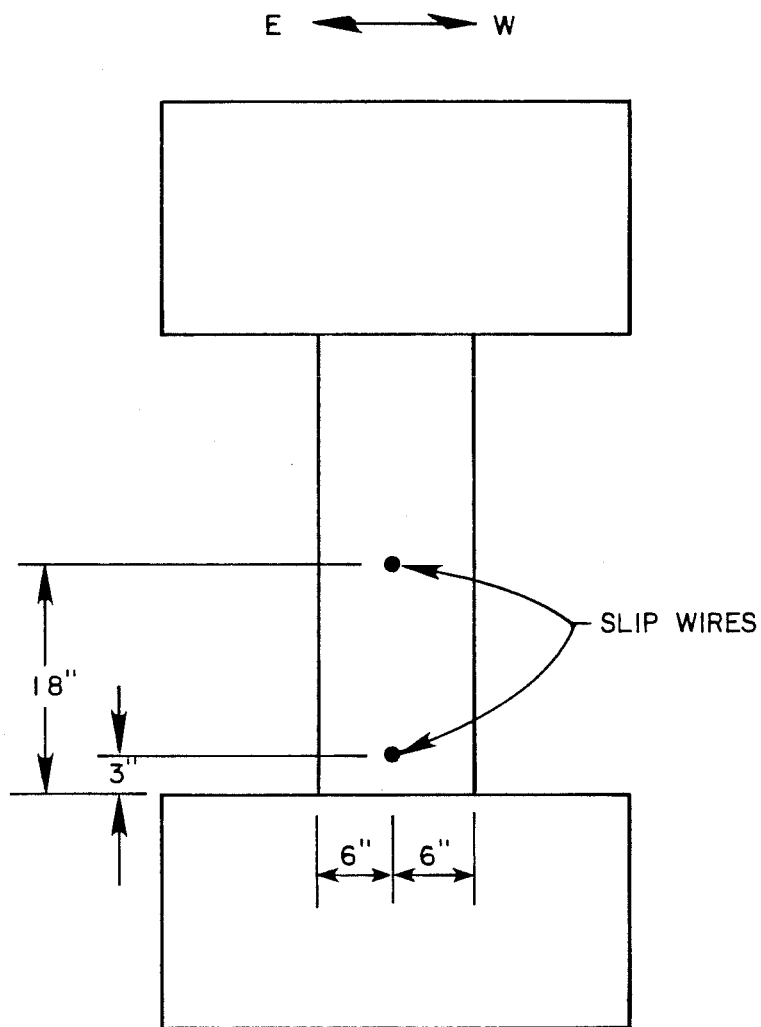


Fig. 3.13 Slip wire locations.

C H A P T E R I V

BEHAVIOR OF SPECIMENS

4.1 Introduction

Portions of the experimental test results for all specimens (original, strengthened and repaired) are reported in this chapter. Load-deflection curves and envelopes for all specimens are shown. Strain information is reported for Specimen 1-1 and Specimen 1-3 only because strain data from Specimen 1-3 were found to be representative of both the other strengthened specimen (1-2) and the repaired specimen (1-1R). Significant variations among individual tests will be discussed in Chapter 5. Basic data for each test were obtained from load cells, displacement transducers and strain gages. Photographs were used to record crack patterns at the end of each load phase.

The hysteretic behavior of the test specimens under the imposed cyclic deformations and constant axial load is presented in terms of lateral load-deflection curves. Of particular interest are the stiffness of the specimen, its peak lateral capacity at a given deflection level, its loss of lateral load capacity due to cycling, and the overall shape of the hysteretic loops. The slope of the load deflection curve at any point represents the tangent stiffness of the specimen. Envelopes of peak lateral load-deflection values are used for direct comparison of test results. The main objective in analyzing the

test results is to study the differences in behavior between the original column, and the same type of column after strengthening or repair.

4.2 Description of Test Results

4.2.1 Load-Deflection Curves. Load-deflection curves for Specimens 1-1, 1-2, 1-3, and 1-1R are shown in Figs. 4.1 through 4.4. Inspection of the figures reveals recognizable characteristics such as symmetry about the load axis, peak load-displacement envelope outlines and the effect of successive cycles at a constant drift level. Hysteretic behavior is referred to as "stable" when only small changes in lateral capacity are observed under cycling to constant drift levels. Large losses in specimen stiffness are characterized by "pinching" of the hysteretic loops. Poor energy dissipating characteristics of a member are generally typified by nonstable hysteretic behavior with pinching. As expected, pinching is more pronounced for both the original column (Specimen 1-1) and the repaired column (Specimen 1-1R), than for either of the strengthened specimens (Specimens 1-2, 1-3). Peak load-deflection envelopes, shown in Fig. 4.5, connect peak load-deflection values in the first cycle to each drift level, and are used to compare hysteretic characteristics of different tests. North and south displacements generated similar peak load envelopes, and for clarity of presentation only the north displacement curves are shown. For lateral deflections in excess of 1 percent drift, the lateral load capacity of Specimen 1-1 is observed to decay much faster than that of either of the strengthened specimens. The repaired specimen (1-1R) was less stiff than either of the two strengthened specimens, and exhibited

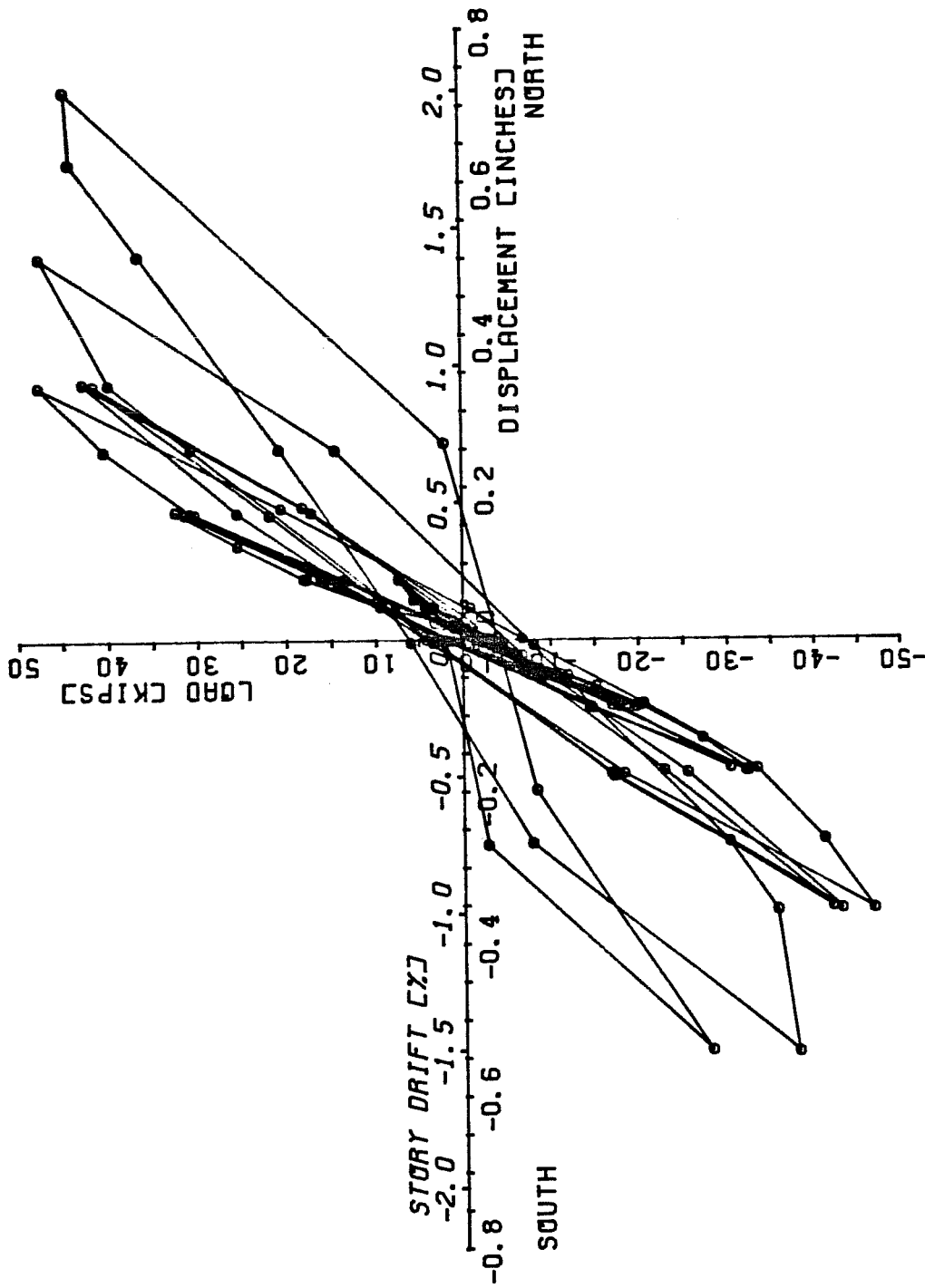


Fig. 4.1 Load-deflection curve, Specimen 1-1.

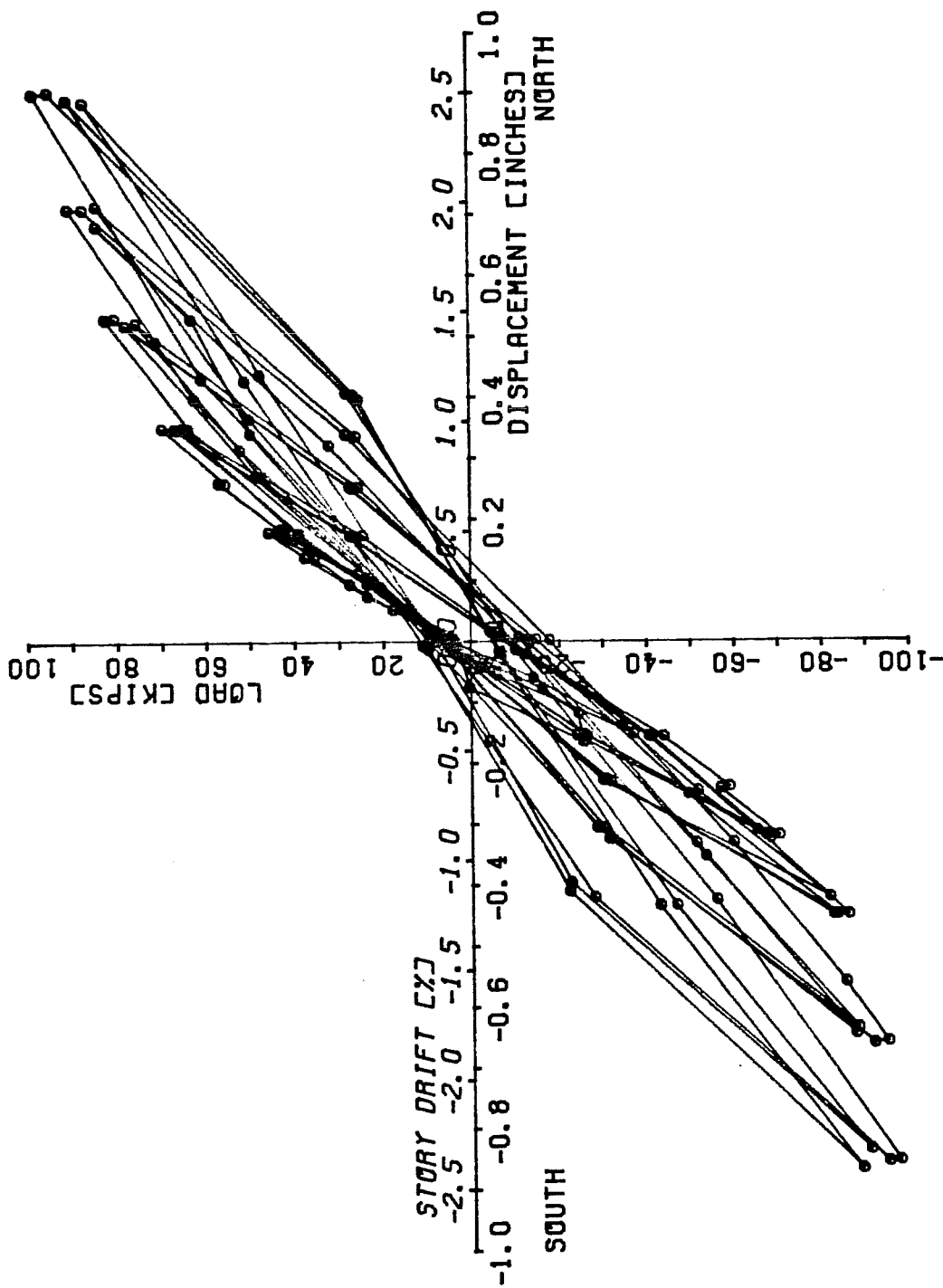


Fig. 4.2 Load-deflection curve, Specimen 1-2.

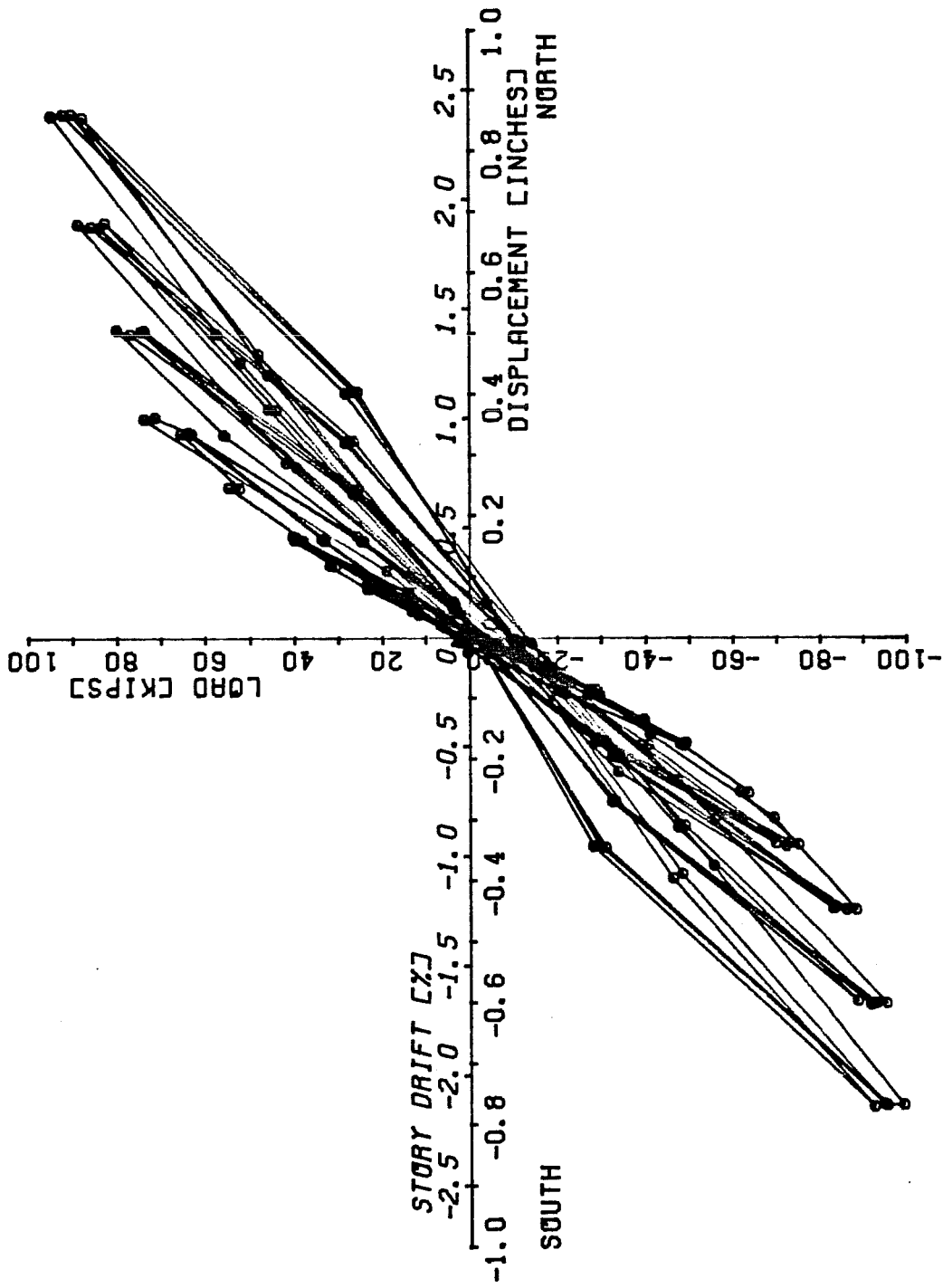


Fig. 4.3 Load-deflection curve, Specimen 1-3.

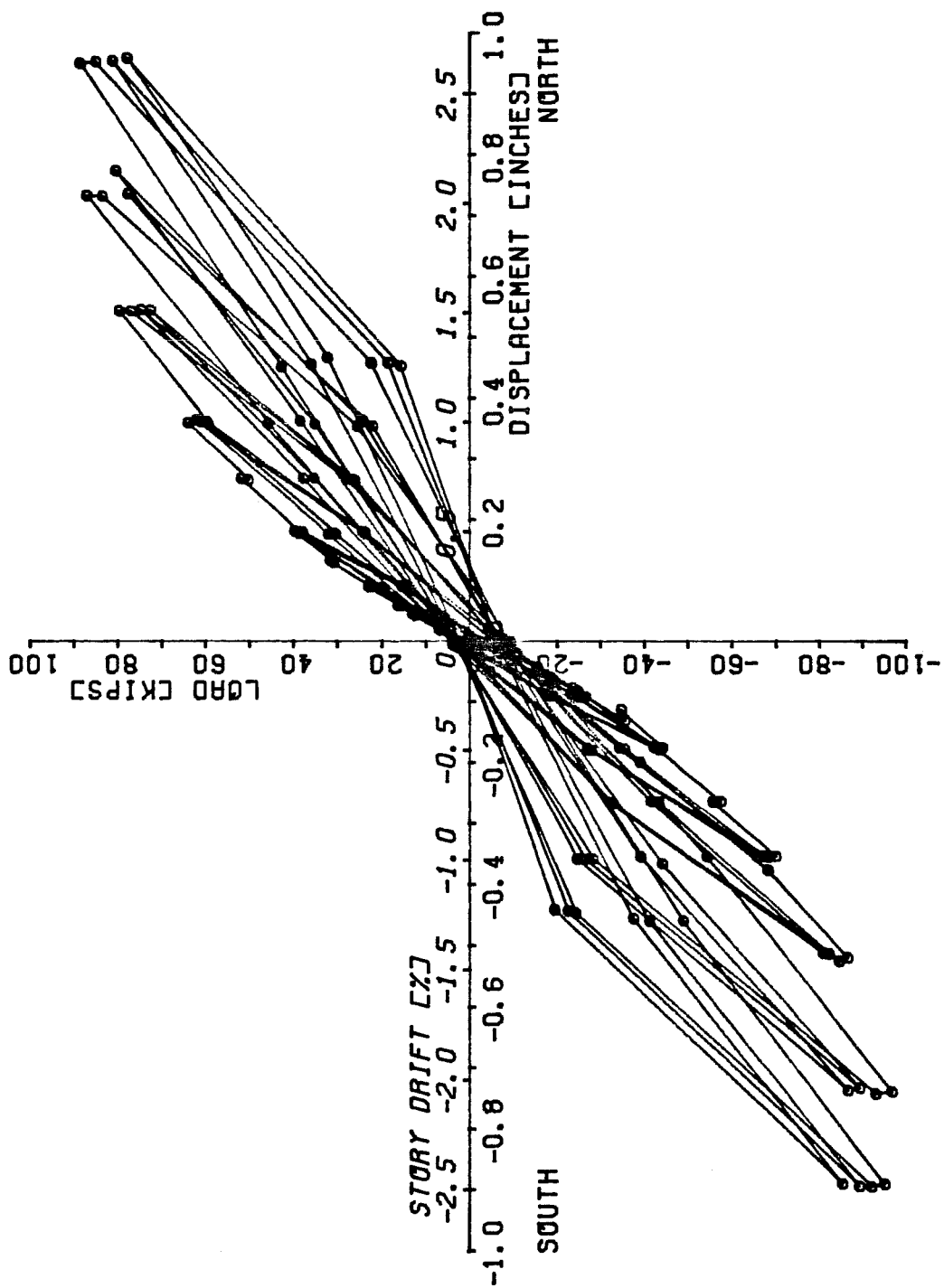


Fig. 4.4 Load-deflection curve, Specimen 1-1R.

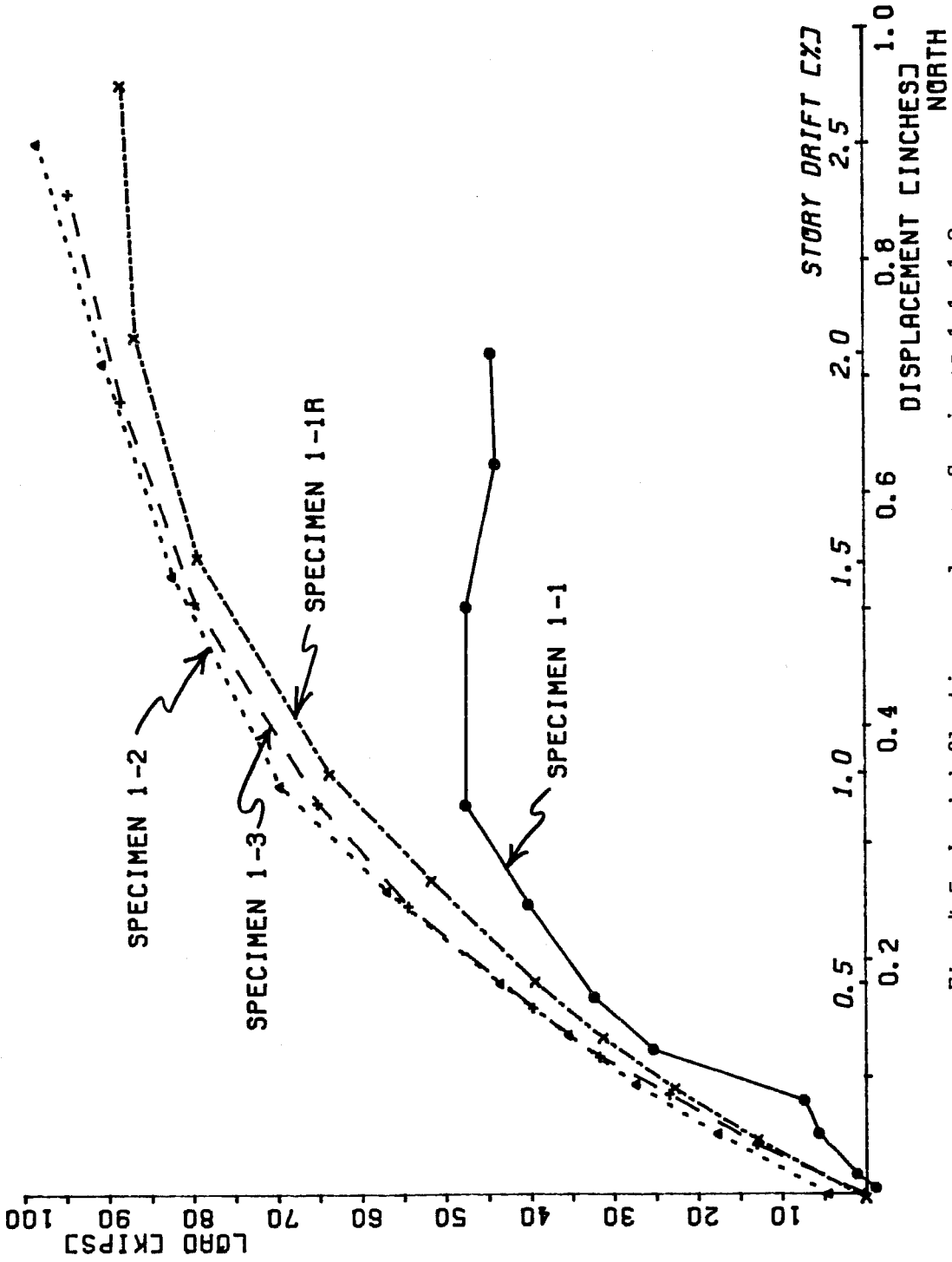
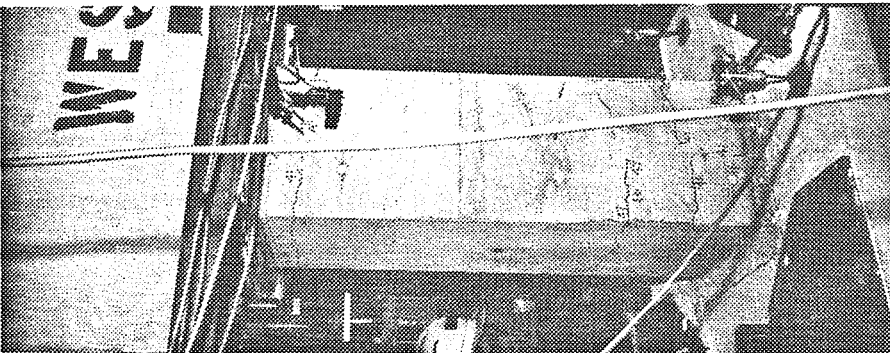


Fig. 4.5 Load-deflection envelopes, Specimens 1-1, 1-2, 1-3, and 1-1R.

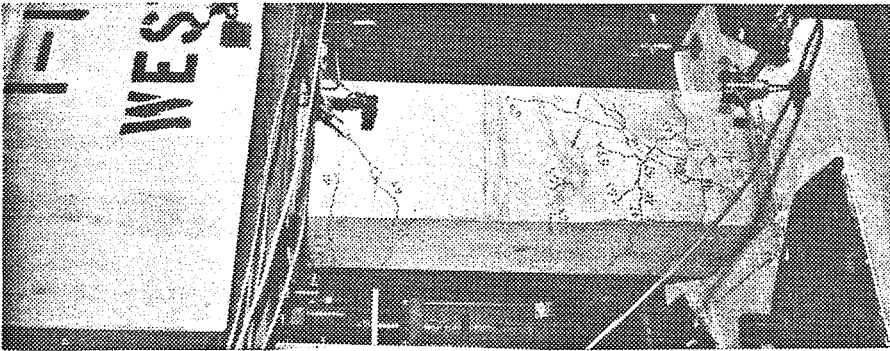
significantly reduced lateral capacity at deflections in excess of 2 percent drift.

4.2.2 Crack Patterns. Crack patterns for each of the tests were photographed at the end of each load phase. Figure 4.6 illustrates typical crack patterns on the northwest faces of Specimen 1-1 after reaching lateral displacements corresponding to 0.5 percent, 1 percent, 1.5 percent, and 2 percent drift. At 0.5 percent drift, flexural cracks developed near the top and bottom face of the column. Inclined shear cracks formed at 1 percent drift, and were approximately $1/64$ in. wide at that displacement level. Cycling at 1.5 percent drift extended those inclined cracks across the column face to a width of $1/32$ in. When 2 percent drift was reached, the inclined cracks widened, and concrete spalling was observed at the column corners, and to a lesser degree on the column face at mid-height.

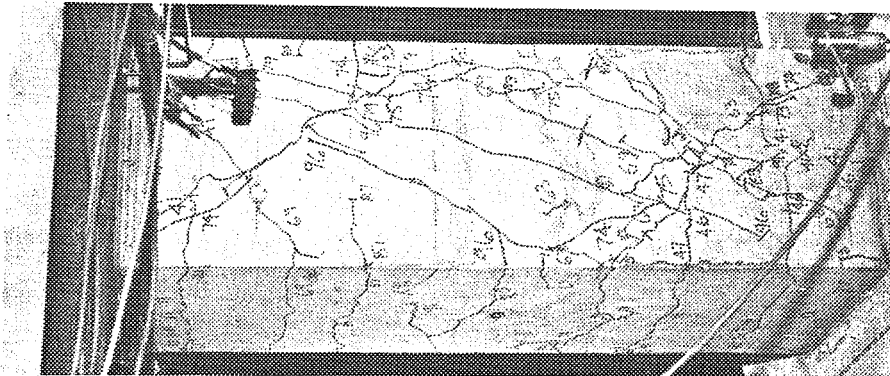
Typical crack patterns for the west face of Specimen 1-3 are shown in Fig. 4.7, for lateral drifts for 1.0 percent, 1.5 percent, 2 percent, and 2.5 percent. Significant flexural cracks developed at the 1 percent drift level and were less than $1/64$ in. wide. Inclined cracks developed from existing flexural cracks at 1.5 percent drift, and a wide crack ($3/32$ in.) on the opposite side of the displacement direction opened up between the shotcrete jacket and the top and bottom end blocks. Continued cycling at 2 percent drift level extended and widened both inclined and end cracks, culminating in crushing and spalling near both top and bottom end blocks at the 2.5 percent drift level. At peak



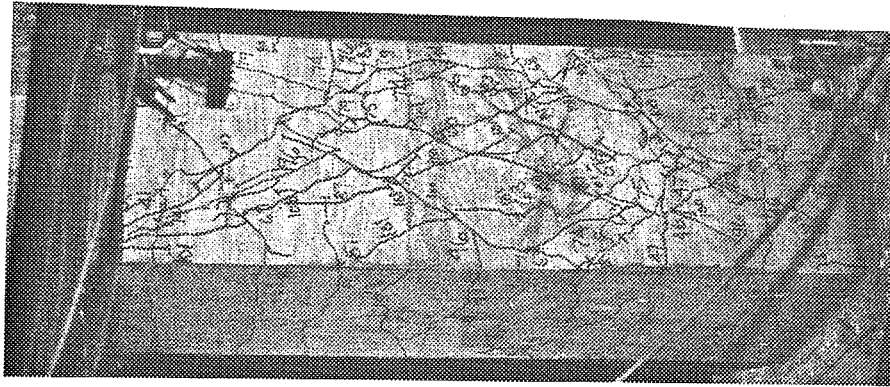
a) 0.5% drift



b) 1.0% drift

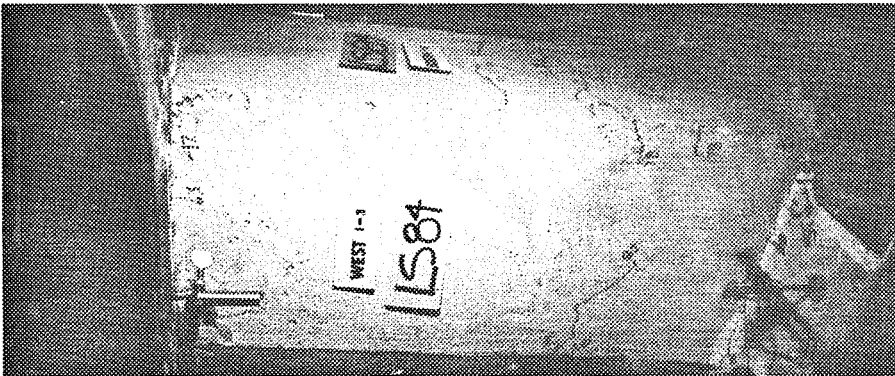


c) 1.5% drift

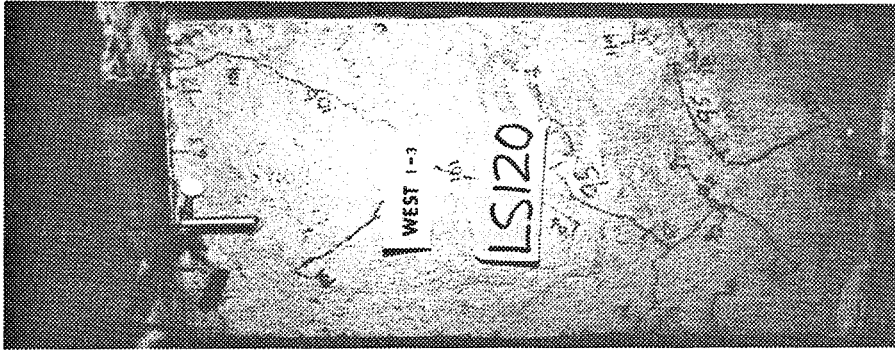


d) 2.0% drift

Fig. 4.6 Crack patterns, NW column faces, Specimen 1-1.



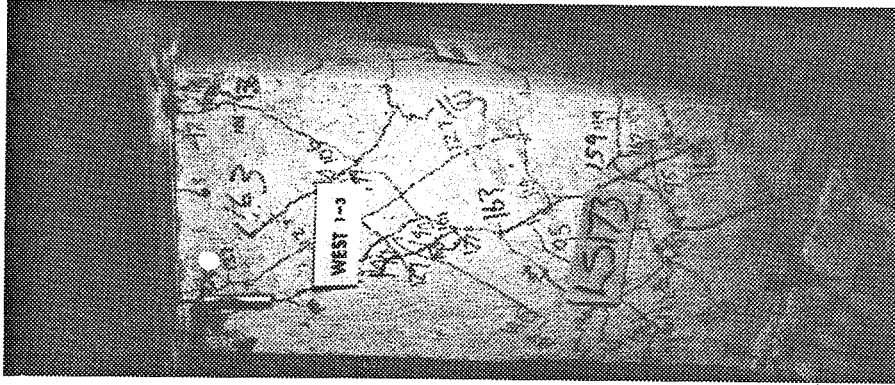
a) 1.0% drift



b) 1.5% drift



c) 2.0% drift



d) 2.5% drift

Fig. 4.7 Crack patterns, Specimen 1-3.

displacements at that drift level, the end cracks were approximately 1/4 in. wide.

4.2.3 Strain Distributions. Strain gages mounted on longitudinal and transverse reinforcement were monitored at each load stage for all tests. Attention was paid to the variations of strain at each drift level, and also to the history of strains at given locations under increasing drift levels.

Longitudinal Reinforcement. Figure 4.8 illustrates, as a function of peak drift levels in the north direction, the distribution of strain along the northwest #6 reinforcing bar of Specimen 1-1. Data correspond only to load stages used to produce the load-displacement envelopes of Fig. 4.5. As expected, the plot indicates the development of tension at the top of the north face, while the bottom north face of the column remains in compression. Figure 4.9 illustrates the comparable situation in Specimen 1-3. Especially noteworthy is the development of tension at both the top and bottom of the north faces as the drift level increases. This will be discussed in Chapter V.

Longitudinal bar strains can be used to characterize the behavior of the original column section. Because the jacket longitudinal reinforcement did not extend into the end blocks, it did not develop large tension forces. Strain information from jacket bars in compression, however, can be helpful for insight into the behavior of the jacket. Figure 4.10 illustrates the history, with increasing drift levels, of strain at the top of both the #6 original column reinforcing bar and the adjacent #3 jacket reinforcing bar. For northerly

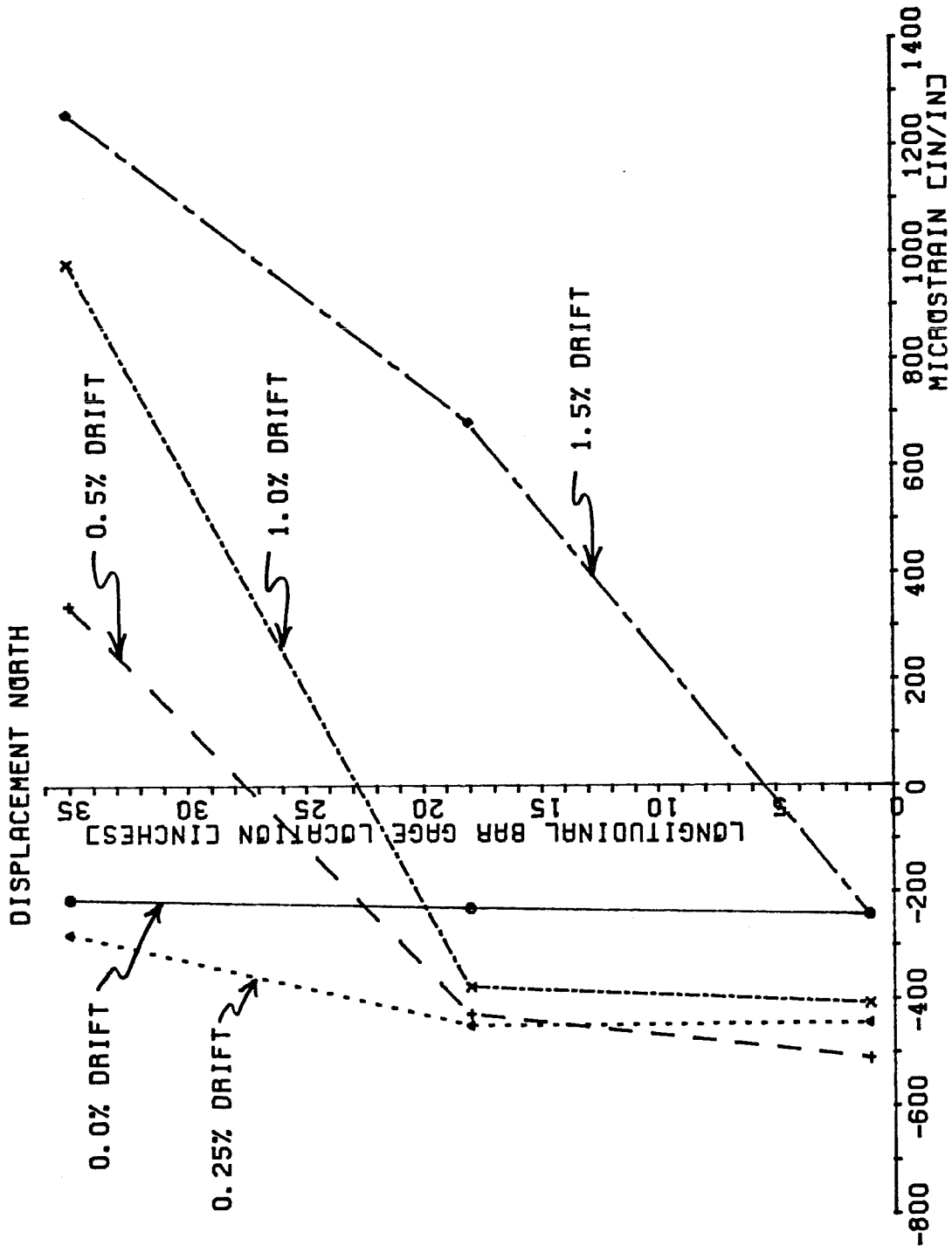


Fig. 4.8 Envelopes of strain distribution, NW longitudinal #6, Specimen 1-1.

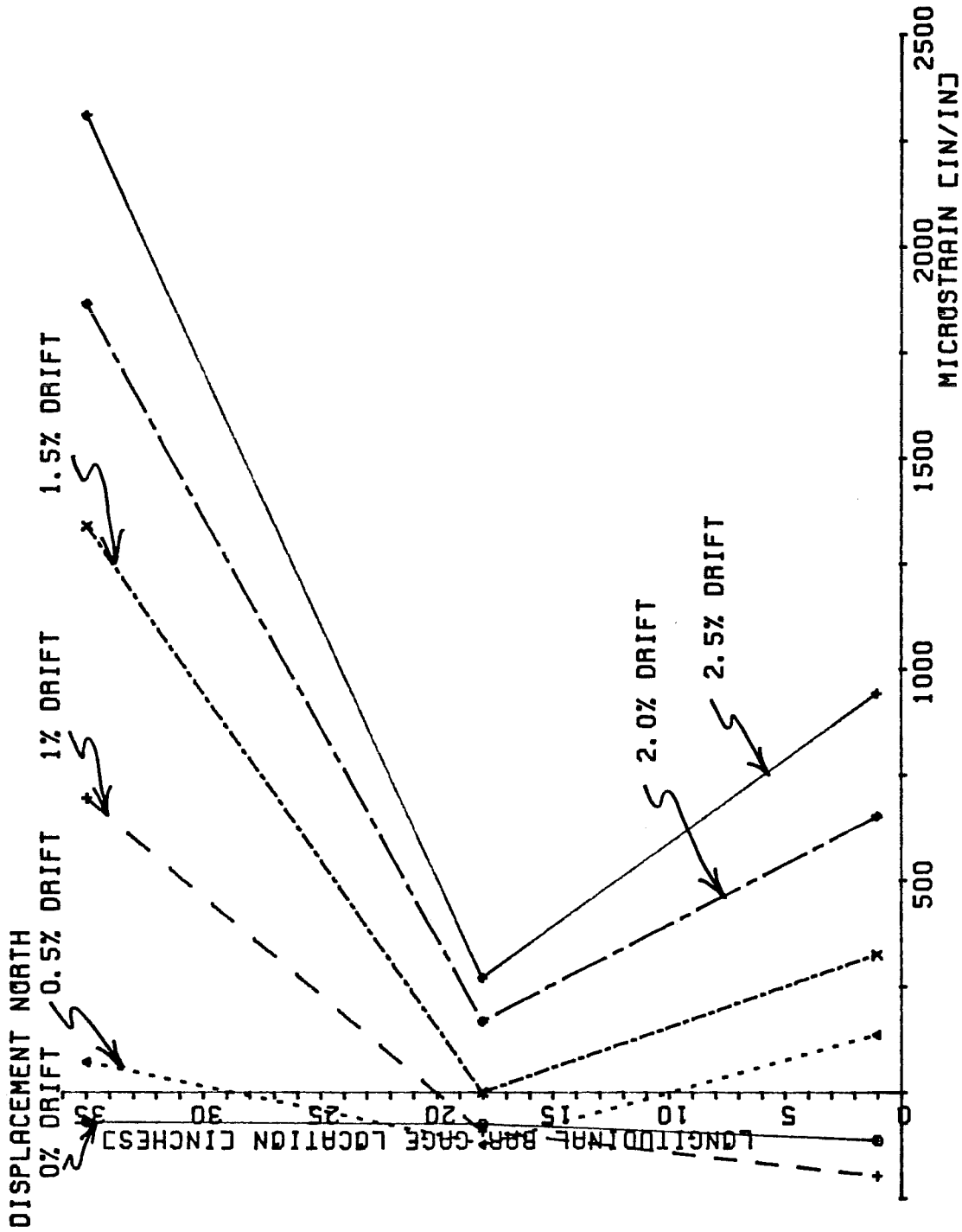


Fig. 4.9 Envelopes of strain distribution, NW longitudinal #6, Specimen 1-3.

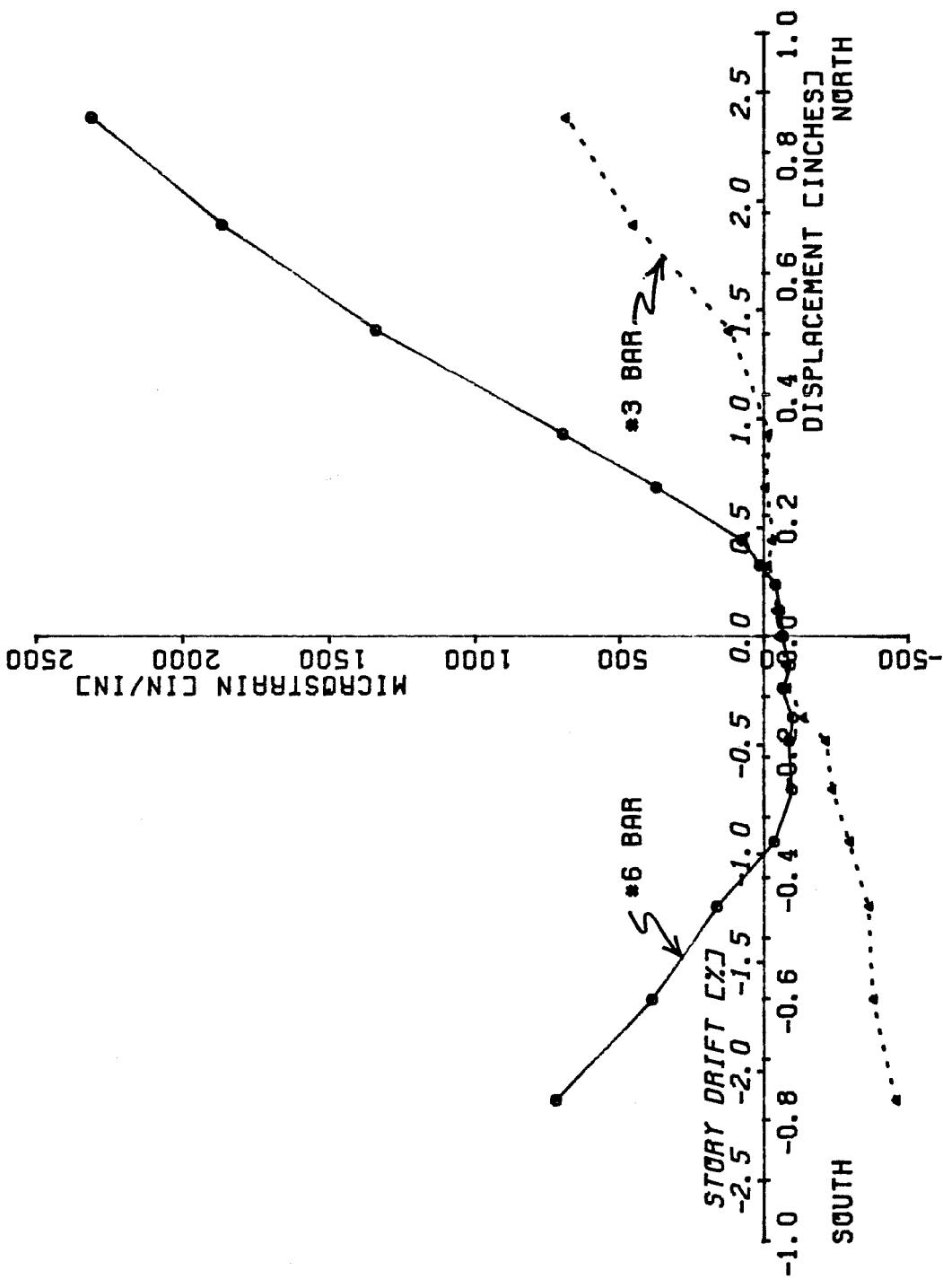


Fig. 4.10 Envelopes of top gage strain, #6/#3 NW longitudinal bars, Specimen 1-3.

displacements, the jacket bar is strained much less than the original column bar. While the jacket bar alternates between tension and compression, as would be expected from conventional beam theory, the original column bar experiences tension at the top under cycling in either direction. This was also observed in Specimens 1-2 and 1-1R, and will be discussed in Chapter V.

Transverse Reinforcement. Figure 4.11 illustrates, for increasing drift levels, the averaged strains from the rectangular ties running in the north-south direction (east-west faces of the column) in Specimen 1-1. The mid-height tie experienced the greatest increase in strain between the 1 percent and 1.5 percent drift levels, which also corresponds to the formation of significant inclined cracks at column mid-height (Fig. 4.6). At 1.5 percent drift, only the top tie remained elastic. Similarly, Fig. 4.12 illustrates the averaged strains for ties running in the east-west direction (north-south faces of the column). As before, the strain increased significantly between 1 percent and 1.5 percent drift level. Figure 4.13 illustrates averaged strains at mid-height of Specimen 1-3 for both jacket and original column rectangular ties. Gages located on east and west face ties exhibited the greatest increase in strain following the formation of inclined cracks between the 1 percent and 1.5 percent drift displacement levels. At peak displacement, only the east-west face jacket ties approached yield.

Crossties. Figure 4.14 illustrates a history of strain in supplementary crossties located at the top, upper mid-height, lower mid-height, and bottom of Specimen 1-3, and running in the north-south

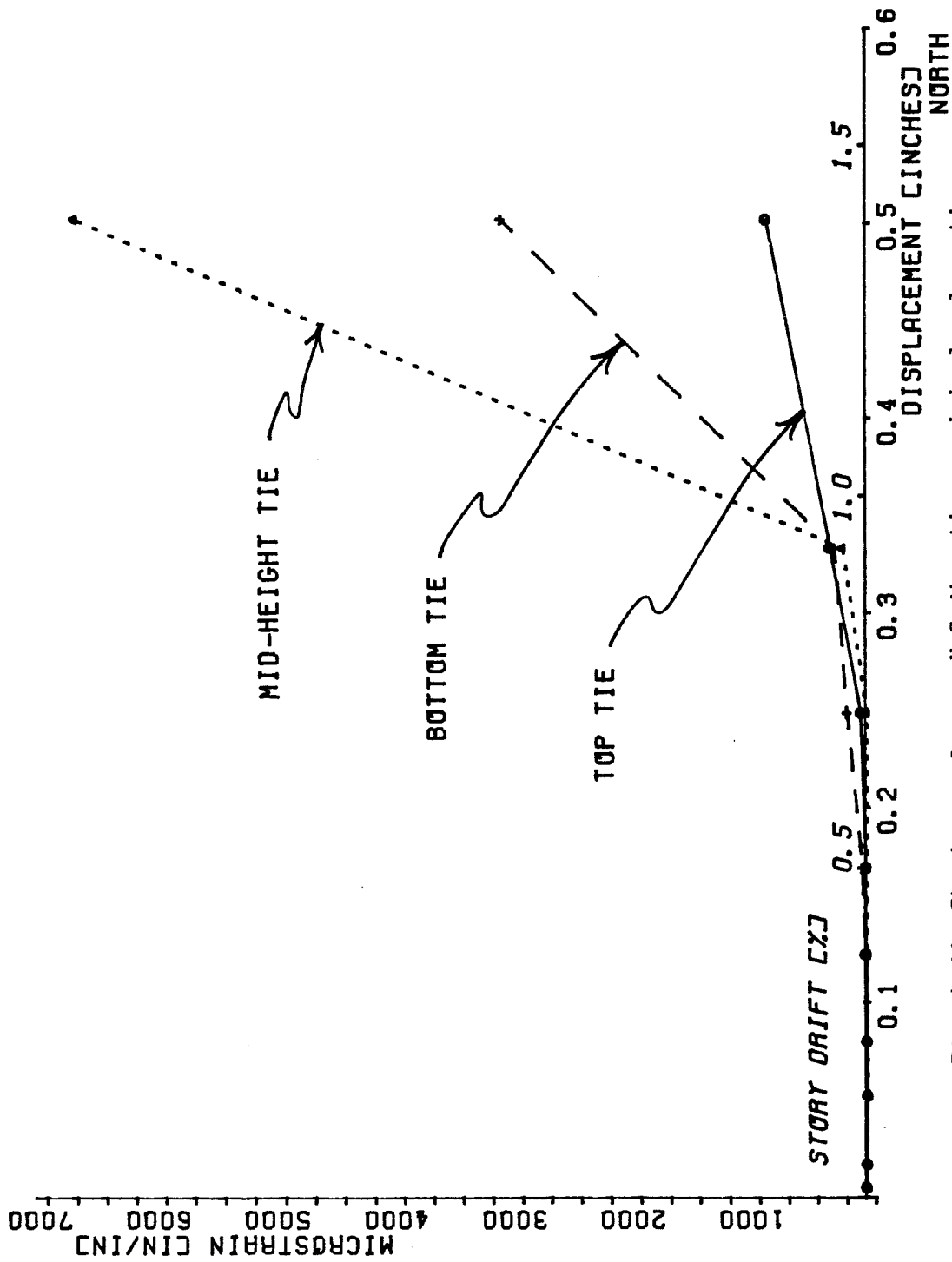


Fig. 4.11 Strain envelopes, N-S direction, original column ties, Specimen 1-1.

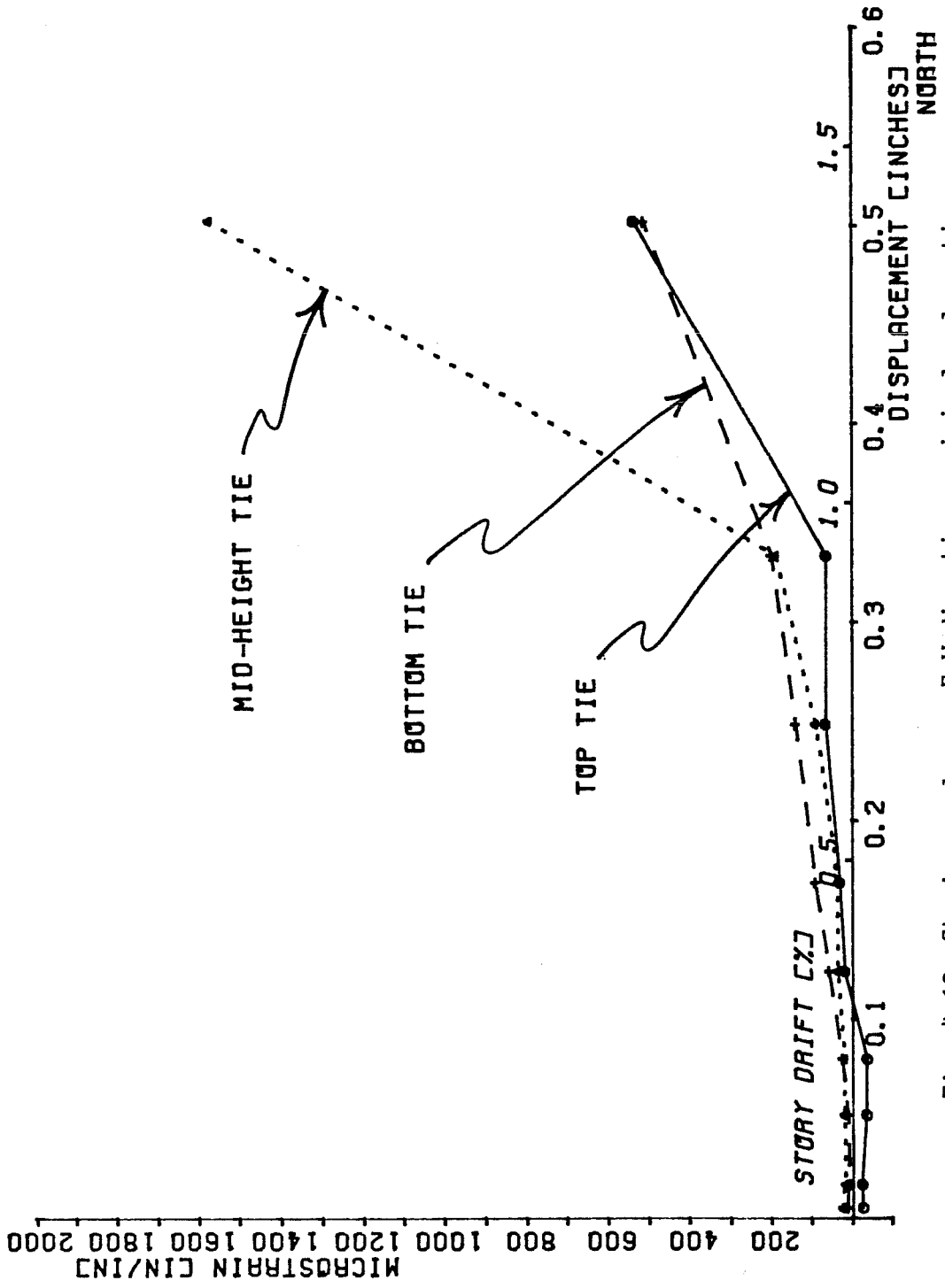


Fig. 4.12 Strain envelopes, E-W direction, original column ties, Specimen 1-1.

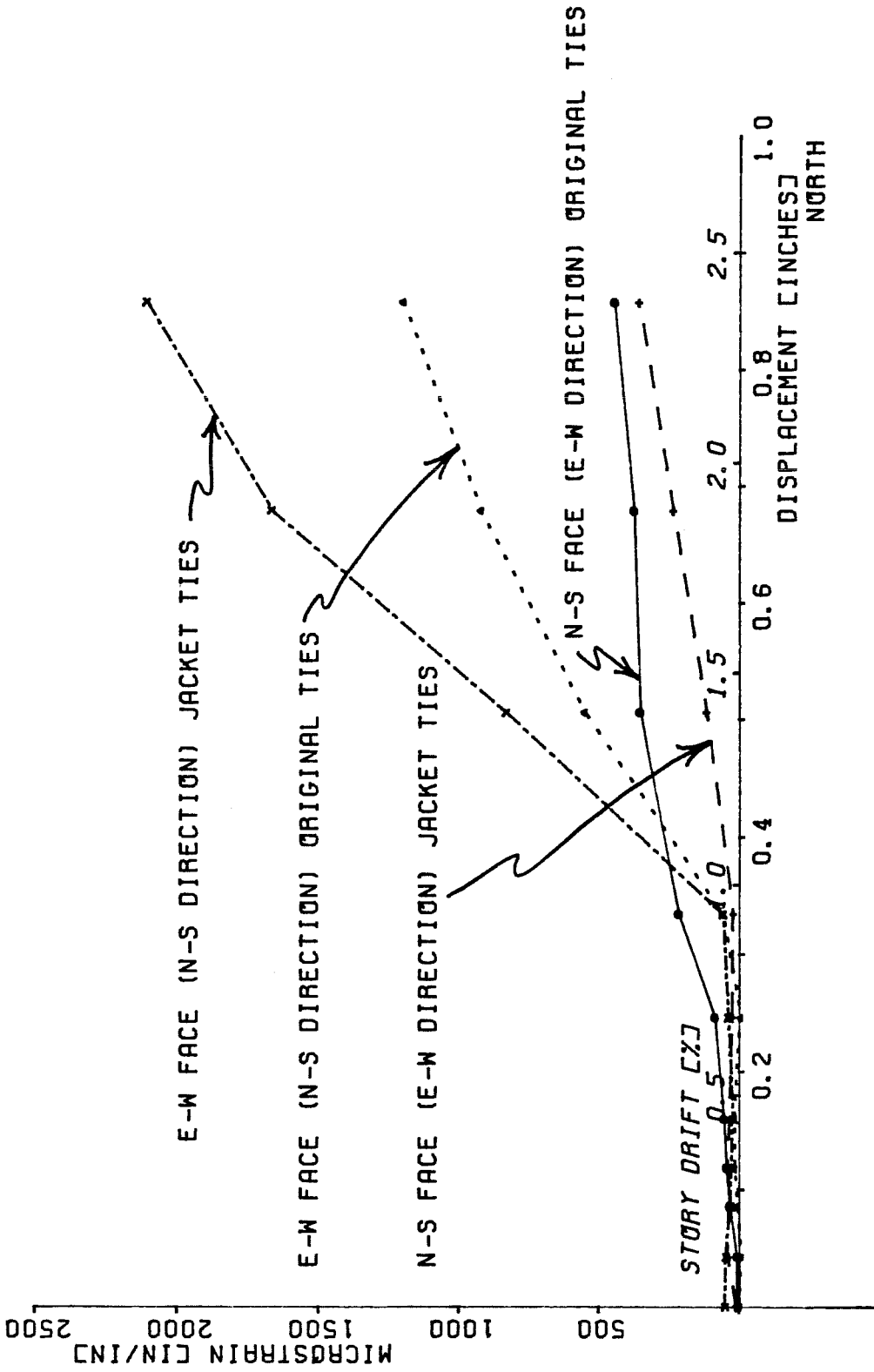


Fig. 4.13 Strain envelopes, mid-height ties, Specimen 1-3.

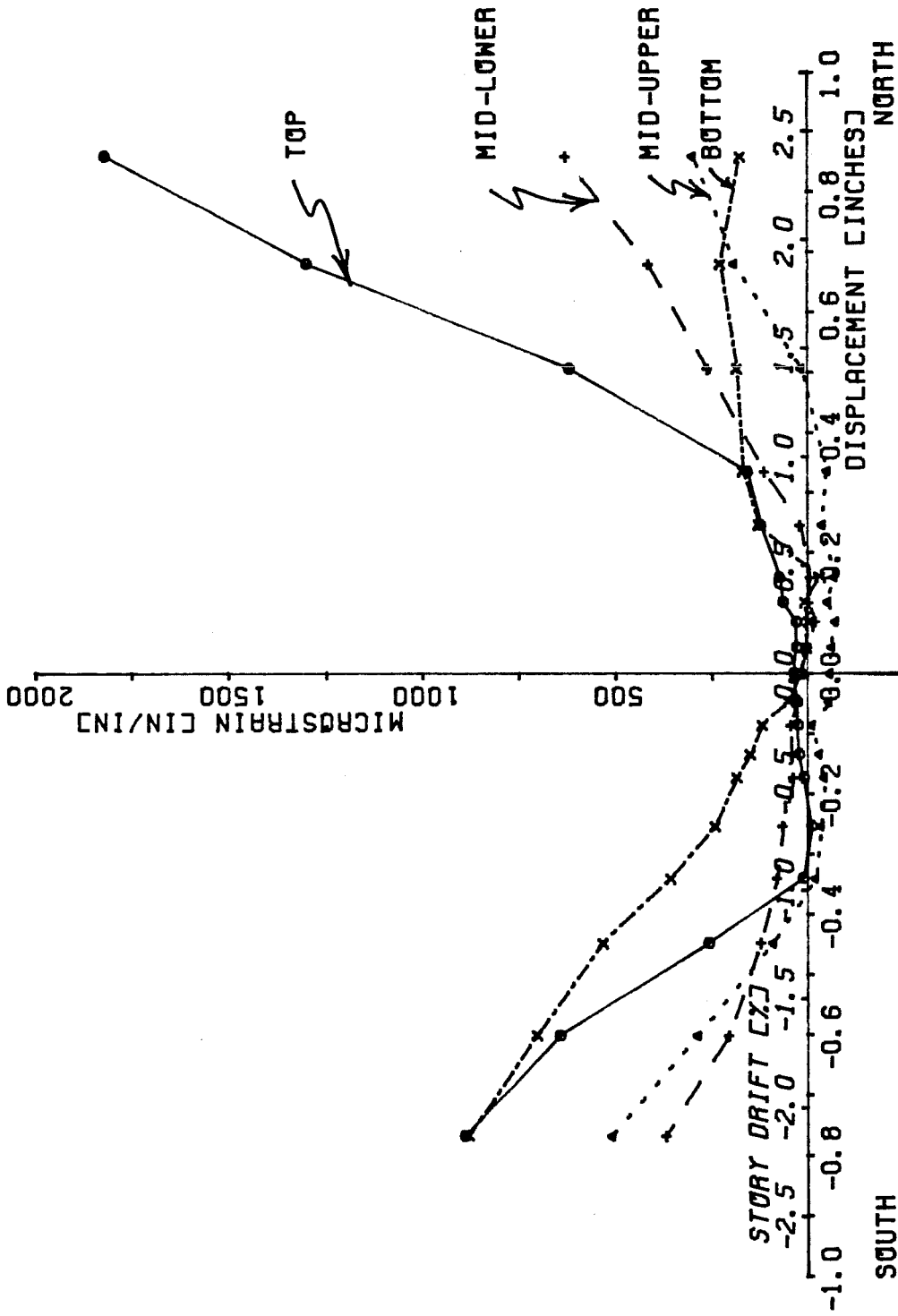


Fig. 4.14 Strain envelopes, N-S crossties, Specimen 1-3.

direction. Figure 4.15 illustrates, for the same specimen, strains in the comparable set of crossties running in the east-west direction. Strains are greater for the north-south ties than for the east-west ones, and increase significantly at about 1 percent drift level.

4.2.4 Slip. For Specimen 1-3, Figs. 4.16 and 4.17 illustrate the vertical slip of the jacket's north face with respect to the original column, at mid-height and near the bottom. Both plots indicate only extremely small relative movement between the jacket and the original column. In both figures, positive slip corresponds to upward motion of the jacket with respect to the original column.

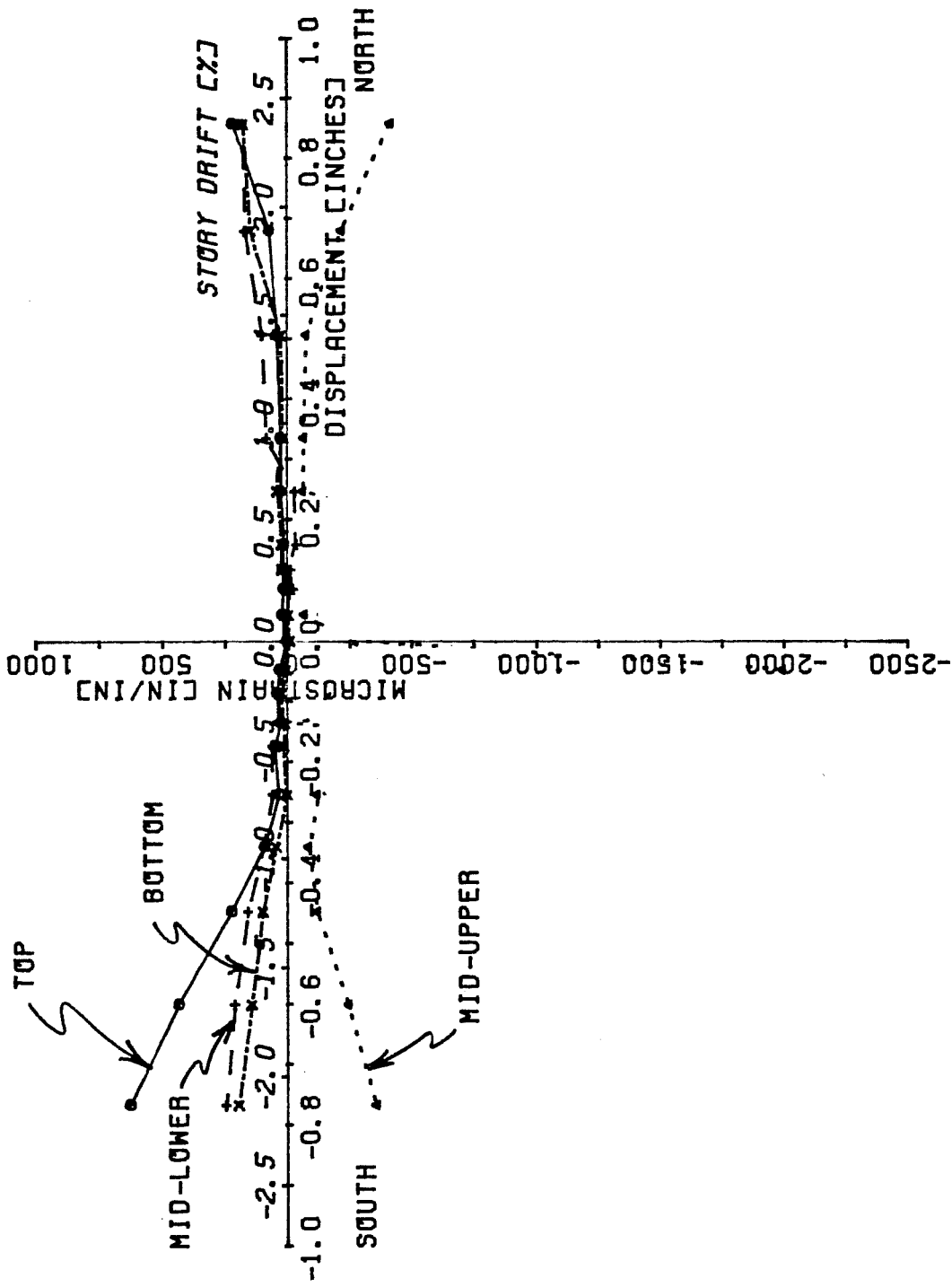


Fig. 4.15 Strain envelopes, E-W crossties, Specimen 1-3.

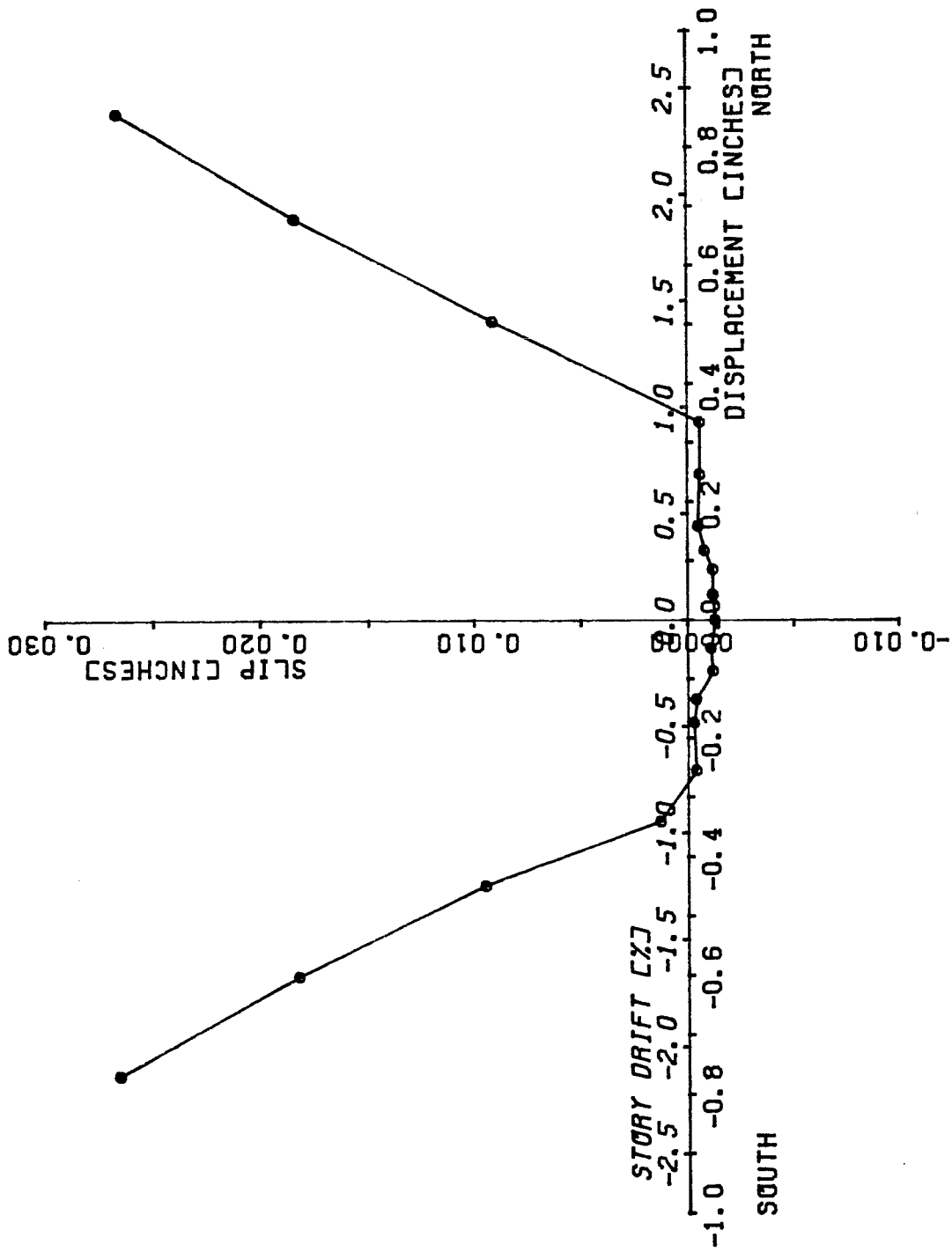


Fig. 4.16 Envelope of mid-height jacket slip, Specimen 1-3.

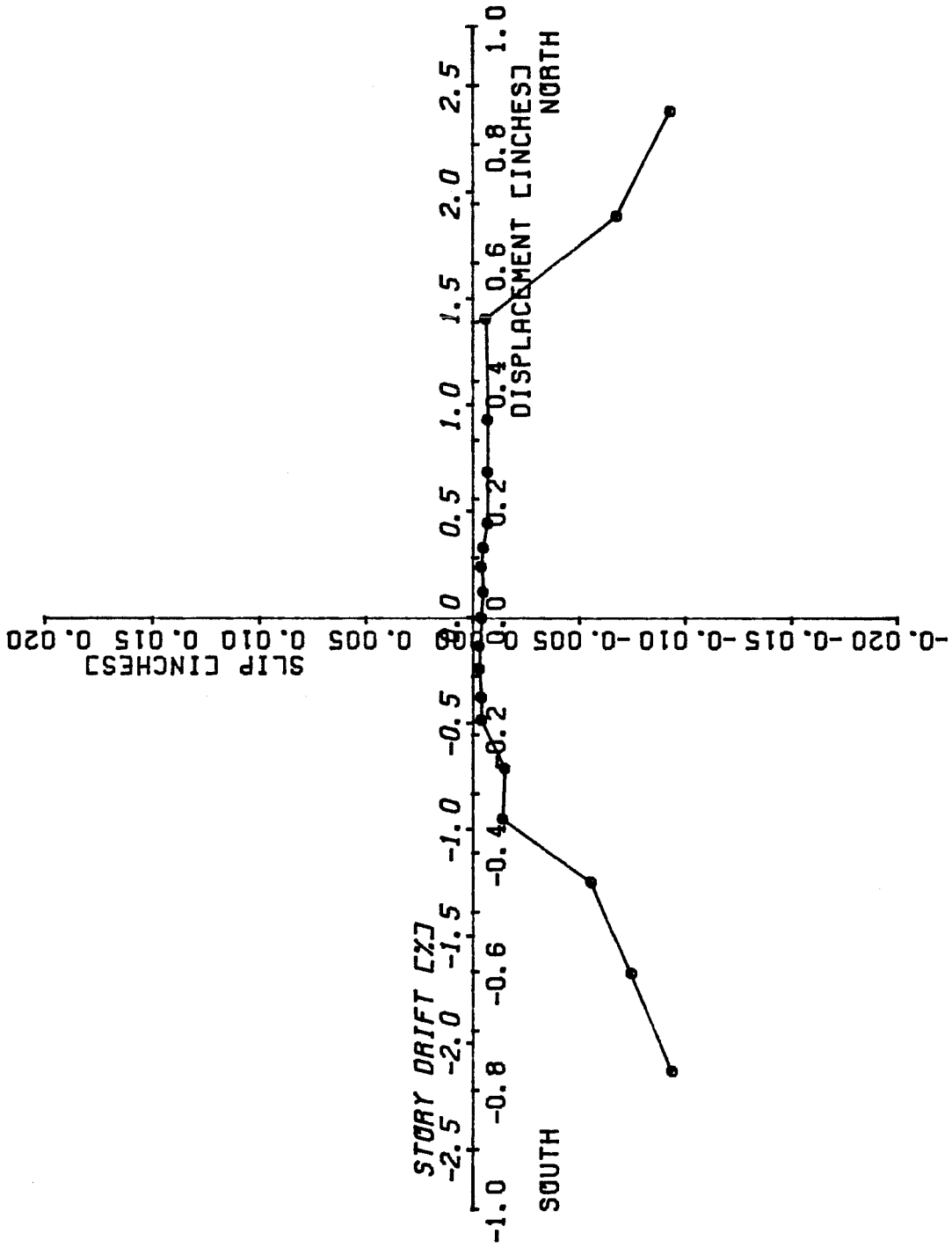


Fig. 4.17 Envelope of bottom jacket slip, Specimen 1-3.

CHAPTER V

DISCUSSION OF TEST RESULTS

5.1 Introduction

In this chapter, the results of four tests on three reinforced concrete short columns will be compared. The first test (1-1) involved the original column specimen, the second and third tests (1-2, 1-3) involved strengthened versions of the original column, and the fourth test (1-1R) involved the repaired first specimen. Similar lateral load histories were used for all tests except the first, in which lateral displacement was limited to 2 percent drift. A constant axial compression of 64.8 kips was applied to all specimens. All the original columns were constructed using identical cross-sectional dimensions and arrangements of longitudinal reinforcement, as shown in Table 2.1. The behavior of the columns will be compared in terms of load-deflection curves, load deflection envelopes, crack patterns, strain distributions, and jacket slip. The experimentally observed behavior will be compared with that predicted analytically.

5.2 Test Results

5.2.1 Specimen Stiffness and Capacity. A global indication of the relative stiffness of each specimen can be developed from inspection of Figs. 4.1 through 4.4. Unstable hysteretic behavior (pinching) is predominant in Specimen 1-1, and much less evident in the repaired or strengthened columns (Specimens 1-1R, 1-2 and 1-3). Specimen 1-1

exhibited stable hysteretic behavior for deformations up to 1 percent drift, but showed considerable loss of stiffness at 1.5 percent drift. Unstable, degrading hysteretic behavior was observed for drift levels in excess of 1.5 percent. The strengthened specimens (1-2 and 1-3) exhibited stable hysteretic behavior for deformations up to 1.5 percent drift, after which pinching and loss of stiffness became apparent. In the first cycle to each drift level, the repaired specimen (1-1R) exhibited load-deflection behavior similar to that of the strengthened specimens, but degraded much faster than the strengthened specimens under constant amplitude cycling beyond 1.5 percent drift. Neither the strengthened nor the repaired specimens exhibited the dramatic loss of stiffness observed in Specimen 1-1 beyond 1 percent drift.

The stiffness of each specimen can be compared graphically using the load-displacement envelopes of Fig. 4.5, which illustrates the improved performance of both the strengthened and repaired specimens compared to the original column (Specimen 1-1). Table 5.1 summarizes the first cycle secant stiffness (applied lateral force divided by lateral displacement) of each specimen for various drift levels. Specimens 1-2 and 1-3 had nearly equal first-cycle stiffnesses, and both were about 10 percent stiffer than the repaired Specimen 1-1R in this respect.

The effect of cycling on specimen stiffness can be seen in Figs. 5.1 through 5.4. The load-displacement envelopes for the first and third cycles to equal drift levels are shown for each specimen. Table 5.2 summarizes the percentage losses in secant stiffness between the

TABLE 5.1 Secant Stiffness in First Cycle to Various Drift Levels

Drift Level	Secant Stiffness (kip/inch)			
	Specimen 1-1	Specimen 1-2	Specimen 1-3	Specimen 1-1R
0.25	204	259	270	235
0.5	192	242	250	218
0.75	162	220	221	193
1.0	143	199	195	178
1.5	95	156	158	146
2.0	62	127	130	119
2.5	---	109	110	93

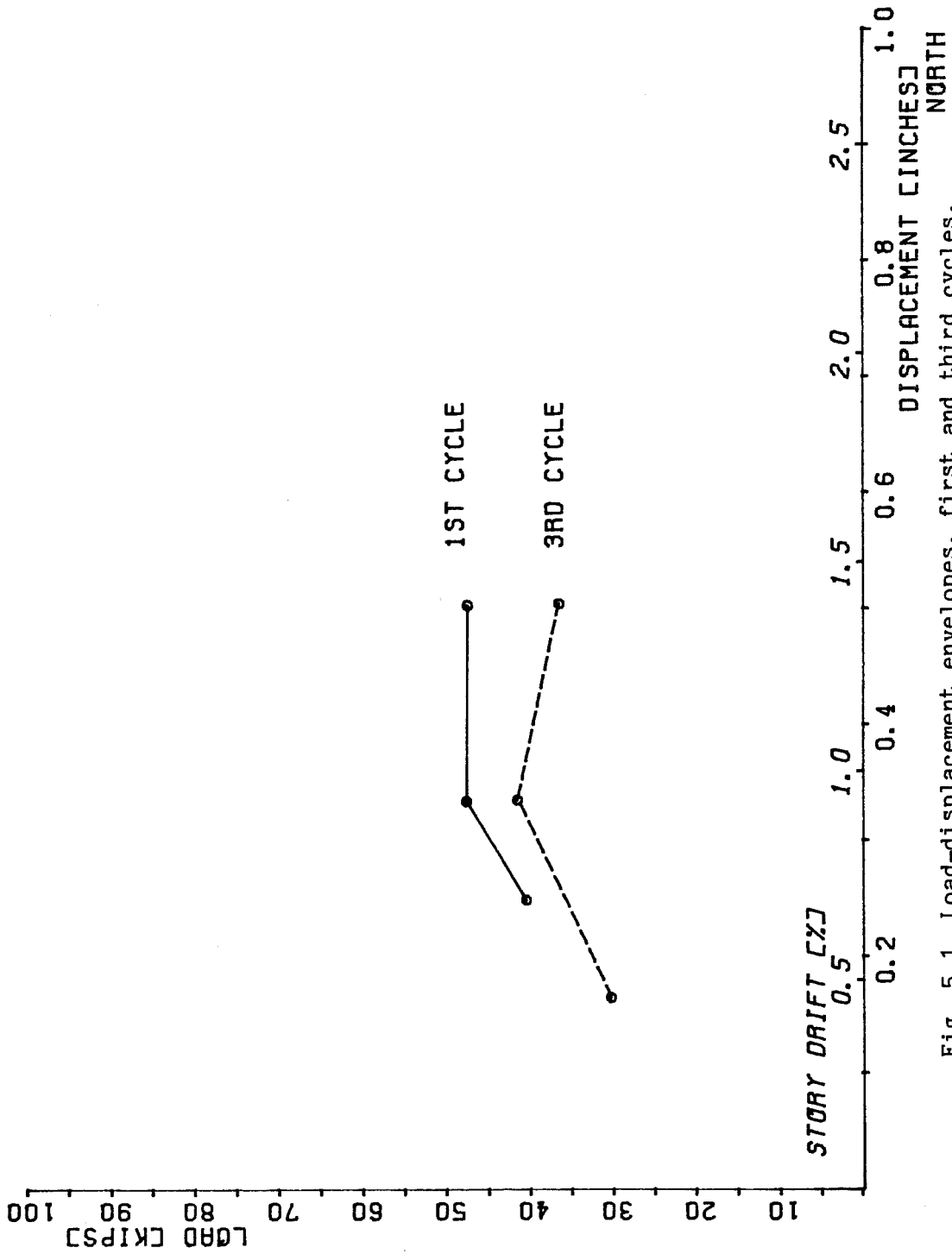


Fig. 5.1 Load-displacement envelopes, first and third cycles, Specimen 1-1.

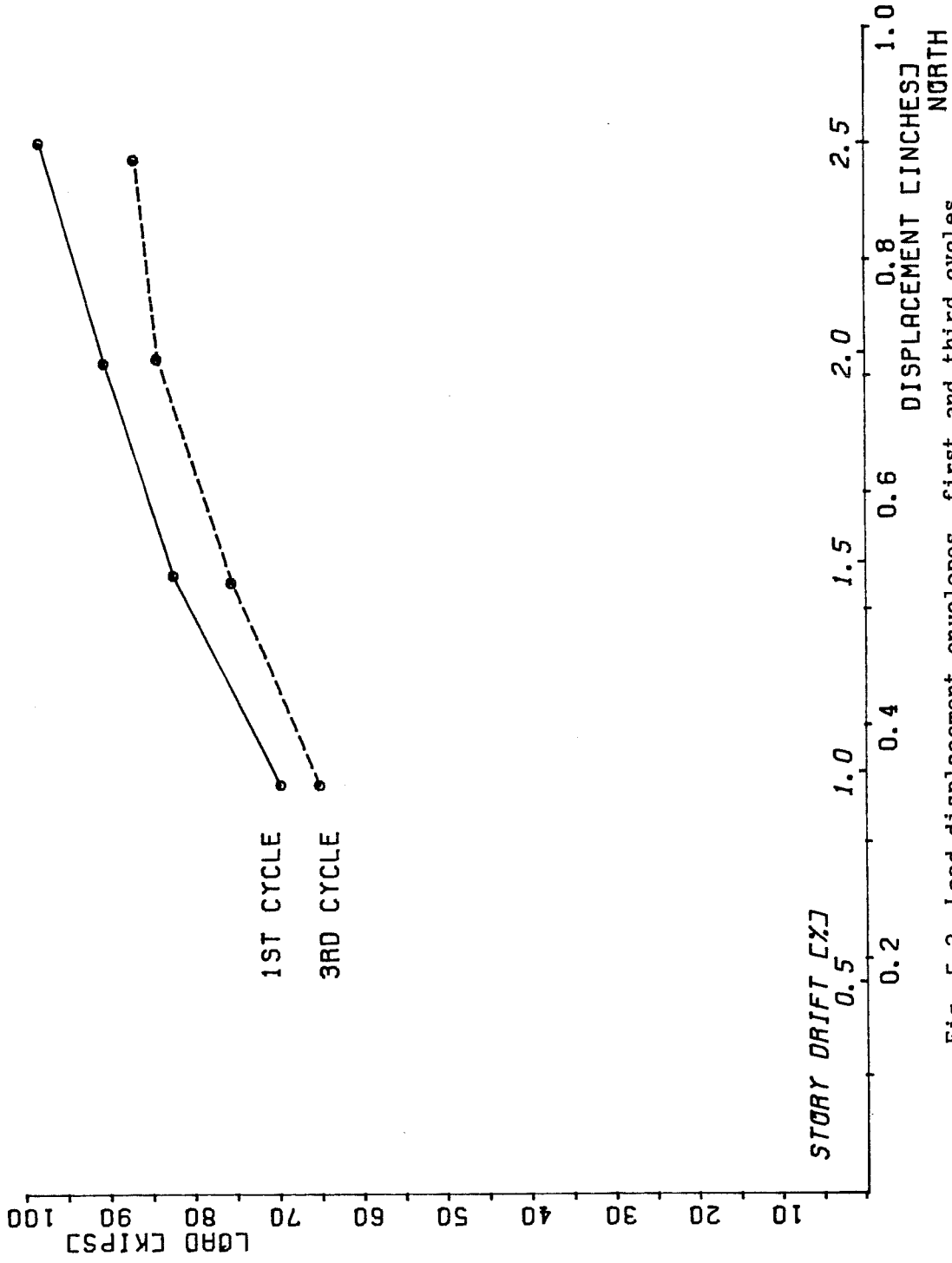


Fig. 5.2 Load-displacement envelopes, first and third cycles, Specimen 1-2.

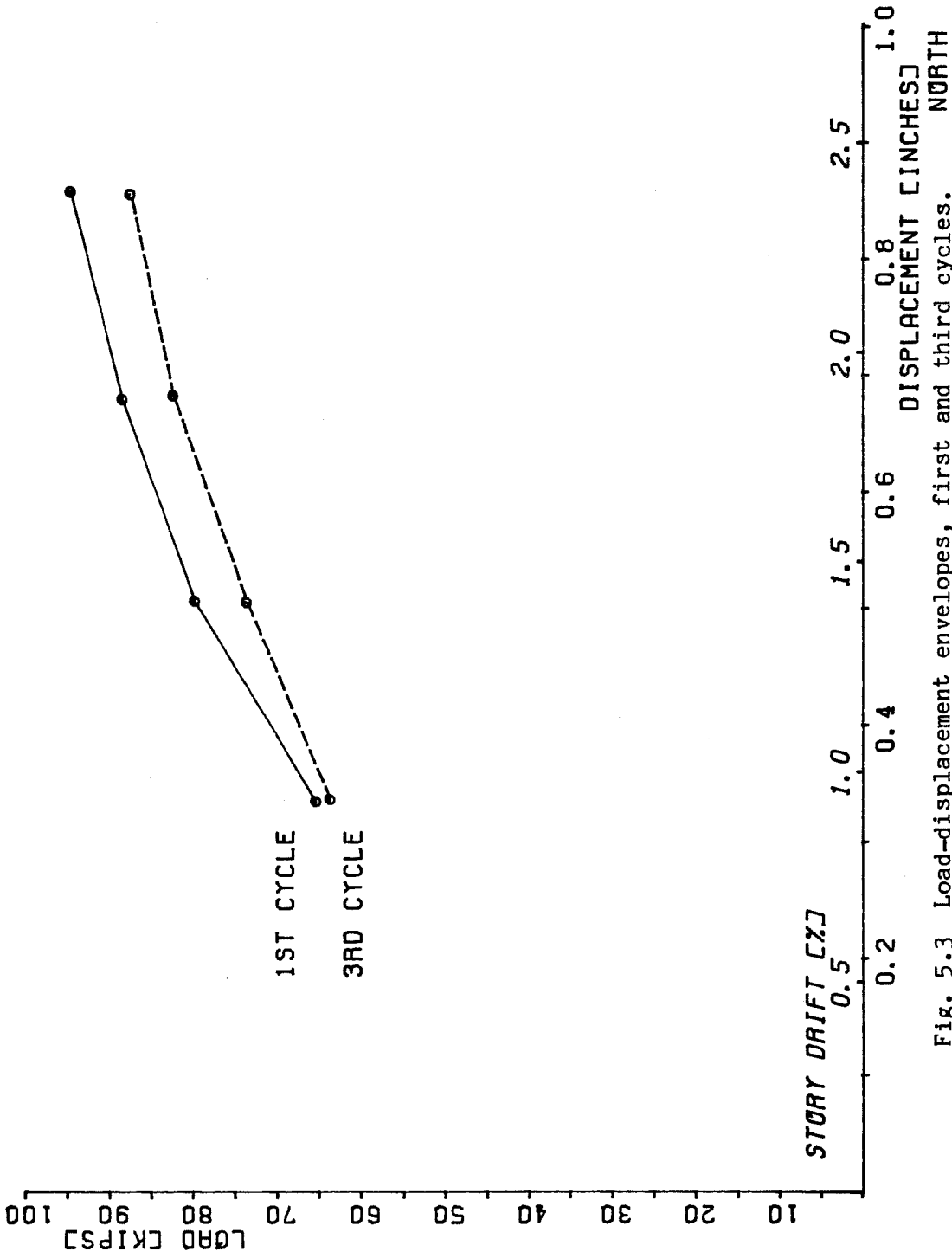


Fig. 5.3 Load-displacement envelopes, first and third cycles. Specimen 1-3.

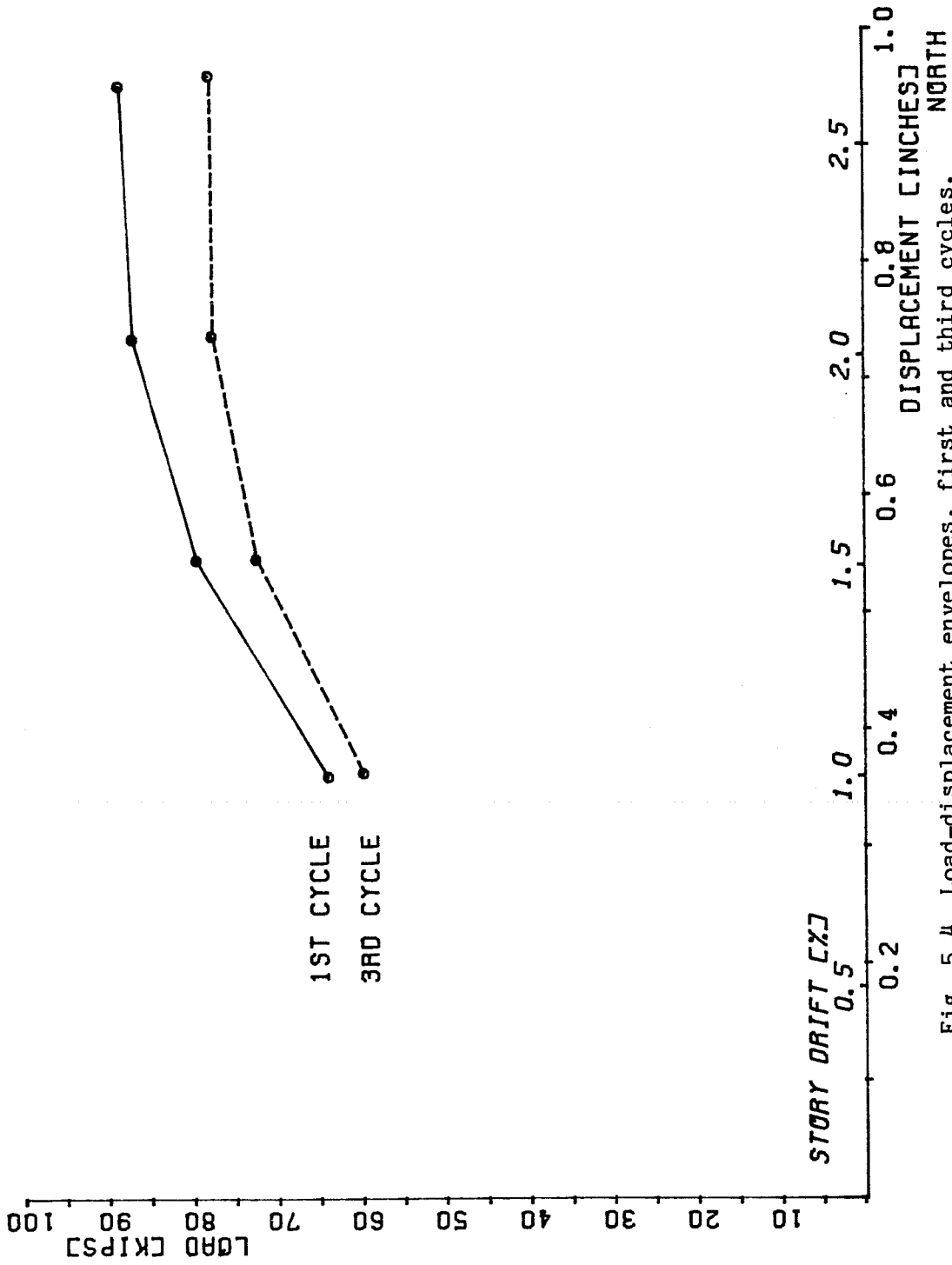


Fig. 5.4 Load-displacement envelopes, first and third cycles, Specimen 1-1R.

TABLE 5.2 Reduction in Secant Stiffness Between 1st and 3rd Cycles

Drift Level	Secant Stiffness Reduction (%)			
	Specimen 1-1	Specimen 1-2	Specimen 1-3	Specimen 1-1R
0.5	7	7	2	5
1.0	13	7	3	7
1.5	23	8	8	9
2.0	--	7	7	11
2.5	--	11	7	12

first and third cycles at a constant drift level. Specimens 1-1 and 1-1R experienced the greatest degradation, and Specimen 1-3 the least.

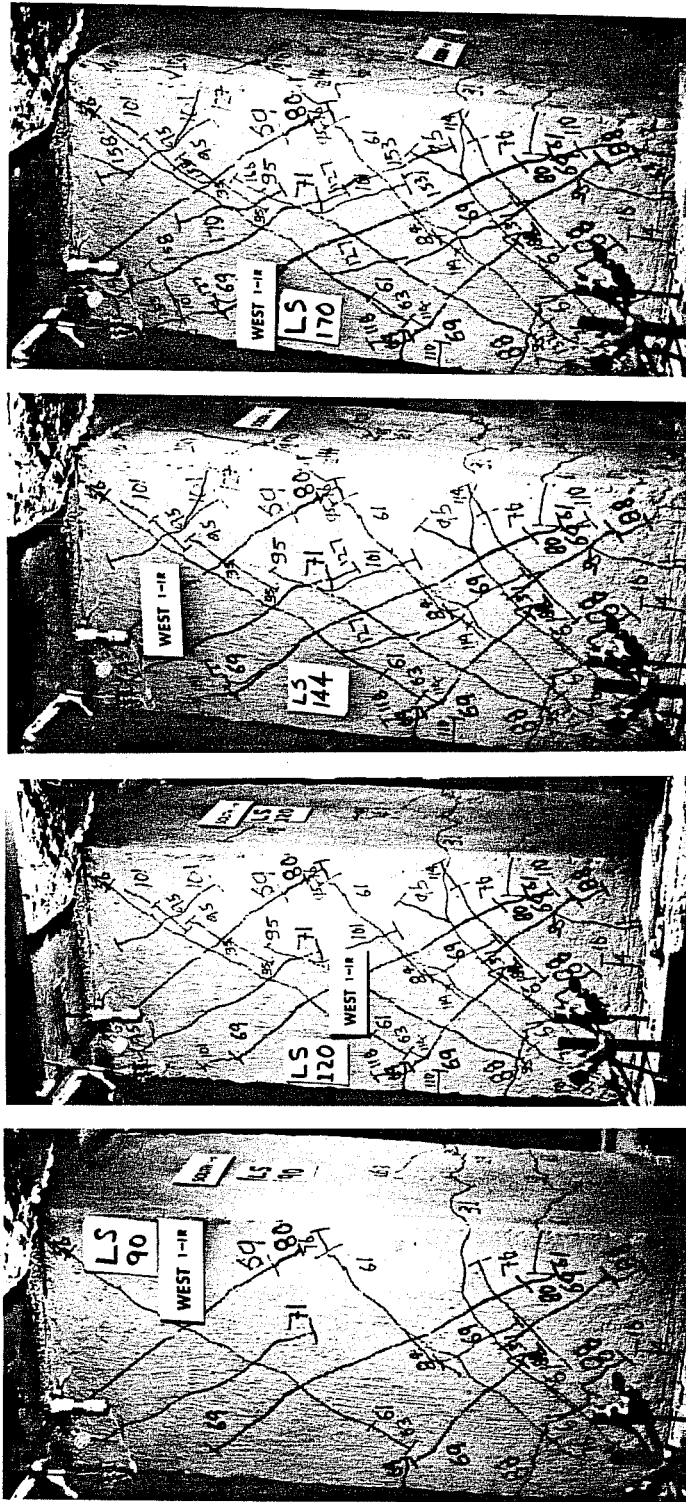
Figure 5.1 also shows that in both the first and third cycles to 1.5 percent drift, the lateral capacity of Specimen 1-1 was less during those same cycles to 1 percent drift. In other words, the lateral resistance of Specimen 1-1 decreased as drifts were increased beyond 1 percent. Other specimens did not degrade as much in this respect. Examination of Figs. 5.2 through 5.4 shows that the jacketed specimens exhibited increased resistance with increased drifts up to 2.5 percent. However, differences were observed among the jacketed specimens, and these can be discussed in terms of comparative tangent stiffnesses. The tangent stiffness, or slope of the load-deflection curve at a given drift level, was approximated by the slope of the straight line connecting a data point on the load-deflection curve with the following point.

Figures 5.1 through 5.4 reveal some additional information about the comparative tangent stiffnesses of each specimen at equal drift levels, and also about the degradation of those tangent stiffnesses with cycling. The tremendous stiffness degradation of the original column (Specimen 1-1) is shown by its negative tangent stiffness past 1 percent drift (Fig. 5.1). While the first-cycle secant stiffnesses of Specimens 1-2, 1-3, and 1-1R are similar, comparisons of Figs. 5.2 through 5.4 show that Specimens 1-2 and 1-3 had much higher tangent stiffnesses than Specimen 1-1R beyond about 1.5 percent drift. In fact, Specimen 1-1R had almost zero tangent stiffness beyond 2

percent drift. Comparison of Figs. 5.2 and 5.3 shows that beyond 2 percent drift, the strengthened specimen with crossties (Specimen 1-3) maintained its tangent stiffness much better under cycling than did the strengthened specimen without crossties (Specimen 1-2).

5.2.2 Crack Patterns. Similar crack patterns were observed in Specimens 1-1 and 1-1R for all levels of deformation. Flexural cracks turned into inclined cracks at about 1 percent drift. Repeated cycling at 1 percent drift widened and extended those cracks, which were evenly distributed over the height of the column. The cracking patterns of Specimens 1-2 and 1-3 resemble each other, but were significantly different from those of Specimens 1-1 and 1-1R. The strengthened specimens showed only flexural cracking at 1 percent drift. Cracks became inclined at 1.5 percent drift. At corresponding drift levels, Specimens 1-2 and 1-3 had fewer cracks and a smaller relative crack width than Specimens 1-1 and 1-1R. Specimen 1-1 exhibited some spalling at column mid-height, while Specimens 1-2, 1-3 and 1-1R all exhibited nearly equal amounts of crushing near the end blocks. Summarizing, Specimens 1-1 and 1-1R exhibited shear-dominated crack patterns, and Specimens 1-2 and 1-3 exhibited flexure or flexure-shear dominated crack patterns. Figures 5.5 and 5.6 illustrate the crack patterns for Specimens 1-1R and 1-2.

A crude indicator of the amount of delamination between the shotcrete jacket and the original column face is the comparative hollowness of the sound produced by tapping with a hammer on the column face. All jacketed columns were investigated in this manner after testing. The east and west faces of each specimen sounded more solid



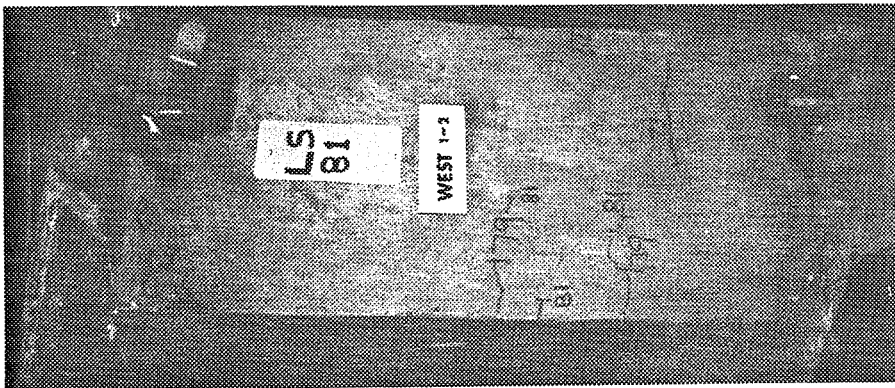
a) 1% drift

b) 1.5% drift

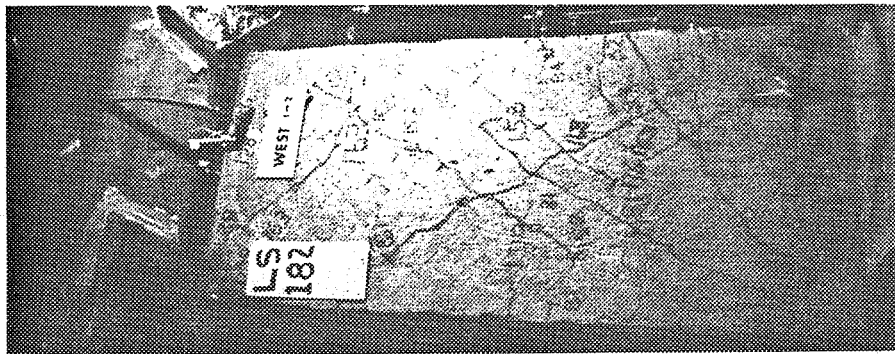
c) 2.0% drift

d) 2.5% drift

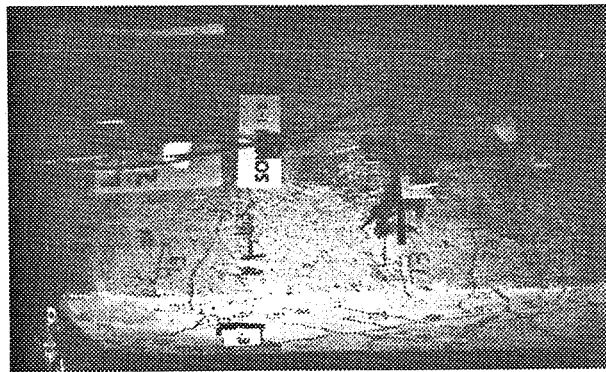
Fig. 5.5 Crack patterns, Specimen 1-IR.



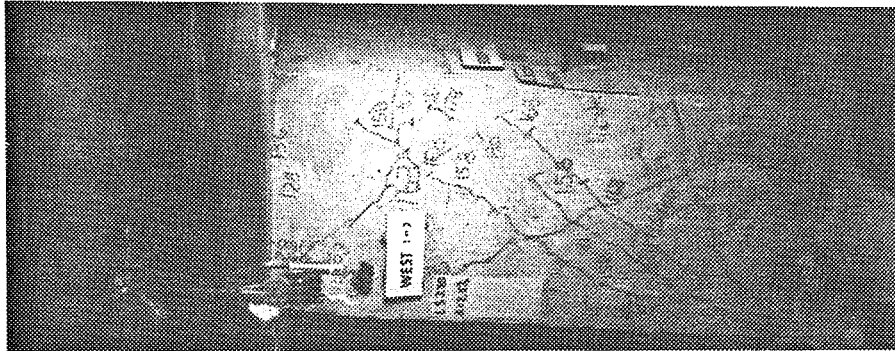
a) 1.0% drift



b) 1.5% drift



c) 2.0% drift



d) 2.5% drift

Fig. 5.6 Crack patterns, Specimen 1-2.

than the north and south faces. Though the east and west column faces exhibited more damage as evidenced by wider and more numerous cracks, the north-south faces would be expected to indicate more delamination because of alternating extreme fiber compression and tension under north-south lateral displacements. The north and south faces of Specimen 1-3 sounded most solid, followed by those of Specimen 1-2. Specimen 1-1R had the hollowest sound.

5.2.3 Strains in Reinforcement. As shown in Figs. 3.10 and 3.11, strain gages were attached to the longitudinal and transverse reinforcement in both the original column and the shotcrete jacket.

Longitudinal Reinforcement. By indicating the presence or absence of bar yielding, strain gages on longitudinal reinforcement provided valuable confirmation of the type of failure of each column. Two types of plots were developed from the data. The distribution of longitudinal steel strain along the column height for increasing drift levels is shown in Figs. 4.8 and 4.9. As shown in Fig. 4.8, the failure of Specimen 1-1 was dominated by shear—longitudinal steel was stressed to about 60 percent of yield at 1.5 percent drift even though a significant loss of stiffness had occurred, as shown by the load-displacement curves of Fig. 4.1.

In contrast, strains reached yield in longitudinal bars at the ends of both the strengthened and repaired specimens, indicating a combined flexural and shearing mode for those specimens. For northerly displacements, the strengthened specimens (1-2, 1-3) had top strains in

excess of yield at 2.5 percent drift, while the repaired specimen (1-1R) reached a strain of about 98 percent of yield at that same drift level.

Comparison of longitudinal bar strains in Specimen 1-1 (Fig. 4.8) versus those of either Specimen 1-2, 1-3 (Fig. 4.9), or 1-1R indicates that the original column had a different strain distribution than that of either the strengthened or repaired specimens. Conventional flexural theory predicts that a beam-column, subjected to equal end moments, and having a point of inflection at mid-height, will have a strain gradient ranging from tension to compression along longitudinal reinforcement. Specimen 1-1, with an aspect ratio of about 1.7, conforms to this conventional expectation. However, as mentioned in Chapter IV, plots indicate that tension develops along the entire length of the longitudinal reinforcement in both the strengthened and repaired specimens. This phenomenon can be explained in terms of two important differences between the original and the jacketed columns: 1) the location of the neutral axis; and 2) the effects of diagonal tension on the internal resisting moment within the column.

Prior to the formation of inclined cracks, and assuming little bond deterioration, longitudinal steel strains are consistent with the predictions of simple bending theory. Analysis using the computer program RCCOLA [15] indicated that regardless of moment direction, the position of the jacketed column's neutral axis placed all of the original column longitudinal reinforcement in tension. Figure 5.7(a) illustrates the effect of this neutral axis location on strains within a

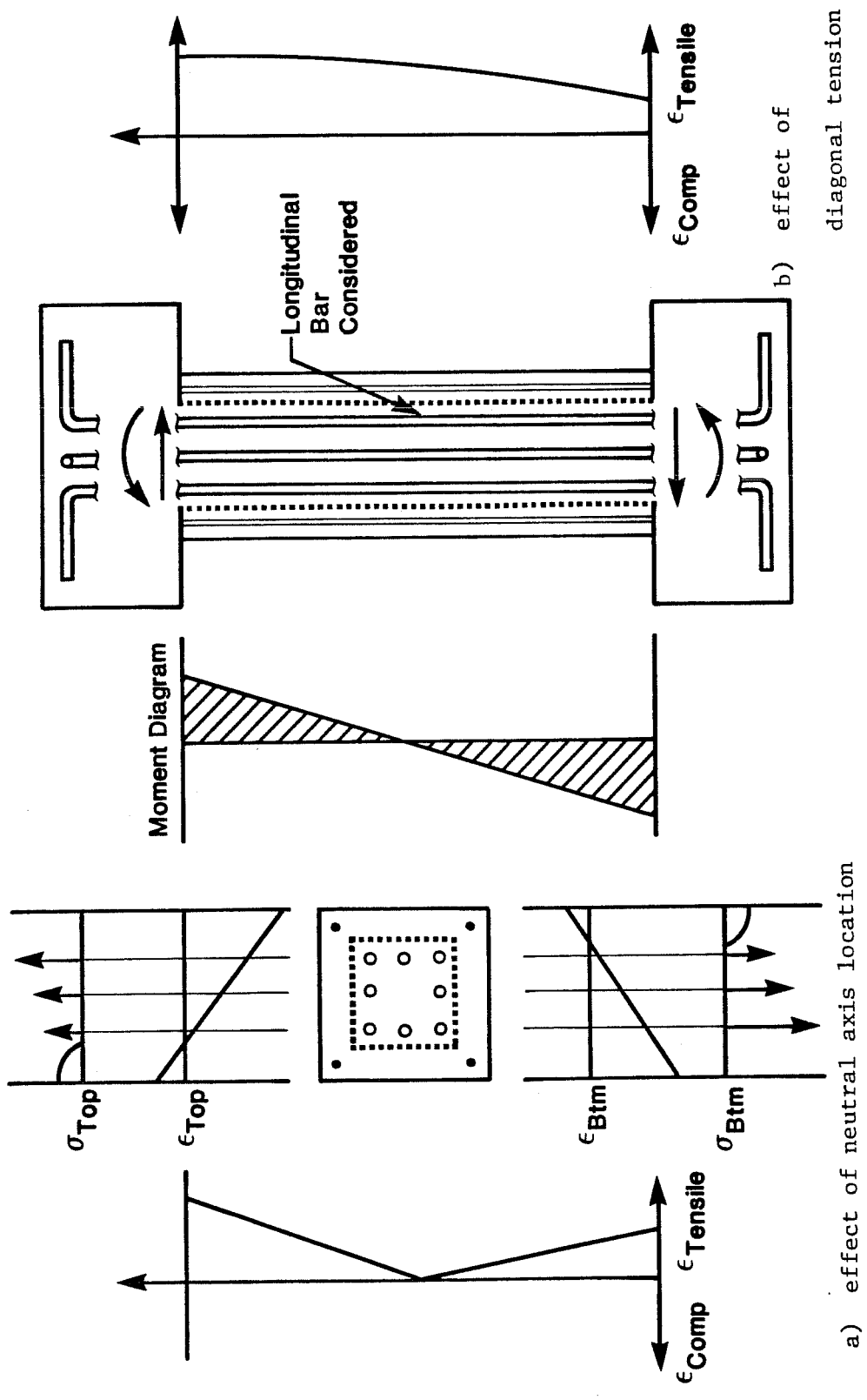


Fig. 5.7 Predicted envelopes of longitudinal bar strains.

single longitudinal bar. The bottom portion of the bar is in tension even though it is located on the "compression" face of the column.

Paulay, in his study of coupling beams [22] has shown that due to the effects of diagonal tension, flexural members with shear span/depth ratios less than about 2 have tensile stresses along the entire length of their longitudinal reinforcement, even at locations where conventional flexural theory would predict compressive stresses. Such a distribution is shown in Fig. 5.7(b) and becomes more dominant with decreasing shear span/depth ratios. The addition of the shotcrete jacket to the original column deepens the section, resulting in Paulay's coupling beam effect.

In all strengthened and repaired specimens, both effects were observed. The position of the neutral axis influenced bar stresses from the start of the tests, and the effects of diagonal tension increased as the tests proceeded. Figure 4.9 shows how the formation of inclined cracks at 1.5 percent drift shifted the strain envelope from one resembling Fig. 5.7(a) to one resembling Fig. 5.7(b). Subsequent larger drifts lengthened the inclined cracks, shifting the strain envelope even more.

The second type of plot developed from measurements of strain in longitudinal reinforcement consisted of histories of strain in the original column and jacket steel under increasing drift (Fig. 4.10). Noting that the jacket reinforcement is not continuous into the end blocks of the specimens, its purpose can conservatively be considered as helpful in construction with no contribution to the section's capacity.

Both the strengthened and repaired specimens exhibited similar behavior in both the original column and jacket reinforcement. Strains in the original longitudinal reinforcement would typically start to increase at about 0.5 percent drift, with relatively large increases occurring with increasing drift. On the other hand, strains in longitudinal jacket reinforcement increased much more slowly with increasing drift for all specimens. For large drift values in the northerly direction, when the reinforcement at the top north face of both the original column and the jacket was in tension, the jacket reinforcement had much less stress than that of the original column. As an index of the effectiveness in tension of the longitudinal reinforcement in the jacket versus that in the original column, comparative longitudinal bar forces at the top north face were calculated by multiplying bar stresses times the corresponding cross-sectional areas. The total tensile force in the jacket bars was only about 6 percent of that in the original column bars. However, at similar displacement levels, the jacket reinforcement in Specimen 1-1R had a higher force, about 17 percent of that found in the original column reinforcement. This appears reasonable because the core of Specimen 1-1R had been badly damaged by the first test; the shotcrete jacket had to carry more of the imposed forces. In any event, the jacket longitudinal reinforcement, which was not anchored at the ends of the columns, did not develop significant tension. As will be discussed in Section 5.3, this observation is consistent with the assumptions made in analyzing the jacketed columns.

Transverse Reinforcement. Distribution of shear between concrete and steel, and relative confining effects of transverse steel were investigated using strain gages mounted on the transverse reinforcement in both the jacket and the original column. Typical plots of averaged tie strains at column mid-height were shown in Figs. 4.11, 4.12, and 4.13.

Transverse reinforcement on the east and west faces of the column resists north and south loads, and also confines the concrete core. All specimens exhibited similar behavior in that drifts in excess of 1 percent caused large increases in strain in transverse reinforcement on the east and west faces (north-south direction). In all specimens, this drift level also corresponded to the formation of inclined cracks at column mid-height.

The average stress developed in parallel legs of an unyielded tie at a specific drift was calculated by multiplying the averaged strain by the modulus of elasticity of steel. The components of those tie forces resisting shear at mid-height were calculated. This gave a measure of total shear resisted by the transverse reinforcement in both the jacket and the original column. For Specimens 1-2 and 1-3 (Fig. 4.13), the force carried by the original column transverse reinforcement, calculated as described above, averaged about 75 percent of that in the jacket transverse reinforcement at drifts in excess of 1 percent. Up to drifts of 2 percent, little if any yielding occurred in the transverse steel of the strengthened specimens. However, this was not the case for the repaired specimen. Inspection of transverse tie strain

data for Specimen 1-1R (Fig. 5.8) indicates that the jacket transverse reinforcement in the north-south direction yielded before 2 percent drift, and reached strains far in excess of those recorded for the jacket ties in the strengthened specimens. Also, the force resisted by the jacket transverse steel was much greater than that carried by the transverse reinforcement in the original column. This is reasonable considering that the original column core of this specimen was badly damaged in the first test, and the original column ties were therefore not fully effective.

Transverse reinforcement on the north and south faces (east-west direction) confined the column core. Strain gages located on north and south face transverse reinforcement in both the jacket and the original column indicated similar behavior for all specimens. Typical envelopes of strain with increasing drift were shown in Figs. 4.12 and 4.13. Strains in transverse reinforcement carried about the same confining force for all specimens.

Crossties. Specimens 1-3 and 1-1R had #3 crossties in both the north-south and the east-west directions. The purpose of these crossties was to provide confinement in the east-west direction and provide both confinement and shear resistance in the north-south direction. Histories of strain versus lateral displacement are shown in Figs. 4.14 and 4.15 for Specimen 1-3, and in Figs. 5.9 and 5.10 for Specimen 1-1R. As was mentioned in Chapter IV, at comparable drift levels the crossties running in the east-west direction consistently experienced less stress than those in the north-south direction. This

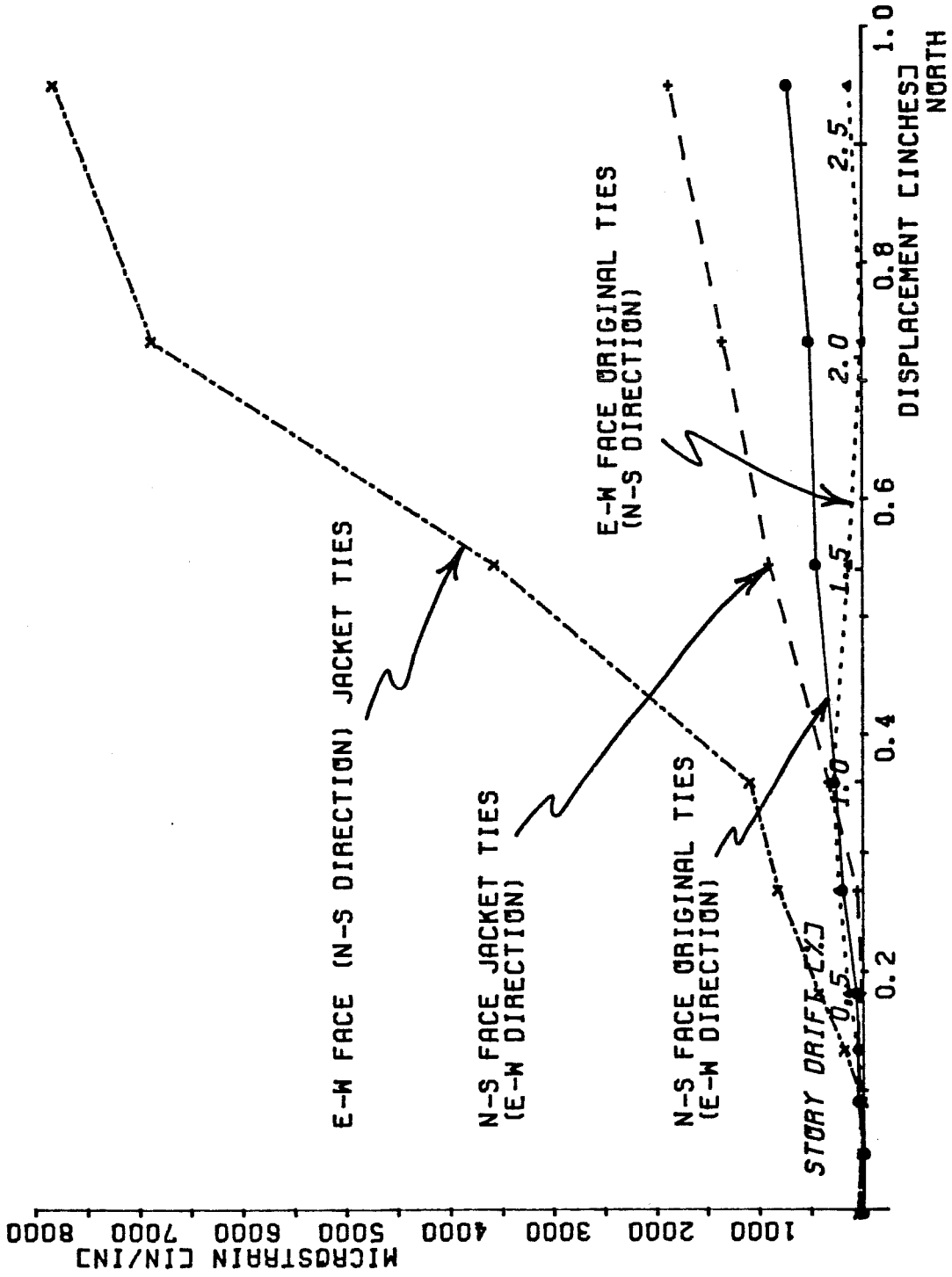


Fig. 5.8 Strain envelopes, mid-height ties, Specimen 1-1R.

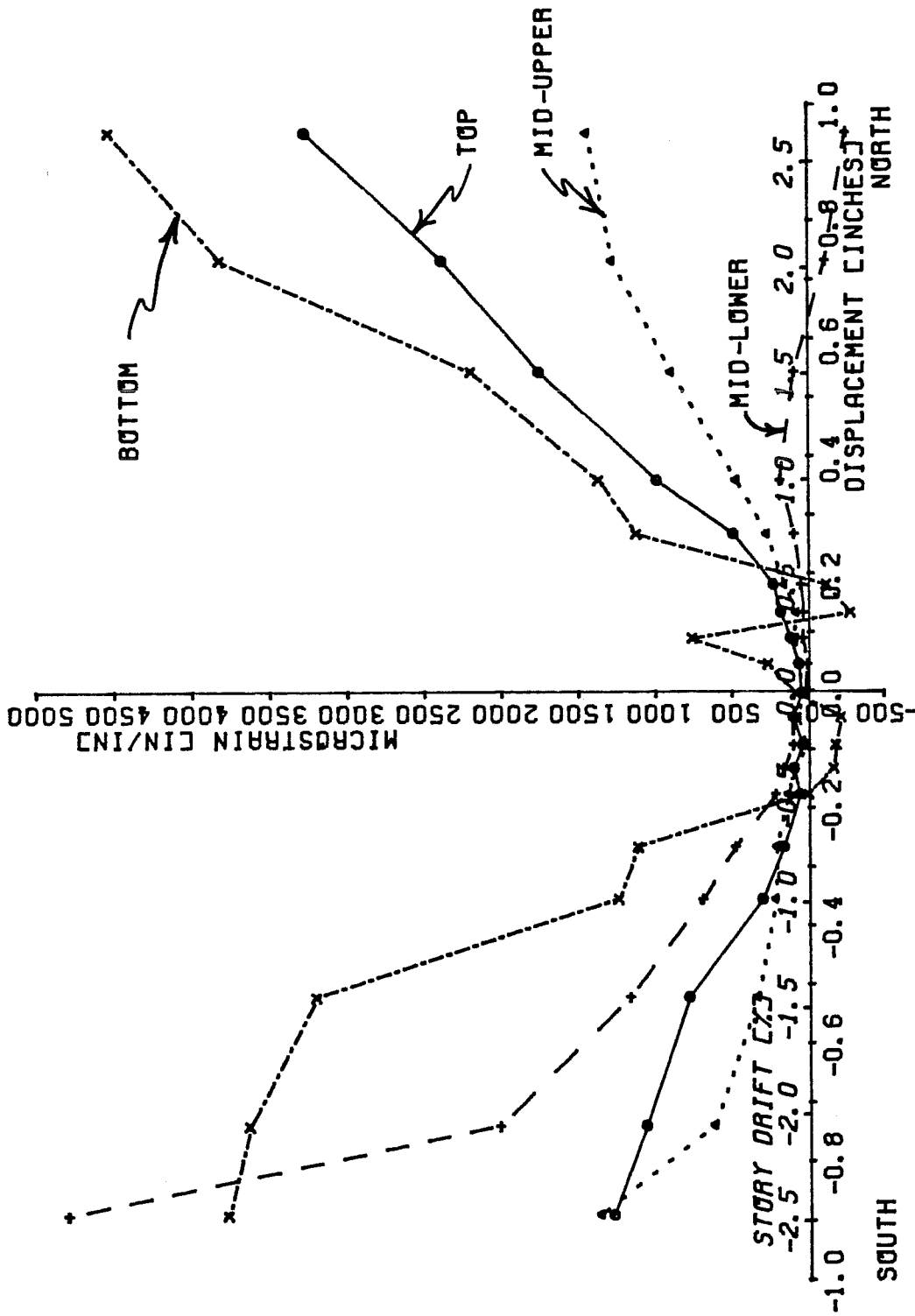


Fig. 5.9 Strain envelopes, N-S crossties, Specimen 1-1R.

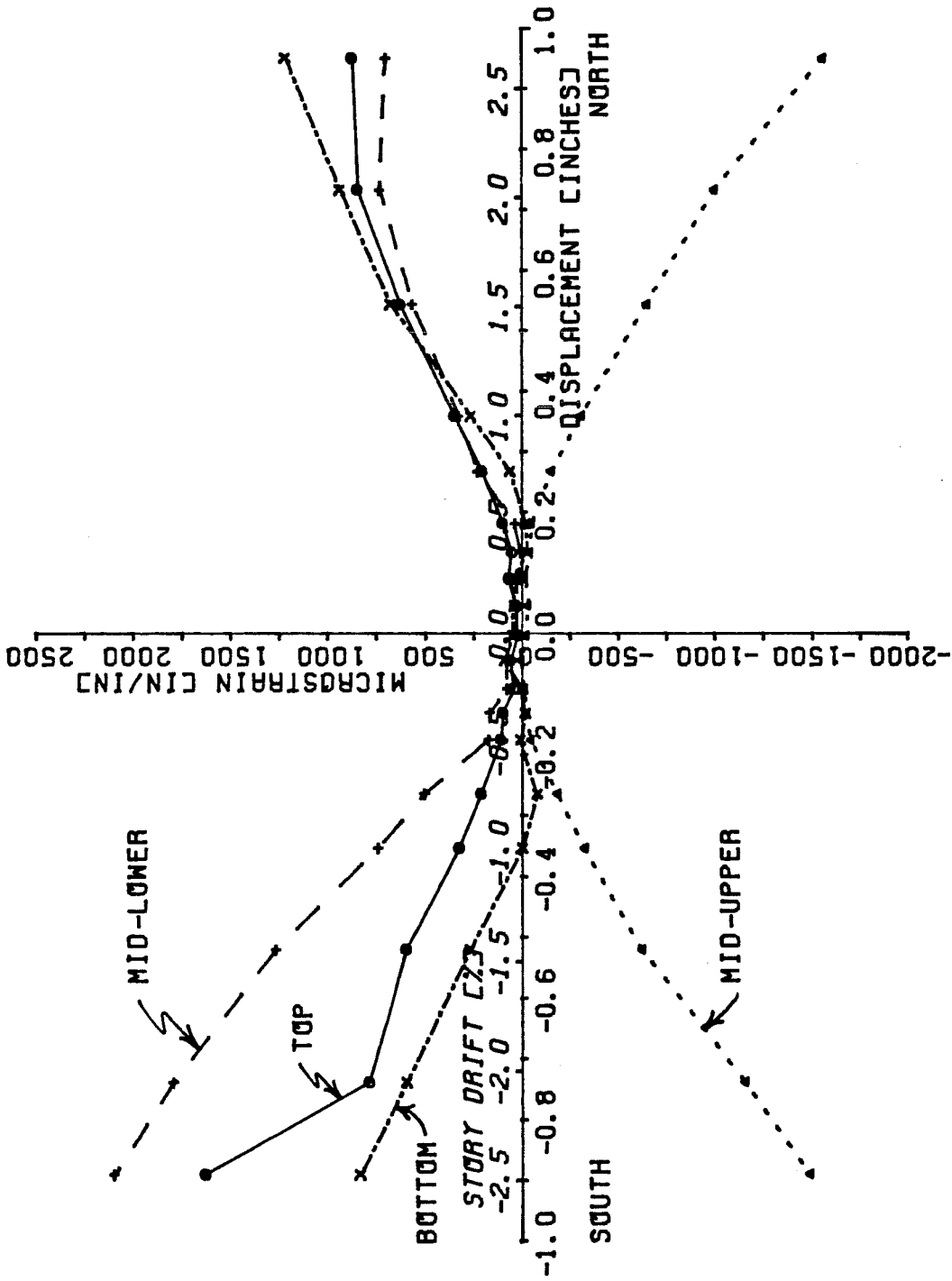


Fig. 5.10 Strain envelopes, E-W crossties, Specimen 1-1R.

is because the north-south crossties had to resist shear in addition to providing confinement. For Specimen 1-3, the east-west top crossties were stressed about 85 percent as much as the north-south ones at 2.5 percent drift. In Specimen 1-1R, for drifts in excess of 1.5 percent, east-west crossties were stressed about 30 percent as much as the north-south ones. A comparison of north-south crosstie stress levels for Specimens 1-3 and 1-1R indicates that crossties in the strengthened specimen (1-3) were stressed about half as much as those in the repaired specimen (1-1R) at comparable drifts.

The north-south crossties in Specimens 1-3 and 1-1R developed significant strains at drifts in excess of 1 and 0.5 percent respectively, corresponding to the formation of inclined cracks and increasing transverse tie strain.

5.2.4 Slip. The jacketing technique used for both strengthened and repaired specimens develops an internal interface which affects the performance of the resulting column. Movement of the shotcrete jacket with respect to the original column would indicate that the cross-section was not resisting flexure monolithically, and could imply that the jacket was not fully effective in confining the original column nor in resisting shear.

Representative plots of jacket movement with respect to the original column were shown in Figs. 4.16 and 4.17. Similar behavior was observed for all strengthened and repaired specimens. In each case, slip wire data appeared to indicate that the mid-height portion of the jacket moved upward relative to the original column at about 1 percent

drift. The bottom portion of the jacket appeared to move downward with respect to the original column at about the same drift. This would suggest the presence of significant cracks between the locations of slip wires in the shotcrete jacket. However, such cracks were not observed.

Care must be exercised in drawing conclusions based on this slip data. First, the magnitude of slip measured in all tests is at the lower limit of the sensitivity of the linear potentiometer used. Second, the linear potentiometer, mounted as shown in Fig. 3.12, could not distinguish between movement of the slip wire and outward movement of its support rod due to lateral expansion of the column. Third, slip in Specimen 1-3, whose jacket was reinforced with crossties, was about twice that of Specimens 1-2 and 1-1R. Intuitively, the crossties would be expected to inhibit relative movement between the shotcrete jacket and the original column.

5.3 Comparison of Observed and Predicted Behavior

The experimentally observed lateral capacity of each specimen was determined using: 1) load-displacement curves (Figs. 4.1 through 4.4); 2) curves of longitudinal steel strains in the original column (Figs. 4.8, 4.9, and 4.10); 3) curves of strains in transverse reinforcement (Figs. 4.11, 4.12, 4.13, and 5.8); and 4) observations of the extent of inclined cracking (Figs. 4.6, 4.7, 5.5, and 5.6).

The original column (Specimen 1-1) was analyzed as described in Section 2.3.3 using the computer program RCCOLA [15]. The program, assuming plane sections remain plane, analyzed a slice of column cross section and computed the column's flexural and shear capacity as shown

in Fig. 2.2. As mentioned previously, the moment-axial force curve as governed by shear capacity is based on University of Texas short column tests [23] rather than conventional ACI [17] equations. Analyses indicated that a shear failure was likely because the predicted capacity in shear was less than that in flexure. Specimen 1-1 did have a shear-dominated brittle failure starting at about 1 percent drift. Longitudinal steel strains at failure were less than yield, and degradation of stiffness under cycling occurred after the transverse reinforcement yielded. The predicted and observed capacities are shown in Table 5.3.

Inspection of Table 5.3 reveals that using ACI shear equations (11-6, 11-7 and 11-17) consistently underestimates the section's shear capacity when compared to the results of the empirical relationship discussed in Section 2.3.3.

The strengthened specimens (1-2, (1-3) were analyzed using the same program (Section 2.6.2) used for the original column. A number of additional assumptions were made in modelling the original column-shotcrete jacket combination:

- 1) No slip was assumed between the original column and the shotcrete jacket. The effect of relative slip would be a smaller predicted capacity based on less than monolithic action;
- 2) Jacket longitudinal reinforcement was assumed not to carry any tensile stress. As shown in Fig. 4.10, a small amount of tension due to bond did develop in the jacket longitudinal

TABLE 5.3 Lateral Capacity

Specimen	Predicted Lateral Capacity (kips)			Exper. Observed Capacity (kips)	Drift (%)	Predicted Capacity/ Observed Capacity
	Flexure	Shear (UT)	Shear (AC)			
1-1	64	40	31	47	1	0.85
1-2	104*	100	72	90	2	1.15
1-3	104*	100	72	88	2	1.18
1-1R	104	100	72	86	2	1.19

reinforcement, and this could be expected to increase the predicted capacity; and

- 3) The shotcrete jacket was assumed to be fully effective in compression. The presence of 1/64 in. shrinkage cracks at each end block would indicate less than full jacket effectiveness at low displacement levels.

The results of the analysis, shown in Fig. 2.7 and Table 5.3, indicated that the predicted capacity in shear was nearly equal to that in flexure. A combination flexure-shear failure mode would be expected, considering the location of the neutral axis developed in the analysis. Specimens 1-2 and 1-3 had flexurally-dominated failures, as evidenced by longitudinal reinforcement strains exceeding yield. Some degradation of stiffness occurred under cycling at larger drifts. The predicted and experimentally observed capacities are shown in Table 5.3.

The repaired specimen (1-1R) also predicted to have nearly equal flexural and shear capacities, could also be expected to fail in combined shear and flexure. Specimen 1-1R did indeed exhibit a combination shear-flexure failure, as evidenced by longitudinal steel strains slightly less than yield at peak displacements, significant degradation of stiffness under cycling, and by strains greater than yield in transverse reinforcement. Inclined shear cracks were both far more numerous and wider in Specimens 1-1 and 1-1R than in either Specimens 1-2 or 1-3.

The summary table (Table 5.3) reveals that for the strengthened and repaired specimens, experimentally observed lateral capacity was

about 10 to 15 percent less than that predicted. This slight discrepancy was probably due to the assumptions, mentioned previously, made in modelling the original column-shotcrete jacket combination.

C H A P T E R V I

SUMMARY AND CONCLUSIONS

6.1 Summary of Investigation

The behavior of strengthened and/or repaired reinforced concrete short columns under cyclic deformations was studied. The primary objective of the study was to evaluate the effectiveness of various techniques for strengthening or repairing short columns.

Based on an 18-in. square prototype column, three column test specimens were constructed to two-thirds scale, using identical geometry and reinforcement. As summarized in Table 2.1, the original specimens had a 12-in. square cross section reinforced with eight #6 longitudinal bars, sets of 6 mm ties spaced at 8 in., and 1 in. cover. Spacing of the transverse reinforcement, though greater than what would currently be specified, was intended to represent the practice of column design in seismic regions of the U.S. in the 1950's and 1960's.

One of the original specimens was tested (Specimen 1-1), repaired, then retested (Specimen 1-1R). Repair of that specimen consisted of removing loose cover, adding #3 longitudinal bars at each corner, epoxying #3 crossties in each direction at 9 in., hooked around a #6 mid-face bar, and adding 6 mm deformed transverse ties at 2.5-in. spacing. The original column was then encased with a 2.5-in. shotcrete jacket which provided a 1-in. cover over the added reinforcement,

resulting in a 17-in. square column. The repair technique is summarized graphically in Table 2.1.

The remaining two specimens (Specimens 1-2 and 1-3) were strengthened prior to testing. Specimen 1-2 was strengthened by adding #3 longitudinal bars at each corner, 6 mm ties at 2.5-in., and a 2.5 in. shotcrete jacket, resulting in 1-in. clear cover and a 17-in. square column. Specimen 1-3 was strengthened similarly to the repaired specimen (1-1R) using #3 longitudinal bars at each corner, 6 mm ties at 2.5 in., plus crossties hooked around #6 longitudinal bars at mid-face. Table 2.1 summarizes the strengthening technique used for each specimen.

The specimens were tested using the apparatus shown in Figs. 3.4 and 3.6, designed to permit north-south lateral movement of one column end while preventing rotations. A single displacement history, summarized in Fig. 2.20, was used for all tests. Typically, each specimen was subjected to three reversed cycles of lateral displacement to drifts of 0.5, 1.0, 1.5, 2.0, and 2.5 percent. A constant axial load of 64.8 kips was applied in all tests. During each test, measurements were taken at each load stage to determine the applied forces, lateral deflection, and strains in the longitudinal and transverse reinforcement. Fixity of the column ends was also monitored. Cracks were marked at each peak deflection.

6.2 Summary of Test Results

6.2.1 Original Column Specimen. Specimen 1-1 exhibited stable hysteretic behavior for deformations up to 1 percent drift (Fig. 4.1), after which considerable loss of specimen stiffness occurred under

cycling (Fig. 5.1). Failure appeared to be dominated by shear, as evidenced by pinching of the hysteretic loops, and the development of longitudinal reinforcement strains significantly less than yield. Extensive inclined cracks (Fig. 4.6) developed at 1 percent drift and steadily lengthened with cycling.

As shown in Fig. 2.2, analyses indicated that the original column's shear capacity was significantly less than its flexural capacity, and hence a brittle shear failure was predicted. The original column specimen did behave satisfactorily at drift levels less than 0.5 percent, as long as its response was essentially elastic. However, its loss of strength and stiffness at larger drifts indicated that the original specimen could not provide adequate cyclic lateral resistance in the inelastic range.

6.2.2 Strengthened and Repaired Specimens. The strengthened and repaired specimens were designed to fail in a more ductile manner than the original column specimens. Analysis of the strengthened specimens (Fig. 2.7) predicted a combination flexure-shear failure, as the section's shear capacity was about equal to its flexural capacity. The shotcrete jacket was assumed to behave integrally with the original column and improve inelastic strength and stiffness due to the confining interaction of the transverse and longitudinal steel. The analysis assumed: 1) no relative movement or slip would occur between the original column and the shotcrete jacket; 2) jacket longitudinal reinforcement would not carry any tensile stress; and 3) the shotcrete jacket would be fully effective in compression. Slip between the jacket

and original column and the formation of significant cracks at the end blocks would be expected to reduce monolithic action, resulting in a smaller capacity.

Both the strengthened and the repaired columns exhibited greater ductility than the original column. Both strengthened specimens (Specimen 1-2 and 1-3) exhibited similar load-deflection behavior (Figs. 4.2 and 4.3), having stable hysteretic loops for deformations up to 1.5 percent drift, after which loss of stiffness became apparent (Figs. 5.2 and 5.3). Failure appeared to be flexurally dominated, as evidenced by the development of strains in excess of yield in the original column longitudinal reinforcement. As shown in Table 5.1, jacketing both with and without supplementary crossties resulted in much greater stiffness and strength than that of the original, unstrengthened specimen. As shown in Figs. 4.7 and 5.6, inclined cracks developed in both strengthened specimens at drifts in excess of 1 percent, coinciding with increases in measured strains in the transverse reinforcement. Supplementary crossties did not significantly increase specimen strength nor stiffness in the first cycle to a given drift level, but were beneficial in delaying strength and stiffness deterioration under repeated cycles to drift levels exceeding 2 percent.

The repaired specimen (1-1R) exhibited stable hysteretic behavior for deformations up to 1.5 percent (Fig. 4.4), after which it began to lose stiffness under cycling (Fig. 5.4). Failure appeared to be a combination of shear and flexure, as evidenced by yield of the

original column longitudinal reinforcement, coinciding with the appearance of pinching of the hysteretic loops.

The repaired specimen had much greater lateral stiffness and strength than the original specimen, and about 10 percent less than the strengthened specimens at the first cycle to a given drift level (Table 5.1). Inclined cracks developed in the repaired specimen (Fig. 5.5) at 1 percent drift, coinciding with increases in measured strains in the transverse ties and crossties, in excess of yield at large drifts. Inclined cracks were longer, wider, and more numerous in the repaired specimen than in either of the strengthened specimens. The repaired specimen degraded much faster than either of the strengthened specimens under repeated cycles to drift levels exceeding 2 percent.

6.3 Conclusions

1) A two-thirds scale model of a typical column designed for seismic areas in the 1950's and 1960's performed poorly under reversed cyclic lateral deformations exceeding 0.5 percent drift. As predicted by analysis, the column's shear span/depth ratio and reinforcing details resulted in a brittle, shear-dominated failure. Reinforced concrete buildings constructed in seismic zones, and using such columns as their primary lateral force resisting mechanism, should be checked for elastic lateral capacity sufficient to resist their design forces. If the elastic capacity is insufficient, requiring that strong ground motions be resisted inelastically, serious losses of strength and stiffness will result when the columns are subjected to reversed lateral deformations in excess of 0.5 percent drift. This situation can be remedied either

by strengthening the columns to produce a more ductile member, as described here, or by providing additional elastic capacity in the form of shear walls or bracing.

2) A number of techniques can be used to strengthen existing columns in order to improve their performance under reversed lateral deformations. In this study, encasement of the original square column with a shotcrete jacket reinforced with corner longitudinal bars and closely-spaced ties significantly increased its stiffness and lateral capacity. In selecting and placing the jacket longitudinal reinforcement, care was taken to develop a column whose failure would still be ductile in spite of the decrease in shear span/depth ratio caused by jacketing. A 2-1/2 in. spacing of jacket transverse reinforcement provided increased confinement and shear resistance, and was not hard to fabricate. An upper bound to the lateral capacity of such a strengthened column can be calculated assuming integral behavior of the shotcrete jacket and the original column. Shear capacity was predicted using equations developed in recent tests of short columns, as ACI equations were consistently found to under-estimate the shear capacity.

3) The strengthening technique described above was varied in an attempt to increase the confinement provided by the jacket. Additional midface longitudinal bars were placed in the jacket, and connected by crossties grouted with epoxy through the original column. Analyses indicated that this modification would not significantly effect the specimen's monotonic stiffness or strength, and results did not show significant increases in stiffness or capacity. However, the crossties

did decrease the rate of strength and stiffness degradation under repeated cycles of reversed lateral displacements exceeding 2 percent drift. Failure appeared to be flexurally-dominated, and the level of lateral deformation imposed may not have been large enough to clearly define the additional confining effect of the crossties. Relative slip between the shotcrete jacket and the original column was very small for all jacketed columns, so the addition of crossties did not improve column behavior in this respect.

4) When a badly damaged column was repaired by encasing its core with a shotcrete jacket reinforced with closely-spaced ties, and with crossties connected to midface longitudinal bars, the strength and stiffness were nearly equal to those of an undamaged column strengthened with the same kind of jacket. The crossties and midface bars contributed significantly to the confining effect of the jacket transverse reinforcement. For columns with geometries and reinforcement similar to those discussed here, encasement with a shotcrete jacket is a practical and effective technique for increasing shear strength and ductility.

6.4 Additional Research

Based on the results of the current investigation, the following future research is suggested:

1) Study is needed regarding the effects of varying the proportions of both the column and the jacket. The performance of a strengthened section may differ considerably depending on the relative proportions of the added jacket to the original column.

2) The effect of epoxy injection of cracks in a damaged column needs study. Repair of the original column core may improve the deterioration of strength and stiffness observed when the repaired specimen was cycled repeatedly to large drift levels.

REFERENCES

1. Hanson, R. D., "Repair, Strengthening and Rehabilitation of Buildings--Recommendations for Research," University of Michigan, Report No. UMEE 77R4, October 1977.
2. Hanson, R. D., "Repair and Strengthening of Reinforced Concrete Members and Buildings," Proceedings, Workshop on Earthquake Resistant Reinforced Concrete Building Construction, University of California, Berkeley, July 1977.
3. Sugano, S., "Aseismic Strengthening of Existing Reinforced Concrete Buildings," Seminar, Seismology and Earthquake Engineering, International Institute of Seismology and Earthquake Engineering, Building Research Institute, Japan, March 1980.
4. "Guideline for Seismic Retrofitting (Strengthening, Toughening and/or Stiffening) Design of Existing Reinforced Concrete Buildings," Ministry of Construction, Japan, March 1977 (translated into English, 1980).
5. Jirsa, J. O., Maruyama, K., and Ramirez, H., "Development of Loading System and Initial Tests--Short Columns under Bidirectional Loading," CESRL Report No. 78-2, Civil Engineering Structures Research Laboratory, The University of Texas at Austin, September 1978.
6. Jirsa, J. O., Maruyama, K., and Ramirez, H., "Short RC Columns under Bidirectional Load Histories," Journal of Structural Engineering, ASCE, Vol. 110, No. 1, Paper 18511, January 1984, pp. 120-137.
7. Ramirez, H., and Jirsa, J. O., "Effect of Axial Load on Shear Behavior of Short RC Columns under Cyclic Lateral Deformations," PMFSEL Report No. 80-1, The University of Texas at Austin, June 1980.
8. Woodward, K. A., and Jirsa, J. O., "Influence of Reinforcement on RC Short Column Lateral Resistance," Journal of Structural Engineering, ASCE, Vol. 110, No. 1, Paper 18513, January 1984, pp. 90-104.
9. Moore, M. E., "Shear Strength and Deterioration of Short Lightweight Reinforced Concrete Columns under Cyclic Deformations," unpublished Master's thesis, The University of Texas at Austin, May 1982.

10. Mahin, S. A., Bertero, V. V., Chopra, A. K., and Collins, R. G., "Response of the Olive View Hospital Main Building during the San Fernando Earthquake," Report No. EERC 76-22, Earthquake Engineering Research Center, University of California, Berkeley, October 1976.
11. Selna, L. G., Morrill, K. B., and Ersoy, O. K., "Shear Collapse, Elastic and Inelastic Biaxial Studies of the Olive View Hospital Psychiatric Day Clinic," Proceedings, U.S.-Japan Seminar on Earthquake Engineering, Berkeley, 1973.
12. Nielson, N. N., and Nakagawa, K., "The Tokachi-Oki Earthquake, Japan, May 16, 1968: A Preliminary Report on Damage to Structures," International Institute of Seismology and Earthquake Engineering, Report No. 2, Tokyo, Japan, June 1968.
13. Sugano, S., "Guideline for Seismic Retrofitting (Strengthening, Toughening and/or Stiffening) Design of Existing Reinforced Concrete Buildings," Proceedings, Second Seminar on Repair and Retrofit of Structures, Ann Arbor, Michigan, May 1981.
14. Personal communication, Loring A. Wyllie, Jr., H. J. Degenkolb Associates, Engineers, February 1983.
15. Farahany, M. M., "Computer Analysis of Reinforced Concrete Cross-Sections," unpublished Master's thesis, The University of Texas at Austin, December 1983.
16. ACI Committee 318, Building Code Requirements for Reinforced Concrete (ACI 318-63), American Concrete Institute, Detroit 1963.
17. ACI Committee 318, Building Code Requirements for Reinforced Concrete (ACI 318-77), American Concrete Institute, Detroit 1977.
18. Personal communication, Joe Chappell, Quality Gunite Co., Austin, Texas, October 1983.
19. Adhesive Engineering Company, Technical Bulletin A/E 478, San Carlos, California, November 1982.
20. Grace and Company, Darex Pumping and Twining Laboratory, Test Results, Report No. DX80-7000, Cambridge, MA, 1980.
21. John S. Edison, Inc., Operators Manual: Model 10FC Hydraulic Load Maintainer and Cycling Unit, Burbank, California, 1970.
22. Paulay, T., "Coupling Beams of Reinforced Concrete Shear Walls," Journal of the Structural Division, ASCE, Vol. 97, No. 3, March 1971, pp. 843-862.

23. Jirsa, J. O., and Umehara, H., "Shear Strength and Deterioration of Short Reinforced Concrete Columns under Cyclic Deformations," PMFSEL Report No. 82-3, Phil M. Ferguson Structural Engineering Laboratory, The University of Texas at Austin, July 1982.

V I T A

Bart John Bett was born in Ashland, Ohio, on March 22, 1959. After completing his work at Black River High School, Sullivan, Ohio, in 1977, he entered Bowling Green State University. After two years of work at Bowling Green, he transferred into the cooperative education program at Purdue University in June 1979. Employed in alternate semesters by the Chicago Bridge and Iron Company of Oakbrook, Illinois, he received the degree of Bachelor of Science in Civil Engineering from Purdue University in May of 1982. In September 1982, he entered The Graduate School of The University of Texas at Austin.

Permanent address: 585 Twp. Rd. 101
West Salem, Ohio 44287

This thesis was typed by Patricia Henderson.